Proteomic screen of dorsal root ganglion neuron growth states reveals Glypican 1 as an autocrine and paracrine activator of axon growth

Dissertation

zur

Erlangung des Doktorgrades (Dr. rer. nat.)

der

Mathematisch-Naturwissenschaftlichen Fakultät

der

Rheinischen Friedrich-Wilhelms-Universität Bonn

vorgelegt von

Kai Alexander Fährmann

aus Marl

Bonn, April 2025

Angefertigt mit Genehmigung der Mathematisch-Naturwissenschaftlichen Fakultät
der Rheinischen Friedrich-Wilhelms-Universität Bonn

Gutachter/Betreuer : Prof. Dr. Frank Bradke
Gutachter: Prof. Dr. Walter Witke

Tag der Promotion: 01.07.2025
Erscheinungsjahr: 2025

Table of contents

Table of figures

Abbreviations

AA	Amino acid
ABC	Ammonium bicarbonate
ACN	Acetonitril
ADF	Actin depolymerizing factor
ADP	Adenosine diphosphate
AI	Artificial intelligence
AKT	RAC-alpha serine/threonine-protein kinase
Arhgap	Rho gtpase activating protein
ARP	Actin-related protein
ATP	Adenosine triphosphate
Basp1	Brain acid soluble protein 1
Bmpr1a	Bone morphogenetic protein receptor, type 1a
bp	Base pairs
Brap	BRCA1-associated protein
BSA	Bovine serum albumin
C-terminal	Carboxy-terminal
CAP1	Cyclase-associated protein 1
CCA	Chloroacetamide
CD	Circular dicroism
Cdc42	Cell division control protein 42 homolog
ChABC	Chondroitinase ABC
CMV	Cytomegalovirus
CP	Actin capping protein
CSPG	Chondroitin sulphate proteoglycan
ctag	Carboxy-terminally tagged
DCC	Deleted in colorectal carcinoma
Ddx18	ATP-dependent RNA helicase DDX18
Dnajc6	Putative tyrosine-protein phosphatase auxilin
Dnm1	Dynamin-1
Dnm1l	Dynamin-1-like protein
Dync1i1	Cytoplasmic dynein 1 intermediate chain 1
E	Embryonic day

ELISA	Enzyme-linked immunosorbent assay
ERK	Extracellular-signal regulated kinases
EV	Extracellular vesicle
FA	Formic acid
Farp1	Rhogef (arhgef) and pleckstrin domain protein 1 (chondrocyte-derived)
FCS	Fetal calf serum
G3bp2	Ras GTPase-activating protein-binding protein 2
Gap43	Growth associated protein 43
GDP	Guanosine diphosphate
GFP	Green fluorescent protein
GO	Gene ontology
Gpc1	Glypican 1
GPI	Glycosylphosphatidylinositol
GTP	Guanosine triphosphate
HA	Human influenza hemagglutinin tag
His	Histidine
hHA	Hidden HA
HS	Heparan sulfate
HSPG	Heparan sulfate proteoglycan
hSyn	Human synapsin
JNK	Jun N-terminal kinase
KD	Knock-down
Kiaa1045	Protein KIAA1045
Kif5a	Kinesin heavy chain isoform 5A
KO	Knock-out
L	Lumbar
LANUV	Landesamt für Natur und Verbraucherschutz
LFQ	Label-free quantification
MACF1	Microtubule Actin Cross-linking Factor 1
Map1a	Microtubule-associated protein 1A
Map7d2	MAP7 domain-containing protein 2
Mapt	Microtubule-associated protein tau
MT	Microtubuli

Mthfd2	Bifunctional methylenetetrahydrofolate dehydrogenase/cyclohydrolase
MTOC	Microtubuli organizing centres
N-terminal	Ammino-terminal
NaCl	Sodium chloride
NaOH	Sodium hydroxide
Ncdn	Neurochondrin
NCE	Nominal colision energy
Ndrg4	Protein NDRG4
Nes	Nestin
NG2	Neural antigen 2
ntag	Amino-terminally tagged
Osbpl3	Oxysterol-binding protein-related protein 3
p38Mapk	p38 Mitogen-activated Protein Kinase
Pcbp3	Poly(rC)-binding protein 3
PFA	Paraformaldehyde
Pgm2l1	Glucose 1,6-bisphosphate synthase
Plcb3	1-phosphatidylinositol 4,5-bisphosphate phosphodiesterase beta-3
PLL	Poly-L-lysine
PM	Plasma membrane
PNL	Peripheral nerve lesion
Ppp1r2	Protein phosphatase inhibitor 2
PTEN	Phosphatase and tensin homolog
PTM	Post-translational modification
Pygb	Glycogen phosphorylase, brain form
Rbms1	RNA-binding motif, single-stranded-interacting protein 1
Rcc1	Regulator of chromosome condensation
Rhoa	Ras homolog gene family, member a
ROCKs	Rho-associated coiled-coil-containing protein kinases
SCI	Spinal cord injury
SEC	Size-exclusion chromatography
Sh3glb2	Endophilin-B2
Shh	Sonic hedgehog

Sprr1a	Small Proline Rich Protein 1A
Stmn2	Stathmin-2
Trim2	Tripartite motif-containing protein 2
Trim46	Tripartite motif-containing protein 46
TTL	Tubulin-tyrosine-ligase
Tusc5	Tumor suppressor candidate 5 homolog
v/v	Volume per volume
Vti1b	Vesicle transport through interaction with t-SNAREs homolog 1B
γ-TuRC	γ-tubulin ring complex

Summary

Following an injury in the adult central nervous system (CNS), axons fail to regenerate because of repressed intrinsic growth competence and a cellular environment that lacks growth support. Interestingly, injured axons of dorsal root ganglia neurons (DRG) can become growth competent and regenerate under specific conditions. The molecular program underlying their regenerative growth, however, has remained unclear. Thus far, studies of growth and regeneration in DRG axons have focused on candidate- or pathway-specific approaches or employed RNA sequencing for unbiased studies. However, transcriptomes only weakly predict the actual proteome. Especially non-transcriptional mechanisms, such as target degradation via autophagy or the proteasome or secretion of targets, can escape such transcriptomic analyses. Consequently, we set out to investigate the proteome of growing and regenerating DRGs. We used three previously published growth paradigms, in which DRG axons switch between low growth with high branching, to elongating growth with little branching. Proteomic analysis identified 39 proteins that inhabit the intersection of these growth paradigms. An overexpression screen of the identified candidates revealed multiple growth effectors. The largest growth effect was elicited by the cell-surface proteoglycan Glypican1 (Gpc1), which has previously been implicated in developmental axon guidance in both mammals and invertebrates. Overexpression of Gpc1 was sufficient to induce axon growth in cultured neurons, where it can overcome the growth inhibition conferred by chondroitin sulfate proteoglycans (CSPGs). Secretion of Gpc1 to the plasma membrane was necessary to bolster growth. Functional knock out of its heparan sulfate binding domain indicated that Gpc1 modulates cell-surface signalling receptors. We demonstrated that Gpc1 acts both autocrine and paracrine. Gpc1-overexpressing cells confer growth competence to WT neurons via extracellular vesicles which label positive for Gpc1. Further, we show that overexpression of Gpc1 changes the whole- and phospho proteome of the cell, to mirror a number of characteristics we found in the original growth paradigms. Together these results reveal Gpc1 as a promising candidate for growth activation, as it acts extracellularly to activate intracellular growth mechanisms, a challenge on which many other growth activators fail. *In vivo* studies will reveal the merit of Gpc1 in regenerating axons following CNS injury.

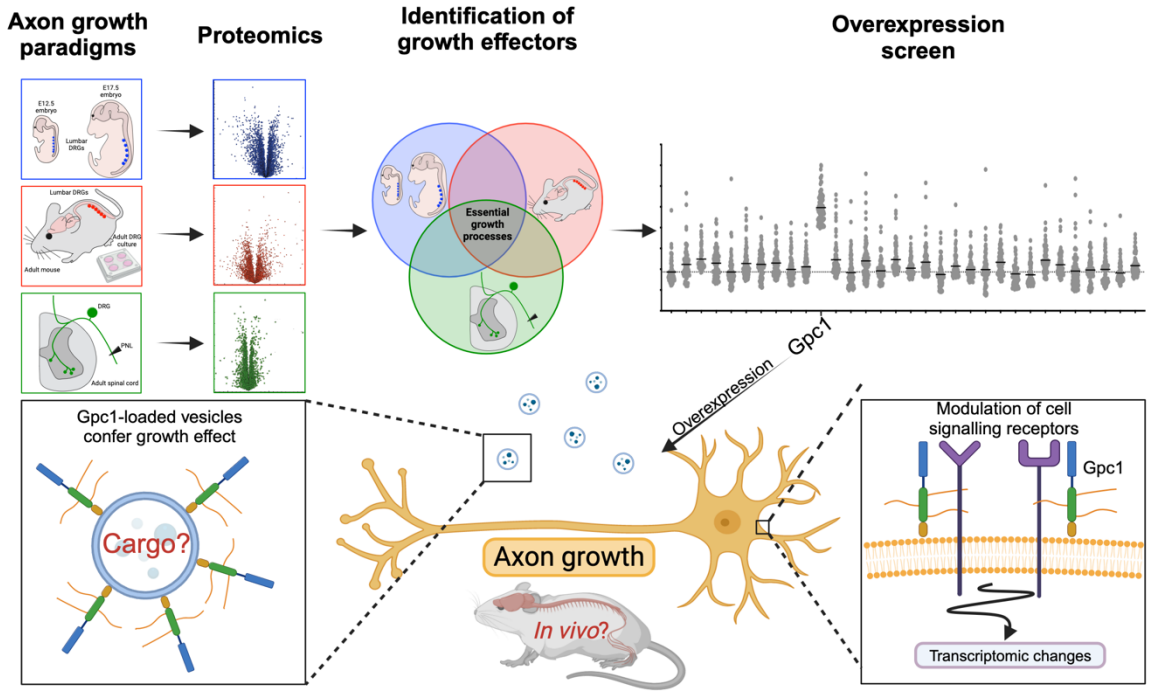

Figure 1: Graphical summary of the proteomic screen and consequent discovery of Gpc1 as a growth activator in DRG neurons.

Introduction

Neurons are the wiring within the brain and the cables from our brain to our muscles. These cables, in the form of axons and dendrites, span large distances, in humans up to 1 m (Hagemann et al., 2022) – 50.000-fold of the diameter of many cells (Goethals and Brette, 2020)– and maintain their function from before we were born, hopefully, until we die (Magrassi et al., 2013). This fact is even more impressive given that almost all neurons we have are born during gestation (Gage, 2019). Thus, neurons are long-ranged and long-lived cells that need to be carefully maintained, to provide function for up to a century or even longer.

As neurons form the functional connections between cells, loss of neurons is typically associated with a loss of function, be it cognitive, motor or sensory. As regeneration in the central nervous system (CNS) is abortive (Ramon y Cajal, 1928), function once lost is hardly ever reacquired. In the following chapters, I will lay out how neurons grow in development and regeneration. I will discuss intra- as well as extracellular cues that modulate axon growth, how these can be manipulated and and where gaps in our knowledge exist that invite the identification of new growth modifiers. I will also discuss mass spectrometry-based proteomics as a main tool used in this thesis to interrogate cellular growth processes and compare axon growth and regeneration to other cellular growth and migration phenomena. Finally, I will give an introduction to Glypican 1 (Gpc1) the main growth-enhancing molecule investigated in this thesis.

Axon growth in development and regeneration

Almost all neurons are generated during gestation. They are typically derived from some form of a progenitor cell, for which the neuron represents the terminal stage of differentiation (Hobert, 2011). Initially, the immature neuron is symmetrical. It needs to break this symmetry to establish neurites, which in most cases mature into one axon and multiple dendrites. This process can either be post-migratory, i.e., occurring after the progenitor cell has migrated to its final destination (Serbedzija et al., 1990), or co-occur with migration (Namba et al., 2014). In both scenarios, the breaking of symmetry is a non-random process which is highly regulated, yet not fully understood. Both intra- and extracellular cues influence when neurites begin to form and which neurite becomes the axon, destining the remaining neurites to become dendrites (Alfadil and Bradke, 2023). While specific regulatory cues will be discussed in a later chapter, the main intracellular effector of neuronal polarization is the cytoskeleton (Tahirovic and Bradke, 2009). Broadly, the cytoskeleton consists of three key polymers, filamentous actin, microtubuli (MT) and intermediate filaments. Since actin and MT are the most researched in the context of neuronal polarization and axon growth, I will focus on them in this introduction. As the molecular scaffold of the cell, these two highly dynamic structural proteins allow for cellular morphogenesis. The molecular structure and key interactors of these filaments will be discussed in a later chapter. Initially during neuronal polarization, filopodia and lamellipodia formed by filamentous actin, push out in a stochastic manner from the round cell body, bulging out the plasma membrane (PM), to allow for the penetration of MT (Flynn, 2013; Schelski and Bradke, 2017). Consequently, this very early step of axon initiation requires a malleable actin network and stable MT. Such MT are then bundled, stabilizing the MT array even more (Dent et al., 2011). The initial protrusions then form growth cones, the neurite's sensing organ as well as the steering unit through the extracellular environment. Much focus has been directed to the question whether the growth cone is propelled forward from the axon shaft or whether it is pulling itself through its surroundings, the latter being the prevailing theory for over thirty years (Lin et al., 1994; Mitchison and Kirschner, 1988). In this model, cellular adhesions form anchor points, by which the growth cone wrenches itself forward. Only recently, advances in imaging techniques and culturing systems, allowed our group to thoroughly investigate growth cone motility in a 3-dimensional culture model that more closely resembles the conditions found *in vivo*, providing data, that hippocampal neurons move in an amoeboid fashion, being pushed by the extension of MT

(Santos et al., 2020). If this holds true for other types of neurons or in other environments, especially *in vivo*, will have to be investigated.

Whether pushing or pulling, it has been observed that the elongation of a newly formed axon is related to a myriad of changes in the cytoskeleton. Axons are unique in the aspect that they orient almost all MT plus-end-out, meaning with the growing MT tip facing the growth cone (Burton and Paige, 1981; Heidemann et al., 1981). Furthermore, MT of the future axon are more stable than those of neurite who become dendrites (Witte et al., 2008). Interestingly, both stability, as well as MT retrograde flow, a recently found phenomenon reported by our group and others (Burute et al., 2022), seem to play a role in the establishment of a single axon (Schelski and Bradke, 2022). While MT retrograde flow is a recently observed phenomenon and thus, we are yet largely lacking the tools to manipulate it, MT stability can and has been manipulated to affect axon growth. Pharmacological stabilization of MT can lead to the formation of supernumerary axons (Witte et al., 2008) and increased regeneration in spinal cord injury (SCI) (Ruschel et al., 2015a; Stern et al., 2021). Conversely, while axonal MT need to be stable for growth, axonal actin filaments need to be malleable and increasing actin stability hinders axon growth (Bradke and Dotti, 1999). The prevailing theory argues that dynamic actin allows for the penetration of MT, while a rigid actin mesh restricts MT (Coles and Bradke, 2015). Consequently, growing and regenerating axons present more dynamic actin and manipulations to reduce actin stability positively affect axon regeneration (Bradke and Dotti, 1999; Tedeschi et al., 2019).

Thus, the cytoskeleton is the main effector of axon growth. Most molecules that affect axon growth in some way signal down to the cytoskeleton (Huber et al., 2003). Of course, other processes, such as the availability of energy in the form of adenosine triphosphate (ATP) or the availability of membrane lipids are necessary for growth but not sufficient to induce it. However, changes in the cytoskeleton are sufficient to induce axon formation, growth and regeneration.

Cytoskeletal organization in growth and regeneration

Both MT and actin stability are regulated by a seemingly endless list of interacting proteins. In general, as the cytoskeleton is omnipresent in the cell, a significant proportion of cellular processes involves the cytoskeleton. Thus, it can sometimes be difficult to distinguish if a protein facilitates an interaction with the cytoskeleton, or if that protein directly affects the cytoskeleton, or both. Here, I will discuss actin and MT modifications as well as modifying proteins, and the signalling cascades upstream of cytoskeleton modifications and how they affect growth.

Actin modifying proteins

Actin dynamics are a key factor in axon growth and regeneration. Filamentous actin is made up of monomeric globular actin subunits, which are bound non-covalently into a double-helical filament. In theory, actin filaments can self-nucleate anywhere in the cell, when three actin monomers bind and form a seed. This process, however, is kinetically disfavoured for the many actin binding proteins (ABP) that regulate seeding (Chandrasekaran et al., 2022). Actin filaments in the axon are nucleated off of stationary endosomes (Ganguly et al., 2015), focal adhesions (Chacon et al., 2012) or existing actin filaments (Mullins et al., 1998). A newly formed filament can now grow, branch, disassemble or be severed. While actin monomers can self-assemble onto filaments, addition of subunits to a filament is 5-10x faster when facilitated by formins (Pollard, 2007; Romero et al., 2004). The only known actin filament branching factor is the actin-related protein (Arp)2/3 complex. Upon recruitment via cortactin, it binds a mother filament and nucleates a daughter filament in a 70° angle. By remaining at the branch site, the Arp2/3 complex mechanically stabilizes the branch point (Liu et al., 2024; Rouiller et al., 2008). A highly branched actin mesh is mechanically more stable, thus restrictive to growth, by hindering the advancement of microtubules (Forscher and Smith, 1988; Schaefer et al., 2008). Destabilizing the actin mesh is mainly achieved via disassembly or severing of filaments. These two processes are highly related via a large number of ABPs. Unbranched axonal actin filaments undergo treadmilling, by polymerizing at their barbed end and depolymerizing at the minus end. ATP-bound monomers preferentially bind the barbed end. While bound to ATP, these monomers stabilize the filament. Is ATP hydrolysed to adenosine diphosphate (ADP), via the actin monomers' inherent ATPase activity, the filament becomes less stable and thus more likely to depolymerize (Kudryashov and Reisler, 2013).

The equilibrium between these two processes determines whether a filament grows or shrinks.

The disassembly rate can be influenced by capping proteins and severing enzymes. While capping proteins, such as actin capping protein (CP), stabilize the barbed end, they also hinder the addition of new monomers to the filament, thus shifting the equilibrium towards disassembly. Severing enzymes, such as actin depolymerizing factor (ADF) or Cofilin family proteins, cleave a filament, thus creating two new filaments. These new shorter filaments are more likely to depolymerize. Severing of filaments can also decrease the branchedness of the mesh, thus potentiating the destabilizing effect of filament severing. As less stable actin networks are more conducive to growth, ADF/Cofilin mediated actin turnover promotes axon growth and regeneration (Tedeschi et al., 2019).

Microtubuli modifying proteins

MT are larger, more stiff filaments compared to actin. They are formed from protofilaments made up of pairs of α- and ß-tubulin heterodimers. 13 protofilaments combine into one microtubule, which is, as the name implies, a hollow structure (Ledbetter and Porter, 1964). MT nucleation is an active field of research and not fully elucidated. Principally, MT nucleate off of MT organizing centres (MTOC), which include the γ-tubulin ring complex (γ-TuRC). The most well studied MTOC is the centrosome. In the centrosome, multiple γ-TuRCs nucleate MT which grow plus-end-out toward the axon tip. Another MTOC is calmodulin-regulated spectrin-associated protein 3 (CAMSAP3), which nucleates MT acentrosomally (Meng et al., 2008). Which MT nucleation strategy is utilized is cell-type and task-specific and when and why cells prefer one mechanism over the other is not fully elucidated. For example, in the CNS, neurons rely on centrosomal MT nucleation for migration, while it is dispensable for polarization (Vinopal et al., 2023). What types of MT nucleation are employed in regeneration is still a topic of research.

Once nucleated, MT polymerize towards the plus end, which is often visualized by tracking fluorescently labelled microtubule-associated end-binding 3 (EB3), which binds the plus-tip and is propelled forward upon polymerization, giving rise to “comets” in microscopy. While polymerization speed is largely constant, as long as a critical concentration of tubulin subunits is maintained, catastrophe and pausing events are more highly regulated. Catastrophe is the rapid disassembly of a MT. The polymerization speed, pausing rate, and comet-lifetime, which is inversely proportional to the catastrophe rate, are the main factors for analysing MT dynamics. Catastrophe starts from the plus-end and can dissolve the MT

completely, or stop at stabilized positions along the MT (Tropini et al., 2012). MT stability is orchestrated via the nucleotide binding state of the tubulin subunits, as well as post-translational modifications (PTM). When incorporated, ß-tubulin subunits are guanosine triphosphate (GTP) bound. These more stable subunits form a protective cap at the end of the MT, protecting it from catastrophe. Only later on, the GTP in ß-tubulin subunits hydrolyse to the less stable GDP bound state. This change in the bound nucleotide leads to a change in the spatial conformation, weakening interactions between protofilaments and therefore causes a disruption of the MT structure. As for stability modifying PTMs, acetylation at lysine residue 40 (Hubbert et al., 2002; Piperno et al., 1987) as well as detyrosination are associated with higher stability, while tyrosination is viewed as a marker for more dynamic MT (Webster et al., 1987). Interestingly, tyrosination is required for branching in both DRGs and cortical projection neurons (Barnat et al., 2016; Ziak et al., 2024), underlining our view of branching and growth as being at least somewhat in opposition to each other. Detyrosination has also been shown to be essential for the correct formation of neural circuitry. The main detyrosinating enzyme is tubulin-tyrosine-ligase (TTL). Knock out of TTL is embryonic lethal and leads to cortical malformation, highlighting the importance of post-translational modifications for microtubule integrity and correct neural development (Erck et al., 2005).

MT dynamics are furthermore modified by MT associated proteins (MAP). While the term MAP lacks separation precision and is often applied to all kinds of proteins that interact with MT, such as the aforementioned nucleating factors or motor proteins that traffic cargoes along the MT, here we refer to MAPs mainly as those proteins, that affect MT stability or bundling. For example, the Alzheimer's disease related protein tau, has been shown to be involved in the bundling of MT (Biswas and Kalil, 2018). Other MAPs involved in bundling in axons are MAP1B, which has been implicated in growth and branching of DRGs (Bouquet et al., 2004) and Tripartite motif-containing protein 46 (Trim46), which bundles correctly oriented MT in the axon initial segment, thus reinforcing axonal identity (van Beuningen et al., 2015). Bundling further stabilizes MT. Another way to destabilize MT are severing enzymes, the most prominent of which are Spastin and Katanin. Interestingly, these preferably cleave MT at stabilized positions (Lacroix et al., 2010; Sudo and Baas, 2010), creating two less stable filaments post-cleavage and thus appear as a key regulator of MT stability.

Cytoskeletal crosstalk

The crosstalk between actin and MT allows for cellular morphogenesis. I have already discussed how a dense actin mesh hinders the progression of MT. However, actin in combination with ABPs and MAPs can also contribute to the bundling and guidance of MT. The ABP Drebrin for example also binds EB3, pulling elongating MT into dendritic spines (Merriam et al., 2013), links actin filaments to MT in the formation of filopodia which turn into neurites (Poobalasingam et al., 2022), and positions MT correctly for the delivery of membrane components in astrocytes during scar formation in traumatic injury (Schiweck et al., 2021). Another plus tip interacting protein that guides MT specifically in the axon is Navigator 1 (NAV1). It crosslinks nonpolymerizing MT to filamentous actin in actin-rich domains of the growth cone and thus stabilizes the MT array, contributing to axon guidance (Sanchez-Huertas et al., 2020). Microtubule Actin Cross-linking Factor 1 (MACF1) is a giant scaffolding protein, which binds both actin filaments and MT, organizing the structure of the actin mesh and facilitating proper neuronal development (Salem and Fecek, 2023). Another prominent protein facilitating cytoskeleton crosstalk is tau. Having both actin and MT-binding domains, it acts as a molecular linker and facilitates the growth of actin filaments along MT (Elie et al., 2015), enabling MT bundling in the process (Biswas and Kalil, 2018).

There are many more proteins that link actin and MT structures and their crosstalk is tightly regulated and dependant on cell types, developmental stages and disease states (Dogterom and Koenderink, 2019). This summary is intended to give an indication of how complex the neuronal cytoskeleton is and how two systems that are often regarded as static scaffolds dynamically interact to steer and enable cellular processes.

Signalling molecules

With this many moving pieces, a system as complex as the neuronal cytoskeleton must be tightly regulated. Here, I will elucidate some of the signalling cascades that unravel inside the cell. The extracellular triggers for these signalling cascades will be focus of the next chapter.

If the cytoskeleton is the main effector of cellular morphology, Rho family GTPases are the conductor of the cytoskeleton (Fig. 2). Three main protein sub-categories within the Rho family modify the cytoskeleton at different stages of cellular polarization. These are isoforms of Rho, Rac, and Cell division control protein 42 homolog (Cdc42). Interestingly, Rho and Rac/Cdc42 act in an antagonistic manner, i.e., pathways that are inhibited by Rho

are activated by Rac/Cdc42 (Stankiewicz and Linseman, 2014). This allows for fine-tuning of cytoskeletal dynamics, by modulating Rho and Rac/Cdc42 activity. Indeed, all three members of the Rho family GTPases have been implicated in axon guidance and generation as well as arborization of dendrites (Threadgill et al., 1997).

Rho activates p38 Mitogen-activated Protein Kinase (p38Mapk) (Zhang et al., 1995), c-Jun N-terminal Kinase (JNK) (Teramoto et al., 1996) and Rho-associated coiled-coil-containing protein kinases (ROCKs) (Schmandke et al., 2007). While p38Mapk and JNK affect mainly transcription -which also might signal back onto the cytoskeleton- and facilitate Rho's role in cell survival, ROCKs are more directly upstream effectors of the cytoskeleton. ROCKs activate phosphatase and tensin homolog (PTEN), which, incidentally, has been shown to be a major suppressant of axon regeneration (Park et al., 2008) and is an upstream inhibitor of RAC-alpha serine/threonine-protein kinase (AKT) (Stankiewicz and Linseman, 2014). AKT, via the inactivation of MT destabilizing factors including GSK3ß, enables MT stabilization (Kim et al., 2022). Interestingly, stabilization of MT can further activate AKT via an AKT/dynactin p150 complex which localizes to stable MT, thus offering a feedback mechanism for MT stabilization (Jo et al., 2014) Additionally, by phosphorylating Cyclase-associated protein 1 (CAP1), AKT modifies actin dynamics (Vandermoere et al., 2007; Zhou et al., 2014). Furthermore, by hindering the expression of cell death genes, AKT contributes to neuronal survival (Brunet et al., 2001). Thus, the inhibition of AKT via Rho family proteins hinders axon growth. Recently, our laboratory provided data that the effects of RhoA activation differ between cell types. In neurons, RhoA activation via CSPGs lead to activation of Myosin II which compacts actin, thus blocking MT protrusion in growth cones. In astrocytes, however, such RhoA activation was shown to inactivate Yes-activated protein signalling via actin compaction, but independent of MT.

Rac and Cdc42 activate Phosphatidylinositol-4,5-bisphosphate 3-kinase (PI3K), which transfers signals via phosphorylated lipids, activating AKT. Interestingly, some forms of lipid-phosphorylation also serve as an activator of Rac, thus enabling signal feedback (Campa et al., 2015). Another avenue for signal amplification is Rac activation of p21-activated kinases (PAK) (Johnson and D'Mello, 2005), which is also activated via the PI3K pathway (Thillai et al., 2017). PAK then activates extracellular-signal regulated kinases (ERK). ERK activation is beneficial to neuronal survival (Ley et al., 2003) and is involved in axon growth and axon guidance (Hausott and Klimaschewski, 2019). Interestingly, however, ERK activation destabilizes MT, at least in tumour cell models (Harrison and Turley,

2001). While it is unclear, that this holds true in neurons, this poses another fascinating regulatory mechanism for the stability of dendritic and axonal MT. Per Harrison and Turley, the destabilization of MT via ERK is dependent on the G-protein Ras, which in neurons localizes to the soma and dendrites, but not axons (Pierret et al., 2001). Thus, ERK might serve to reenforce axon identity by destabilizing the MT network of non-axonal neurites.

Concluding, the neuronal cytoskeleton is a highly regulated ever dynamic system, influenced by a long list of proteins, which regulate cell morphology. Together, they enable the neuron to define and grow axons and dendrites and navigate the extracellular environment to establish functional circuitry. To achieve this, the interplay of extracellular and intracellular signalling is indispensable.

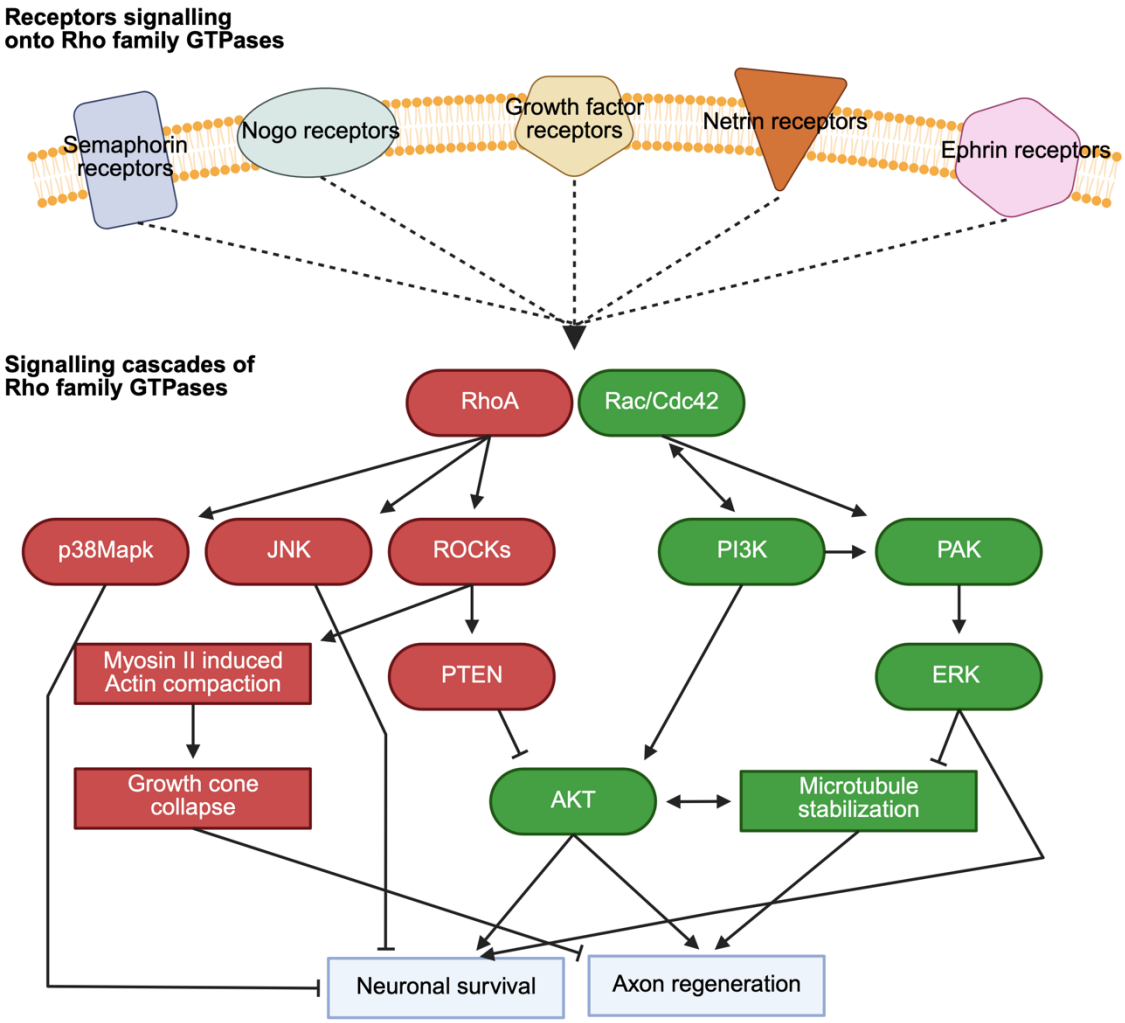

Figure 2: Overview of Rho family GTPase protein signalling cascades.

Overview of selected key up and downstream interactors of Rho family GTPases and their effect on neuronal survival and axon growth and regeneration. Dashed arrows indicate signalling onto Rho

GTPase family proteins and can be both activating and inhibitory, depending on the exact receptor makeup and receptor-ligand interaction. Solid lines indicate activation (arrows) or inhibition (blunt ends) and are mostly indirect interaction, via intermediate phosphorylation targets. RhoA and Rac/Cdc42 act antagonistic to each other. While the activation of Rac/Cdc42 leads to the downstream activation of AKT, which activates axon growth and regeneration, activation of RhoA leads to the downstream inhibition of AKT and growth cone collapse, hindering axon regeneration and neuronal survival.

Axon guidance during development via extracellular cues

A newly formed axon must navigate a complex and ever-changing environment to reach its target area and successfully integrate into the neural circuitry. As discussed above, at the same time, the cell body might also be migrating through different brain regions. Accordingly, the cell needs to sense its environment, while the environment must communicate to the cell where it is and where to go. The cell's sensing organ is the growth cone, while the ECM communicates via extracellular cues (Alfadil and Bradke, 2023). Axon guidance is a fine balance of attractive and repulsive cues. When a growth cone senses a cue, that information is relayed to the cell via the signalling cascades affecting the cytoskeleton discussed above.

Guidance cues can be broadly categorized into long- and short-ranged. Long-range cues are secreted by cells distal from the tissue they affect. They include diffusible factors such as neurotrophins, growth factors, and ephrins, as well as ECM molecules like laminin. Short-range cues operate within the local environment and are consequently expressed at key points in development where special guidance is require, such as turning points (Dorskind and Kolodkin, 2021; Myers et al., 2011; Stoeckli, 2018). Interestingly, some molecules can function both as long- and short range cues, depending on their secretion levels (Simpson et al., 2000). This introduces a key principle in axon guidance, concentration gradients. Gradients confer directionality by attracting or repulsing a growth cone evermore, the deeper into the gradient it penetrates. For example, the Netrin and sonic hedgehog (Shh) gradients at the floorplate of the spinal cord attracts commissural axons towards the ventral midline (Sloan et al., 2015). From this turning point, another gradient emanates, a slit gradient, that repulses axons (Farmer et al., 2008). This exemplifies another key feature of axon guidance, differential responsiveness to extracellular cues. While initially, the commissural axons are attracted by Netrin and Shh and non-responsive to slit, at the floor plate they alter their growth cone receptor pattern, which makes them repelled by slit, while becoming less responsive to the formerly attractive cues (Sabatier et al., 2004).

A major family of guidance molecules are netrins. They act as both long- and short-range cues and direct growth in the spinal cord and brain. Interestingly, netrins can be both attractive and repellent cues, depending on the receptor pattern on the growth cone. Netrin-1 attracts axon that present deleted in colorectal carcinoma (DCC) but repels those which present Netrin receptor Unc5, while different ratios between the two receptor types can fine tune axon guidance (Kruger et al., 2004). Via interactions with cell membranes and

ECM molecules, netrins have also been proposed as mechanotransductive guidance molecules (Boyer and Gupton, 2018).

Semaphorins are a family of major repulsive cues and are among the first repulsive cues to be identified (Kolodkin et al., 1993; Luo et al., 1993; Raper and Kapfhammer, 1990). This family, spanning more than 20 proteins, is involved in axon guidance in the brain and spinal cord, as well as regulation of cellular morphology in the cardiovascular, immune and reproductive system, the liver, kidney, lungs and muscles (Alto and Terman, 2017). Semaphorins consist of soluble, GPI-anchored or transmembrane proteins which are defined by a sema domain. These domains are also present on their main receptors of the neuropilin and plexin families and facilitate the ligand-receptor interaction (Lu et al., 2021). That interaction then signals onto RhoA, to modulate axon growth and cell motility via modification of the cytoskeleton (Sun et al., 2012). Astonishingly, Semaphorins are such a dominant repulsive cue, that they repel even highly growth competent conditioned DRG axons and have consequently been theorized as a major restricting factor in spinal cord regeneration (Pasterkamp et al., 2001).

Ephrins are a fascinating group of short-range cues. They are membrane-bound, largely to neuroepithelial and neuronal progenitor cells during development and to neurons and astrocytes in the adult (Homman-Ludiye et al., 2017; Stuckmann et al., 2001). They interact with Eph receptors which are often expressed on the same cell types. Upon contact of Ephrin- and Eph-expressing cells, a bidirectional signalling cascade is initiated, meaning both cells receive a stimulus that can be attractive or repulsive (Egea and Klein, 2007). This positions Ephrin-Eph interactions as a feedback tool in neural development, facilitating intra-cell-type crosstalk. Indeed, Ephrin-Eph signalling defects have been linked to neurodevelopmental disorders, neurodegenerative disease as well as intellectual disability (Rasool and Jahani-Asl, 2024). In neurons, Epherin-Eph singling relies on Rho family GTPases to modify integrin-based cell adhesions (Davy et al., 1999; Davy and Robbins, 2000) and rearrange tissue organization via actomyosin contractility (Kindberg et al., 2021).

With the human brain being the most complex structure in the universe, allegedly, hundreds of different types of neurons, originating from different areas of the brain, targeting yet again different areas, need to find their way in a pretty much exactly predetermined fashion. Having introduced five families of cues, merely scratches the surface of an immense group of molecules that facilitate pathfinding. However, having to guide around 80 billion neurons, instructing them to correctly form billions of synapses, the question

arises, how a significantly smaller number of guidance cues accomplishes that task? Afterall, the human genome contains only around 19.000 protein coding genes (Ezkurdia et al., 2014) and even while one gene can give rise to multiple proteins, and not all forms of axon guidance are based on proteins -discussed in a later chapter- (Sheng et al., 2022) , it becomes highly unlikely that each different class of cells has one specific guidance cue to follow. Evidentially, each class of neuron presents a unique combination of receptors, tailored to its specific environment and intended path. This pattern of pathfinding molecules than dynamically responds to the cues it encounters *en route* and over time, changing its responsiveness to precisely arrive at its final destination (Stoeckli, 2018). Cumulatively, axon guidance is a highly orchestrated spatiotemporal procedure which is fine-tuned by different cues, receptor and mechanical properties of the neural tissues. Deciphering all levels of this cacophony of interplaying systems will require further research, but enrich our understanding of neural circuit formation and likely present new therapeutic approaches to neurodegenerative and neurodevelopmental disease, as deeper knowledges of the processes involved in growth, will open new avenues to hinder inhibition and bolster beneficial pathways.

The Tedeschi paradigms of dorsal root ganglion axon regeneration

In this thesis, I reapply an approach, that has been successfully utilized by our group previously, based on the work of Andrea Tedeschi. It employs three paradigms of DRG axon regeneration, in which the neurons can be observed to be in one of the two following states, either high-growth-low-branching or low-growth-high-branching (Fig. 3A) (Tedeschi et al., 2016). For the purposes of this thesis, we view the two processes of growth and branching as mutually exclusive. By comparing different molecular programs, that result in a similar morphological phenotype, we pose that molecules that behave the same in all three paradigms, are causally related to the morphological phenotype of the cell (Fig.3 B). Why use three paradigms though, if one could also focus their attention on only one? Briefly, a growing cell, be it regenerating or developmentally growing, goes through a myriad of changes all at once. When comparing for example the transcriptome of our first paradigm, embryonic DRGs in mid and late gestation, more than half the detected transcripts (11.000/20.874) significantly change their expression levels (Tedeschi et al., 2016). Distinguishing which genes are involved in the establishment of cell morphology versus other concurrent processes, for example angiogenesis, becomes sheer impossible. Consequently, identifying the overlap between three similar but distinct paradigms, provides a way to thin out the data and remove processes which might be relevant in one paradigm, e.g., angiogenesis in an embryo, which is fully absent in our cell culture model. In the following, I will elucidate the three paradigms which are based on Andrea Tedeschi's work and thus termed the Tedeschi paradigms.

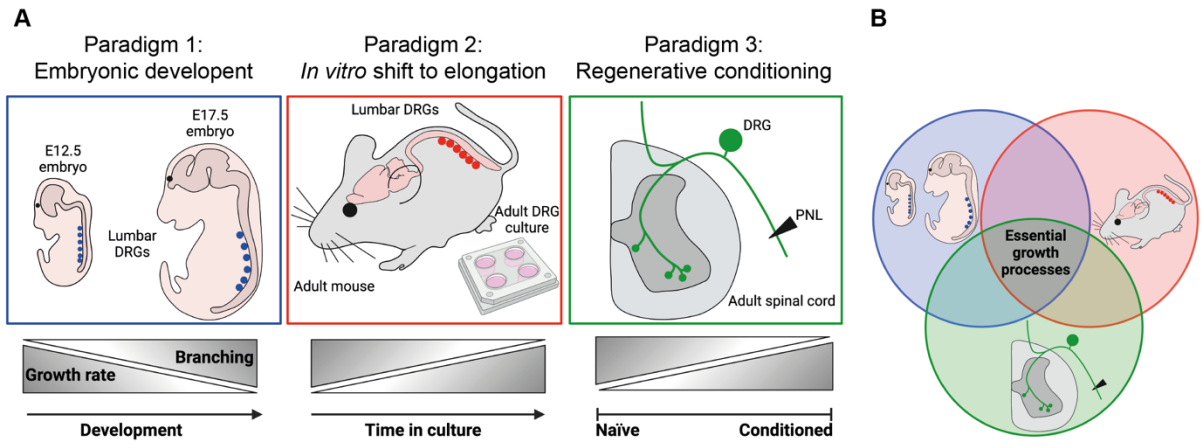

Figure 3: Overview of the Tedeschi axon growth paradigms.

(A) Schematic representation of the Tedeschi paradigms and their axon growth behaviour. All three paradigms have a high-growth-low-branching state and a low-growth-high-branching state, between

which they transition during development, over time in culture or following a peripheral nerve lesion (PNL). (B) Schematic representation of the logic of the paradigms. Comparing morphologically similar but molecularly distinct paradigms allows for gene prioritization.

Paradigm 1: Embryonic DRG neurons in mid and late gestation

In paradigm 1, we compare embryonic lumbar DRGs from mid gestation, embryonic day (E) 12.5, with those from late gestation E17.5. The dorsal root ganglion starts to be formed around E8.5, with the ventral migration of neural crest cells (NCC) from the neural tube (Serbedzija et al., 1990). Once reaching the intersomitic area, the NCCs will differentiate both into the neural precursors as well as the glial cells of the dorsal root ganglion (Teillet et al., 1987). Beginning at E12.5, the axons of the newly differentiated DRGs, penetrate into the spinal cord (Honma et al., 2010). At this point, they need to migrate up the spinal cord to synapse onto neurons of the dorsal horn. Consequently, as the DRG axons need to cover quite some distance, their molecular program is primed on growth, while downregulating branching (Tedeschi et al., 2016). Later on, once the axons reach the dorsal horn, they need to establish functional connections. Synapses within the spinal cutaneous reflex arc could be detected starting from E14-16 (Vaughn et al., 1975). Accordingly, at E17.5, our late gestation time point, the axons of the DRG are already well into a molecular synapsing program, while downregulating growth, as to not grow beyond their target area (Tedeschi et al., 2016). As the onset of synapse formation acts as a molecular off-switch on growth (Hall and Sanes, 1993; Hilton et al., 2022), and it stands to reason that higher DRGs, e.g., cervical compared to lumbar DRGs, reach their targets earlier in development, we focussed our studies on lumbar DRGs, which should be in roughly similar developmental stages.

In summary, in early gestation, DRG axons need to focus all their growth potential into elongating growth, to reach their targets and not form ectopic branches. Once they have reached their target area, they downregulate growth, to focus on branching, which is necessary to form their functional circuits. Our early timepoint E12.5, represent the very early onset of axon growth, when the molecular machinery should be most primed for growth, while the later timepoint E17.5 is already deep into synapse formation with a major focus on branching.

Paradigm 2: Adult DRG neurons in cell culture

Adult neurons are in a constantly growth inhibited state. This is also true for the neurons of the second Tedeschi paradigm, the adult lumbar DRGs in cell culture. Upon plating, DRG neurons rely on a translation-dependent switch to shift from arborizing to elongating

growth. This shift is inhibited by retrograde trafficking of a yet elusive signal from the axon tip (Smith and Skene, 1997). It has been hypothesized that one of the cues hindering elongating growth in DRG neurons is synaptic activity (Enes et al., 2010; Hilton et al., 2022; Tedeschi et al., 2016). This gives rise to the following model: An adult DRG physiologically is connected to its synaptic partners in the CNS dorsal horn as well as peripherally in muscles, internal organs and the skin. Their synaptic activity leads to the trafficking of an inhibitory signal from the axon tip to the cell body. Upon preparation of the dorsal root ganglia and consequent plating of the DRGs, these connections are severed. The growth-inhibitory signal is no longer being trafficked to the soma, which activates a translation-dependent switch, starting the transition of the transcriptome and proteome to growth competence. As more and more of these changes occur, the growth rate increases over time, while branching decreases, thus inversely mirroring the transition from embryonic development. In fact, the transcriptomic profiles of DRGs reverts back to a more embryonic state over time in culture (Hilton et al., 2022; Tedeschi et al., 2016). Accordingly, in this paradigm, we compare neurons at 6 h and 36 h post plating. Here, 6 h represent the molecular program before the translational switch goes into effect and 36 h representing the proteome of neurons that have reverted to a more embryonic, growth-competent state.

Paradigm 3: Adult DRG neurons after regenerative conditioning

One outstanding feature of DRGs is their capacity to regenerate, even in the CNS. Physiologically, DRGs, like other neurons, do not regenerate within the CNS. However, upon a preceding injury to their peripheral nerve, they can overcome the growth inhibition of the CNS and the glial scar, and also regenerate the central branch (Richardson and Issa, 1984). This process, called “conditioning”, is one of the most powerful tools in axon regeneration research, because it allows for functional regeneration into and beyond the lesion site, in the CNS (Neumann and Woolf, 1999). Briefly, the DRG cell body resides in the dorsal root ganglion, adjacent to the spinal cord. It extends an axon, that promptly bifurcates, targeting one arm into the spinal cord and one into the periphery. L3-6 extend their axons into the sciatic nerve. For its easy accessibility, it has become a common experimental model for peripheral lesioning. The sciatic nerve is exposed at mid-thigh level, tied off, to hinder it from reattaching with its distal end, and then transected (Fig. 4A) (Hilton et al., 2019). Is this peripheral nerve lesion (PNL) performed previously to a central nerve lesion, for example a SCI, the conditioned neurons are already in a growth competent state and

can regenerate through the lesion, overcoming CNS growth inhibition and passing the lesion before the glial scar forms an inhibitory barrier. Interestingly, is the PNL performed after the CNS insult, the neurons still intrinsically acquire growth competence, which is hindered by the glial scar, but would allow for regeneration in a minimal scar environment (Ylera et al., 2009).

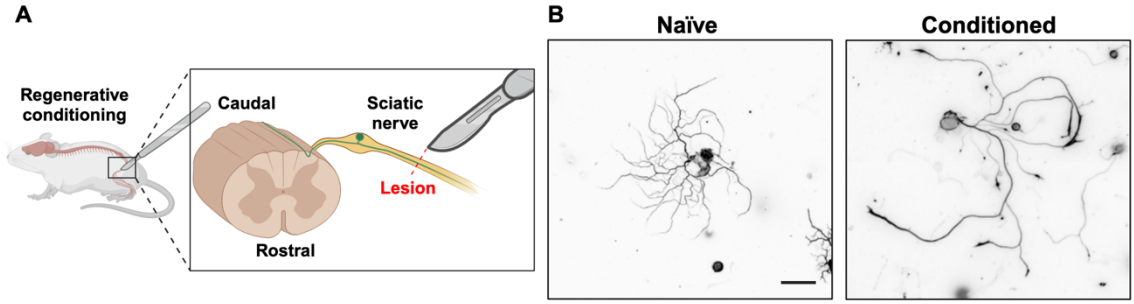

Figure 4: Overview of the regenerative conditioning lesion.

(A) Schematic view of the peripheral nerve lesion surgery. The sciatic nerve is, in part, innervated by L3-6. It is exposed via incision at mid-thigh level, sutured off and transected. (B) Representative images of naïve and conditioned DRG neurons 16 h post plating. ßIII-tubulin staining. Scale bar 75 µm.

When transferred to cell culture, this enhanced growth state of the conditioned DRG is reflected in a characteristic growth pattern. While naïve DRG neurons are basically the same as the earlier time points of paradigm 2 and similar in morphology to late gestation embryonic DRGs, the conditioned DRGs grow long axons with few branches, thus mirroring the early embryonic DRGs as well as the late time points of paradigm 2 (Fig. 4B).

In summary, we employ three growth paradigms, which produce the same morphological phenotype, via similar but distinct molecular patterns. Investigating the differences and overlap between these three paradigms, allows us to more deeply understand axon growth and regeneration.

Failure of axon regeneration after spinal cord injury

The spinal cord and spinal cord injury

The spinal cord and brain form the CNS (Fig. 5A). Its neuronal tracts are protected in the spinal canal within the spinal vertebrae. Its nerves connect to the PNS to transmit motor, sensory, and reflex signals. Motor signals descend down the spinal cord, originating from the brain, reaching neuromuscular junctions via multi-synaptic circuitry. Sensory information is communicated from receptors in the periphery ascending to the brain (Purves, 2018). Finally, reflexes originating from the limbs and many internal organs are processed directly in the spinal cord vial spinal reflex arcs, bypassing the brain entirely for faster response times. Anatomically, the spinal cord is segmented according to the spinal vertebrae. The number of spinal vertebrae varies between species and in mice within strains. Humans present 31 vertebrae (Fig. 5B), while mice have 25-30, depending on the strain (Sengul and Watson, 2012). Broadly, the vertebrae are categorized by their anatomical environment and labelled descending from the skull. In human there are 8 cervical, 12 thoracic, 5 lumbar, and 5 sacral nerves, in mice these numbers slightly vary and are supplemented by 7 to upwards of 30 caudal vertebrae depending on age (Matsuura et al., 1997).

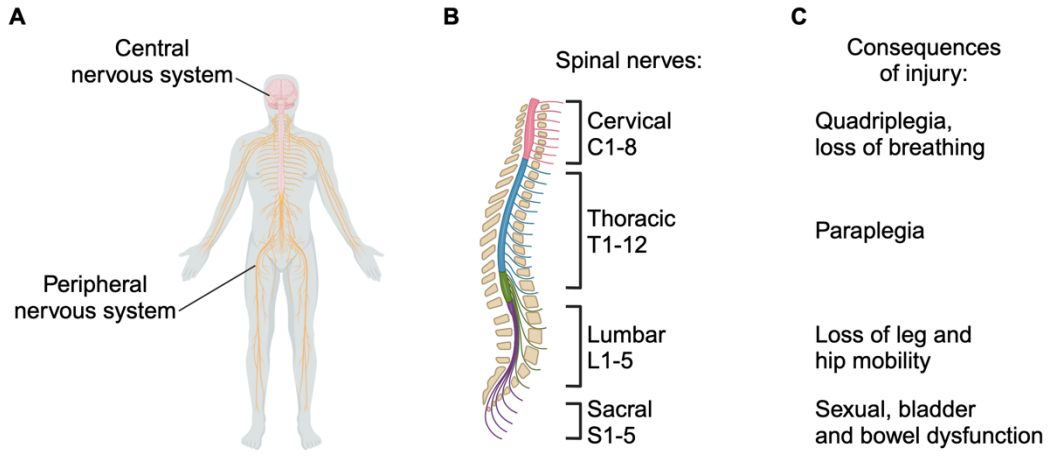

Figure 5: Overview of the architecture of the human spinal cord and consequences of injury dependent on spinal level.

(A) Gross architecture of the human central and peripheral nervous system. (B) Segments of the spinal cord according to the spinal nerves. (C) Consequences of spinal cord injury dependent of the spinal level.

Each vertebra is associated with a dorsal root ganglion, which emanates from the lateral dorsal side of the spinal cord. As discussed above, these ganglia, via their associated neurons and axons, form one of the connections from the PNS to the CNS. Severing these connections disconnects the brain from the PNS, leading to permanent disruption of motor, sensory, and reflex function. Around 1.000.000 people suffer SCIs every year, with falls and road injuries being the major causes, except in conflict-affected areas, where violent causes predominate (Guan et al., 2023). Which functions are lost depends of the injury level and severity (Fig. 5C). Complete transection terminates all function below the lesion site. A low-level transection in the sacral area leads to a loss of voluntary bladder and bowl function, a loss of sexual functions and some loss of function in hips and legs, however, walking can often be restored in such patients. In lumbar injuries, loss of hip and leg mobility is more severe, and unassisted movement becomes less likely, with the other restrictions persisting. Injuries in the thoracic area most likely result in paraplegia, the full paralysis of the lower libs, but trunk mobility and balance, as well as self-sufficient breathing are typically maintained. Cervical transections pose the highest burden, combining all the aforementioned restrictions, while being accompanied by full quadriplegia, i.e., loss of all limb function and trunk mobility, and a loss of the ability to breathe unassisted (Alizadeh et al., 2019). As of yet, there are no curative therapies available to patients of SCI. While rehabilitation can lead to the restoration of some motor function, it relies on the availability of spared neurons to form secondary circuitry. Pharmacological interventions, such as epothilones, Nogo inhibitors or chondroitinase, as well as surgical interventions, including grafts, implantation of biomaterials and stem cell transplantation, this far show only small effects in animal models and phase II clinical trials. Consequently, there is still a need for the discovery and development of novel SCI treatments. Likely, any successful therapy will involve a combinatory approach to multiple facets of SCI (Griffin and Bradke, 2020).

SCIs are complex traumatic insults to the nervous system, disrupting a myriad of cellular processes, whose rebalancing is vital to successful regeneration. Initially, an injury to the neural tissue causes the death of neurons, astrocytes, microglia and oligodendrocytes as well as the disruption of the vascular system. This releases damage associated molecules such as interleukins and ATP, which activate surrounding glial cells, recruit circulating immune cells, and prompt stromal cell proliferation. Within hours to days after injury, macrophages and microglia polarize towards the lesion site, while releasing extracellular matrix (ECM) components, thus stabilizing the lesion border. This creates an increasingly

proinflammatory and growth inhibitory environment. This roughly coincides with the onset of axonal degradation. In the following weeks, reactive astrocytes further wall off the fibrotic core of the lesion site, enriching the environment in inhibitory factors like Nogo and CSPGs, while ongoing axonal degeneration and the associated axonal and myelin debris reinforces the inflammatory environment. Thus, a chronic scar forms which poses both a physical barrier, via the glial border, as well as a growth inhibitory one (Bradbury and Burnside, 2019).

Inhibitory molecules

Above, I have listed some of the major inhibitory molecules. Here, I will elaborate them in more detail and summarize strategies to overcome them in a therapeutic setting.

CSPGs are ECM proteoglycans. They consist of a core protein, which is bound to glycosaminoglycan (GAG) chains. In the nervous system, six types of CSPGs predominate. The four Lecticans: Versican, Aggrecan, Neurocan, and Brevican, as well as Phosphacan and neural antigen 2 (NG2). While they all have slightly different interactions with axon repulsion and guidance at different stages of development and areas in the nervous system, they all inhibit axon growth via chondroitin sulfate moieties in their GAG chains (Bandtlow and Zimmermann, 2000; Iseki et al., 2012). These activate cell surface receptors, such as protein tyrosine phosphatase sigma, leukocyte common antigen related phosphatases, and, interestingly, Nogo receptors, which trigger signalling cascades that activate Rho family proteins, while inactivating the PI3K/AKT pathway (Sharma et al., 2012). Additionally, it has been speculated that CSPGs sterically inhibit ECM interactions, thus decreasing the ability of axons to adhere to their substrates (Tan et al., 2011). Because the inhibitory effect of all neuronal CSPGs is largely dependent on their GAG side chains, GAG digesting enzymes have been a focus of neural regeneration research. Chondroitinase ABC (ChABC) has been shown to effectively digest GAG side chains *in vivo*, prompting functional regeneration in rodent models (Bradbury et al., 2002). A clinical study in canines also found a modest yet significant improvement of limb coordination following SCI (Hu et al., 2018). Clinical studies in humans are yet to be published.

Nogo proteins are among the first identified inhibitors of axon growth (Caroni and Schwab, 1988b). The main axon growth inhibitory isoform being NogoA. Interestingly, NogoA is mainly an intracellular protein, localizing to the endoplasmic reticulon (GrandPre et al., 2000). However, domain Nogo-66, a 66 amino acid (AA) loop within the

Nogo protein, can be exposed on the surface of oligodendrocytes in the adaxonal membrane. Here, it interacts with Nogo-66 receptor to facilitate growth inhibition, via growth cone collapse (Wang et al., 2002). Again, the activation of Nogo-receptors leads to the activation of the RhoA/ROCK pathway and thus to the inhibition of axon growth. Blocking the interaction with Nogo-receptors via antibodies was one of the earliest approaches to combat the growth inhibition of NogoA (Caroni and Schwab, 1988a). Recently, a clinical phase 2b study reported no significant increase in their primary outcome measure of upper limb mobility in human patients of SCI, however, secondary outcome measures indicated potential beneficial effects, warranting further study (Weidner et al., 2025). It has been reported that Nogo antibody treatments are most effective in laboratory models in combination with ChABC delivery (Zhao et al., 2013), according clinical studies, however, are yet to be conducted. Another approach to lessen Nogo inhibition are pharmaceutical Nogo-receptor agonists. One such compound, AXER-204, has recently been shown to be well tolerated in SCI patients, now awaiting studies of functional recovery (Maynard et al., 2023).

The developmental guidance molecules of the Semaphorin family belong to the category of myelin associated growth inhibitory molecules. As discussed above, semaphorins are imperative in the correct guiding and targeting of axons during development. They are expressed from neurons, oligodendrocytes, astrocytes, and meningeal cells, which secrete them, forming a repulsive gradient (Carulli et al., 2021). Via their receptors neuropilin and plexin, semaphorins trigger cytoskeleton remodelling via Rho and Hippo pathways. Interestingly, semaphorins have also been detected within extracellular vesicles (EVs), which could be shown to affect neural stem cell migration (Manini et al., 2019). Such EVs also carried a micro-RNA, miRNA-22, which regulates the expression of a semaphoring family protein, Semaphorin 4C, affecting motor neuron pathfinding (Sheng et al., 2022). Therapeutically, a small-molecule inhibitor of Semaphorin 3A, SM-216289, was found to attenuate repulsive cues and accelerate axon regeneration in the olfactory nerve (Kikuchi et al., 2003) and stimulated growth of neuropilin-1-expressing serotonergic axons following SCI in rats (Kaneko et al., 2006). Clinical trials of this or other small molecules targeting semaphorins, however, are not reported.

I have summarized here some of the key molecules that inhibit axon growth, their origins, mechanisms and curative approaches targeting them. Currently, no treatment targeting growth inhibitors has led to real translational success in human patients. It is clear that the problem of failing to regenerate is multifactorial, consequently, it stands to reason that a

cure would also need to target multiple pathways. Combinatory treatments show great promise (Griffin and Bradke, 2020; Zhao et al., 2013), but also challenges in for example cumulative toxicity. How to functionally recover the spinal cord will be focus of research for the foreseeable future.

Rehabilitation to alleviate symptoms of SCI

Rehabilitation is currently the major therapeutic approach to regain function following SCI. The effects of rehabilitation are multilevel, affecting brain circuitry and different spinal cell types as well as axon regeneration. On the brain level, rehabilitation leads to increased secretion of neurotrophic factors (Graziano et al., 2013) and structural remodelling of the cerebral cortex circuitry responsible for limb movement. This remodelling is in part necessary due to the death of neurons in the somatosensory and motor cortex (Freund et al., 2013; Jurkiewicz et al., 2006), but also a consequence of the enhanced plasticity conferred by rehabilitation (Jurkiewicz et al., 2007). Secondary circuits are also established in the spinal cord. Spared axons can sprout new branches, forming circuits bypassing the lesion, bridging the gap from disrupted axons, thus leading to functional recovery following SCI (Hansen et al., 2016; Hollis et al., 2015). Rehabilitation, furthermore, triggers molecular changes in neurons. Environmental enrichment, as a form of rehabilitation, modifies histone acetylation, boosting growth on an epigenetic level (Hutson et al., 2019).

It is important to note, however, that not all rehabilitation is equal. Different modes of training lead to different outcomes. Girgis *et al.* reported that training rats in a grasping task did increase their ability to perform that task, but worsened performance in horizontal ladder testing (Girgis et al., 2007). More recently, a systemic review found limited and inconclusive evidence for task specific training positively affecting non-related function (Tse et al., 2018). Accordingly, while rehabilitation and the consequent establishment of secondary circuitry leads to a functional improvement, the scope of that improvement is limited; is one function emphasized, another might suffer. Consequently, there is still need for interventions that boost axon regeneration, to reconnect severed circuits, rather than bypassing them.

Proteomics as a tool to investigate cellular processes

As the previous chapters have introduced, there is a sheer uncountable number of proteins involved in the regulation of cell morphology, axon guidance and cellular functions. Those chapters have only briefly discussed the cytoskeleton and signalling mechanisms affecting axon growth. To gain a more holistic understanding of cellular processes, we employ proteomics, to evaluate a large portion of the DRG proteins at once. Proteins are the molecular engines driving almost all cellular processes. Translated from genes, proteins are polypeptides of AA subunits, covalently bonded together. The sequence of 20 different AAs, called primary structure, lays the ground-work for a protein's identity, which manifests in secondary and tertiary structure. The secondary structure describes how stretches of the sequence form basic structures, including helices, folded sheets or unfolded regions. When different secondary structures coalesce, they form tertiary structures, broadly speaking, the architecture of a protein. The correct function of a protein depends on the correct structure on all three levels (Lehninger et al., 2013).

Where multiple proteins interact, we speak of a proteome. A proteome is the sum of all proteins in a defined biological system. This can be the content of a synapse (Lassek et al., 2015), a muscle cell under stress (Bock et al., 2021), a whole liver (Niu et al., 2022), or any other distinguishable sample. The value of proteomics lies in the fact that they can be unbiased. Without previous assumptions, we can ask what changes happen during a process and then discern changes in protein level for thousands of unique proteins, which then inform the consequent research questions.

On the technical level, proteomics rely on mass-spectrometry (MS). In this technique, a mixture of proteins, like from a lysed regenerating neuron, is digested into individual peptides. Combining the knowledge about the cleavage site of the used enzymes – typically trypsin – and the sequences of known proteins, we can predict a large but finite number of possible peptides arising from the digestion. Theses peptides are now separated broadly via chromatographic methods and then measured in the mass-spectrometer. Firstly, the sample is ionized, giving it a charge. Via different methods this charge can now be detected as a ratio of mass to charge. As we know all possible peptides and their associated masses and likely charges, we can identify the peptides. However, peptides with the same AA composition have the same mass, such as two peptides with the sequence "MASS" and "SMSA". To tell these apart, individual peptides are ionized again, supplying enough collision energy to split them. The new fragments are reanalysed for their mass-to-charge-ratio. As the fragment "MA" has a different mass-to-charge-ratio than the peptide "SM",

we can decipher which peptide was the original one. This second round of MS is referred to as tandem MS or MS/MS. The abundance of each detected peptide correlates to its abundance in the sample, thus we can infer the protein levels for all detected proteins. It is important to note that some peptides can be generated from different proteins or multiple times within the same proteins, for example, because two proteins share a domain or a protein repeats a domain. Thus, only unique peptides are used to identify proteins.

Mass spectrometry is not the only unbiased "-omics" technique used in biological research. Unbiased studies in axon regeneration have thus far largely focussed on RNA sequencing (RNAseq), be it bulk (Poplawski et al., 2020; Tedeschi et al., 2016), single cell (Kim et al., 2023; Matson et al., 2022; Renthal et al., 2020) or spatial (Bielefeld et al., 2024; Skinnider et al., 2024). The main advantage of RNAseq-based techniques is the ability to amplify targets, thus lowering detection thresholds. RNAseq studies typically detect above 20.000 transcripts, which represent the lion's share of protein coding genes (Harati et al., 2014). Even recent MS-based studies detect less than half of that number (Bian et al., 2021). However, transcriptomes poorly predict the proteome (Ghazalpour et al., 2011). While the large number of detected transcripts offers a good systems overview, individual candidate proteins might show drastically different levels in the proteome as would have been predicted by the transcriptome. This positions MS-based proteomics as the better tool for candidate identification.

Glypican 1 as a modulator of extracellular signalling receptors

In the following thesis, one protein will stand out as an extraordinary activator of axon growth: Glypican 1 (Gpc1). Here, I will introduce Gpc1 as a modulator of extracellular signalling receptors and summarize its role -or the role of its homologues- in neurodevelopment.

Gpc1 is a 557 AA heparan sulfate proteoglycan (HSPG) of ca. 60 kDa before its maturation. Roughly, Gpc1 can be separated into 4 domains. An amino-terminal (N-terminal) 24 AA secretory peptide, a core protein, a heparan sulfate (HS) binding cassette of three alternating serine and glycine residues, and a 28 AA carboxy-terminal (C-terminal) Glycosylphosphatidylinositol (GPI) anchor domain (Fig. 6) (Svensson et al., 2012). It is trafficked outside of the cell where it is tethered to the PM via a GPI anchor. Upon translocation, the secretory peptide is cleaved (Pan and Ho, 2021).

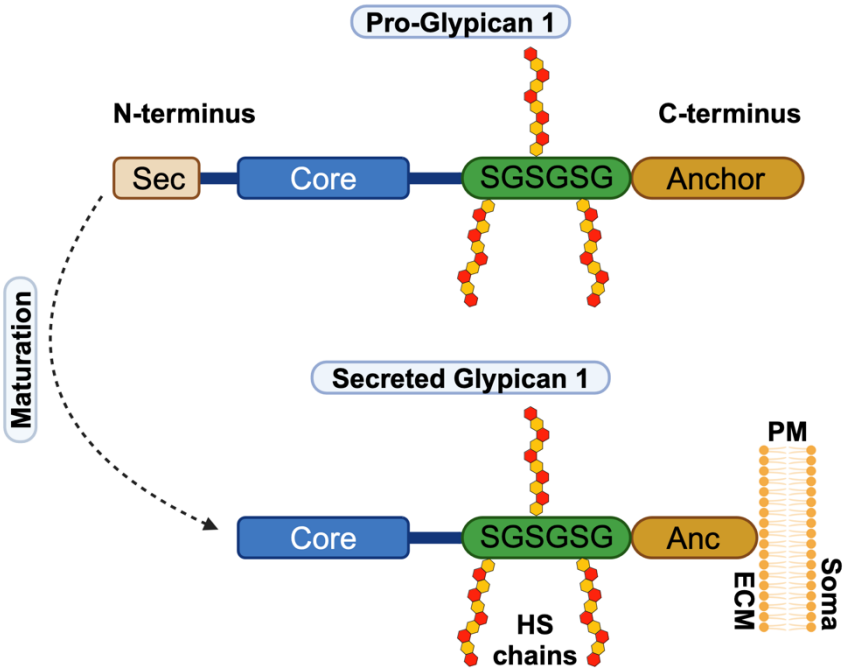

Figure 6: Structure and maturation of Gpc1.

Pro-Glypican 1 harbours a 24 amino acid secretory peptide (Sec) a core protein and a 28 amino acid anchor domain. A cassette of three alternating serine and glycine residues (SGSGSG) close to the C-terminus binds heparan sulfate (HS) chains. Upon maturation, the secretory peptide is cleaved, while Gpc1 is translocated to the plasma membrane (PM) facing the extracellular matrix (ECM). The anchor domain is partially cleaved upon tethering to the plasma membrane.

On the PM, Gpc1 interacts with various cell signalling receptors, one family of them being fibroblast growth factor receptors (FGFR). These receptors are activated by fibroblast growth factors (FGF), which are secreted glycoproteins, active in development and cell homeostasis (Guillemot and Zimmer, 2011). Gpc1 has been proposed as a coreceptor for FGFRs by sequestering FGF, thus making the receptors more receptive to lower concentrations of their ligands (Zhang et al., 2001). Interestingly, Gpc1 also facilitates secretion of FGF, offering up another mode of FGF signal amplification (Sparn et al., 2022). When activated, FGFRs trigger signalling cascades leading into, among others, PI3K and AKT pathways (Geary and LaBonne, 2018).

Similarly, another upstream activator of these pathways which is also regulated by Gpc1, is vascular endothelial growth factor receptors (VEGFR). Known primarily from their role in the development of the vascular system, VEGFR and its ligand vascular endothelial growth factor (VEGF) are also paramount in neurodevelopment (Carmeliet and Ruiz de Almodovar, 2013). Gpc1 interacts with VEGFR via its HS chains, coactivating it and facilitating receptor ligand interactions specifically for VEGF-A (Gengrinovitch et al., 1999).

Development of the nervous system is also majorly influenced by Wnt signalling, which is activated by Frizzled receptors. Wnt is an upstream regulator of GSK3ß, Rac and Rho, thus affecting cytoskeletal reorganization, as well as a regulator of target gene transcription via Ca2+/calmodulin-dependent protein kinase II (Mulligan and Cheyette, 2012). Frizzled, depending on the physiological needs of its expressing cell, forms a receptor complex with R-spondins (Lebensohn and Rohatgi, 2018), which in turn have been recently published to form tertiary complexes with Gpc1 and other Glypicans to enhance Wnt signalling (Dubey et al., 2020).

Lastly, bone morphogenic protein receptors (BMPR) and their ligands bone morphogenic proteins (BMP), besides their namesake role in osteogenesis, regulate the fate and maturation of neural stem cells. For example, a BMP gradient is imperative in the establishment of the dorsal-ventral axis in the developing spinal cord (Bond et al., 2012). Via Rac signalling, BMPs and BMPRs are involved in the development of synapses (Kim et al., 2019). Gpc1 negatively regulates BMPRs in the context of osteogenesis (Dwivedi et al., 2013). Interestingly, this interaction appears to be largely steric. Following up this finding, it was observed that recombinant Gpc1 released from titan nano tubes acted as a BMPR inhibitor, positioning it not only as a therapeutic agent, but also providing data that non-membrane-tethered Gpc1 is biologically active (Bariana et al., 2018).

Thus, Gpc1 has been shown to interact with a long but likely not exhaustive list of cell surface signalling receptors. Among this list are many known neural growth factors, activating signalling cascades established to influence axon growth. Interestingly, it also inhibits receptors involved in synapse formation, BMPRs, while synaptic activity has been shown by our group to be adverse to axon growth (Enes et al., 2010; Hilton et al., 2022; Tedeschi et al., 2016). Consequently, Gpc1 appears to be a major regulator of axon growth and neural development. This is underlined by the observation that absence of Gpc1 during development leads to malformation and aberrant patterning of the brain (Jen et al., 2009) and expression levels of Gpc1 decrease with ageing (Kato et al., 2020; Perrot et al., 2019). The fly homologue of Gpc1, Dally-like, is required for axon guidance and circuit assembly in the drosophila visual system (Rawson et al., 2005) and dysregulation of Gpc1 levels hinders the formation of the trigeminal ganglion in chick embryos (Shiau et al., 2010). Finally, Gpc1 was observed to be upregulated in DRGs following injury in the spinal cord and sciatic nerve (Bloechlinger et al., 2004).

Parallels in cell migration and axon growth

The extension of axons is remarkably similar to the process of cell migration. After all, both are about manoeuvring (a part of) the cell through the extracellular environment. Cell motility is largely driven by the cytoskeleton and, consequently, much of what we know about the cytoskeleton has been learned from the study of migrating cells such as smooth muscle cells (Tang and Gerlach, 2017), fibroblasts (Petrie and Yamada, 2015), and various types of tumour cell models (Fife et al., 2014). Smooth muscle cells, for example, receive the cues that trigger migration via G-protein coupled cell surface receptors, which signal onto ROCKs, PI3K, and Rac, among others. Towards the muscle cell's leading edge, actin polymerizers and depolymerizers become active, making the actin mesh more dynamic, while MT penetrate into the leading edge (Gerthoffer, 2008). Similarly, mouse embryonic fibroblasts rely on stable MT to penetrate into their leading edge, supporting migration, which is governed by Rac and Cdc42 (Kole et al., 2005). Conversely, fibroblasts of the spinal cord are hindered from migration upon stabilization of their MT following SCI (Ruschel et al., 2015b). This emphasises that the migration behaviour of fibroblasts is context specific, possibly to the environment or developmental stage, as it is for neurons. Stabilization of MT is also well established to hinder migration of tumour cells. Both Taxol and Epothilones were approved as cancer therapies, before our group described them as being beneficial to axon growth (Altmann et al., 2000; Martin, 1993). Interestingly, highly migratory tumours express increased levels of neuronal genes (Denny et al., 2016) and hindrance of such gene expression results in decreases in tumour migration (Wu et al., 2016). The outgrowth of metastases follows the formation of filopodia-like protrusions similar to early stages of neuronal development (Shibue et al., 2012) and specific cancers have been observed to form axon-like protrusion, which correlated with high migratory potential (Yang et al., 2019). Finally, dysregulation of the signalling mechanisms which govern axon growth and maturation is also associated with tumorigenesis. All signalling receptors I summarized in the context of Gpc1 and axon growth, also have major associations to cancer (Pan and Ho, 2021). Furthermore, Gpc1 itself is upregulated in liver, pancreatic, colorectal, prostate, and breast cancer (Cao et al., 2024) and high levels of Gpc1 expression correlate with a poor clinical prognosis, for its strong correlation with tumor size and tumor-node-metastasis (Chen et al., 2020). In conclusion, cell migration and axon growth both rely on the cytoskeleton and are activated by the same signaling cascades. Especially in cancer cell migration those parallels become obvious, as what is good for axon growth, is often also beneficial for cancerous growth.

Results

The aim of this study was to investigate the proteome of growing and regenerating DRG neurons to find novel modulators of axon growth and regeneration. To this end, I generated proteomic data sets for the growth paradigms laid out above, developed a cell culture screening method to test for growth effects and characterized the most prominent candidate, Gpc1, with regards to its mechanism of action.

Proteomic analysis of DRG growth states

To identify novel growth modulators in DRG neurons, I set out to produce a proteomic dataset of the three different growth paradigms that our group has successfully employed in the past, to identify growth modulators from RNA sequencing data (Tedeschi et al., 2016). Briefly, embryonic ganglia, as well as conditioned and naïve adult ganglia, were harvested, and flash frozen in liquid nitrogen before lysis. Cell cultures of adult DRG neurons were harvested at the appropriate time points by scraping the cells, before pelleting and flash freezing the dry pellets on dry ice. Thus, this data set includes both whole tissue samples, as well as a culture sample. In mass spectrometry, we detected 3467, 3516 and 4415 proteins in the embryonic, cell culture, and conditioning lesion paradigm, respectively. Taken together, we detected 5674 unique proteins with 2865 of those being detected in all three paradigms. Principal component analysis (PCA) showed that the different conditions separate well within their paradigms, as indicated by non-overlapping 95% confidence intervals for each condition within a paradigm (Fig. 7A-C). Consistent with regeneration literature, RAGs including Gap43 and Sprr1a were upregulated (Fig. 7D-F). These quality control measures confirmed that we have generated a robust proteomic data set, which can be further used to investigate growth effectors in DRG neurons.

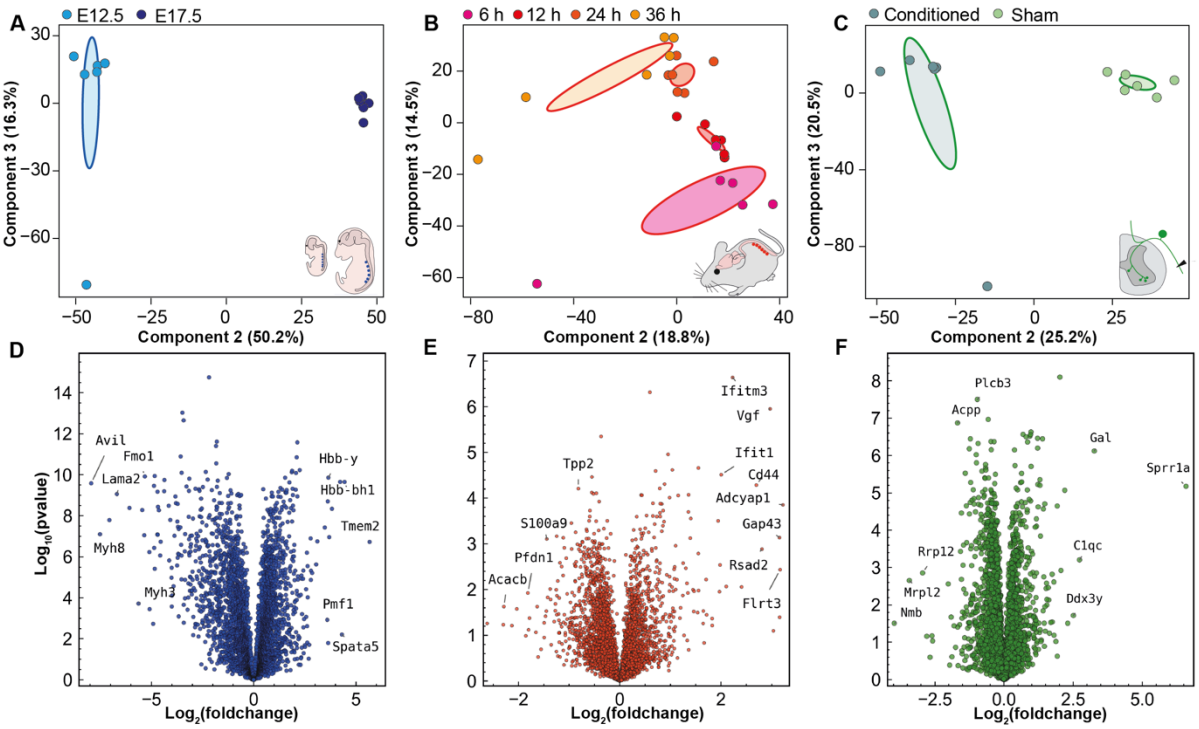

Figure 7: Quality controls of growth state proteomics.

(A-C) Principal component analysis of DRG growth states. Ellipses show 95% confidence intervals per group. (D-F) Volcano plots of detected proteins in the individual paradigms.

Gene ontology analysis of proteomic data

With an average of roughly 3.800 proteins detected in each paradigm, one way to make sense of large datasets like this is gene ontology (GO) term analysis. Briefly, GO term analysis relies on databases of genes tagged with their associated processes, molecular function and cellular localization, here called component. By comparing the abundance of a specific tag, for example the component “plasma membrane”, in the provided gene list, against the general abundance of that term in the data base or a background set, GO term analysis allows to detect statistically overrepresented tags in a list of genes of interest (GOI). In an effort to identify growth activators, I focussed on the proteins upregulated whenever neurons became growth competent. For each paradigm, the upregulated terms were collected individually and then compared to find GO terms that are upregulated in all three paradigms. This provided us with a list of 18 terms that appear essential when DRG neurons become growth competent, including “cell adhesion”, “signal transduction”, “integral component of plasma membrane”, and “extracellular matrix binding” (Fig. 8). Interestingly, hippocampal neurons have been reported to grow without reliance on extracellular matrix adhesions in 3-dimensional cell cultures (Santos et al., 2020), which suggests, that DRG neurons grow in a different mode than other CNS neurons.

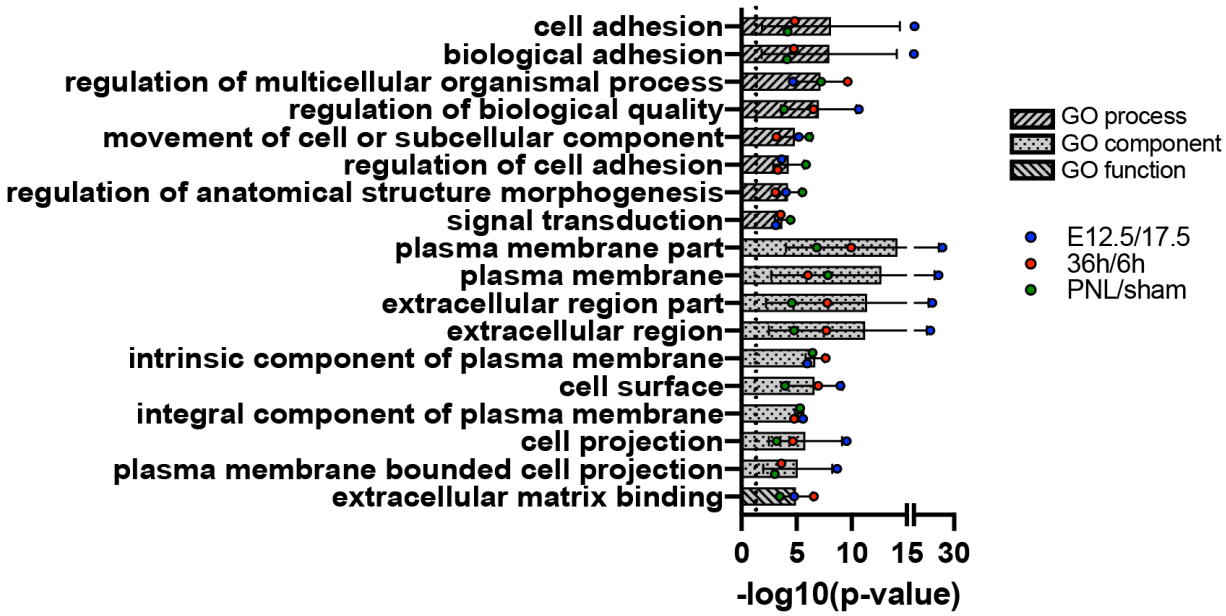

Figure 8: GO terms commonly upregulated in DRG growth states.

GO terms that are overrepresented in proteins upregulated in growing DRGs. Dotted line indicates p=0.05

Equidirectional protein level changes in DRG growth states

As the GO term analysis revealed mostly broad categories instead of specific pathways, I wanted to investigate further into the specific proteins implicated in axon growth. I reasoned, that proteins that change equidirectionally, meaning increase or decrease in all three paradigms when DRGs acquire growth competence, could be cues to essential growth processes, which are "conserved" between the three similar but distinct growth paradigms. Accordingly, I sorted the datasets by proteins that significantly change their levels equidirectionally in all three paradigms. This yielded a list of 39 GOIs (Fig. 9). Again, this list showed known RAGs as being upregulated, including Gap43, Stathmin2 (Stmn2) and Brain Abundant Membrane Attached Signal Protein 1 (Basp1), as well Nestin (Nes), which is considered a marker for stemness. Conversely, a number of downregulated proteins could be placed into growth hindering pathways, including the negative regulator of Ca^{2+}/calmodulin-dependent protein kinase II, Neurochondrin (Dateki et al., 2005) (Ncdn) and Vesicle Transport Through Interaction With T-SNAREs 1B (Vti1b), which could be placed upstream of Munc13, which has been shown by our group to be a growth inhibitor (Emperador-Melero et al., 2018; Hilton et al., 2022; van de Bospoort et al., 2012; Voets et al., 2001). With the list being internally consistent with literature, I reasoned we might find

unknown growth molecules among the remaining genes, which could not be directly related to axon growth.

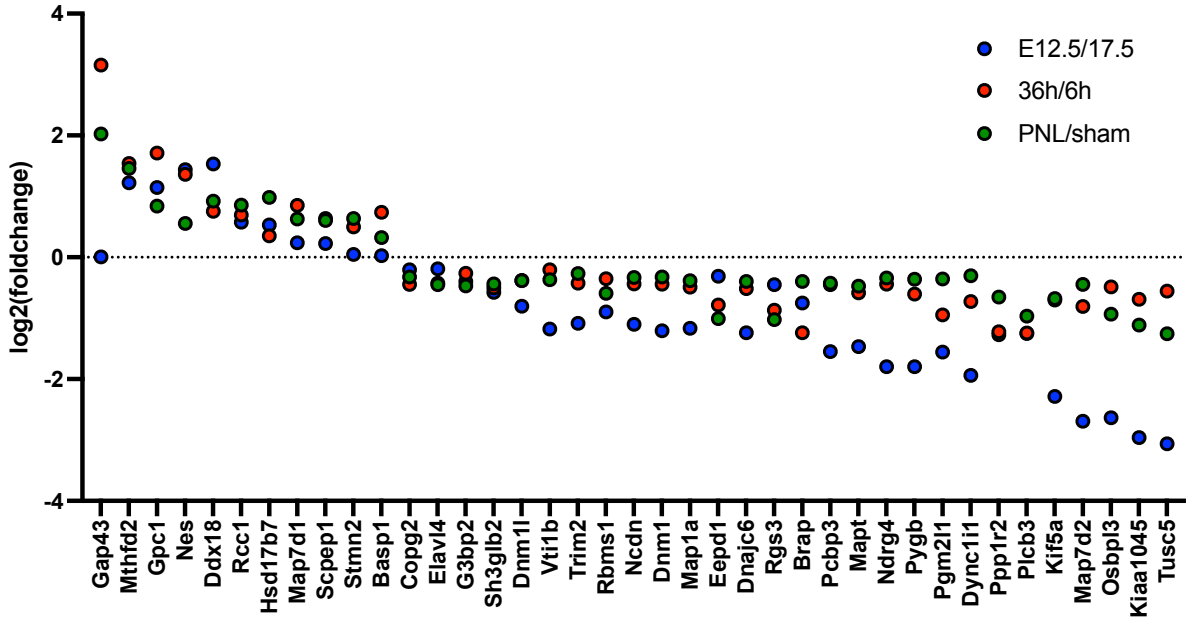

Figure 9: Proteins that are significantly up or down regulated in all three growth paradigms.

Foldchange of GOIs in the MS data set for the axon growth paradigms. Each point indicates the significant change (FDR < 0.05) in one paradigm. The dotted line indicates no change in expression.

Development of a cell culture system to screen genes of interest for axon regeneration

After establishing a list of GOIs for potential growth effectors, I needed to develop a culture system suitable to investigate growth effects in DRGs. Typically, DRGs are used to study regeneration, precisely for their immense growth capacity. A naïve adult DRG neuron will grow on average around 200 µm longest axon– as measured from the neuronal MT marker ßIII-tubulin – within 16 h when cultured on poly-L-lysine (PLL) and laminin, the typical culture conditions used in our laboratory and others. In comparison, a hippocampal neuron, probably the most widely used primary neuron culture (Bradke and Dotti, 2000), will in the same time and conditions only generate around 50 µm of a longest neurite (Fig. 10). This capacity for growth, however, can be disadvantageous when trying to modify growth by overexpression of transgenes. The expression of ectopic genes from plasmids follows its own kinetics, while the transfected axons are already growing. The most suitable method to introduce transgenes to DRGs is nucleofection. A nucleofected cell will have to express, correctly fold, and traffic an overexpressed protein before it can even affect the cell. The earliest we observe fluorescence of ectopically expressed fluorescent proteins in DRGs is 18-24 h post transfection. In that time a DRG neuron might have already grown quite the impressive axon, before the transgene can even affect the cell. This, paired with the heterogeneity of DRG cultures, allows for possible growth effects being overshadowed by already well growing axons. Consequently, the cell culture system I developed aimed to reduce growth of DRG axons without actively inhibiting it. To this end, I cultured DRGs on PLL only, to slow down the growth of the DRGs enough see growth effects. Additionally, I collected two time points per construct, 48 h and 72 h, partially because a candidate might spike axon initiation, thus leading to an increase in the earlier timepoint, without influencing axon elongation, thus losing the growth effect in the later time point, but mainly to be able to check whether a potential candidate would consistently increase growth. A promising candidate would, in the best-case scenario, boost growth consistently over both timepoints.

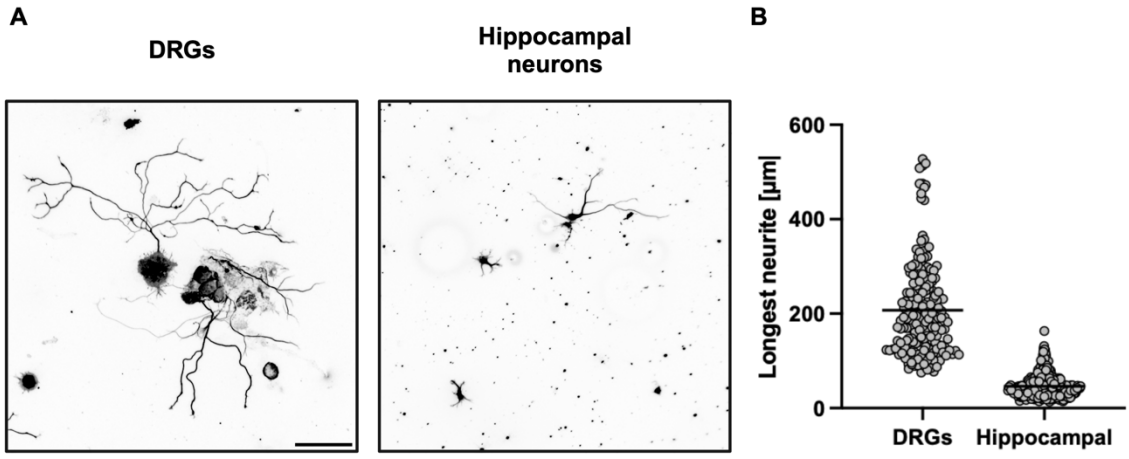

Figure 10: Growth comparison between DRGs and hippocampal neurons.

DRGs and hippocampal neurons were grown for 16 h on PLL and laminin coated coverslips. (A) Representative images of DRGs and hippocampal neurons. ßIII-tubulin staining. Scale bar 100 µm (B) Quantification of the length of the longest neurite. N = 192 and 364, n = 3.

Another consideration was detecting the overexpression of the GOIs. To avoid the problems that might arise with fusing a full protein, such as green fluorescent protein (GFP) or HaloTag, I decided to use the 27 AA 3xHA tag. This small tag is easily detected by antibodies and less likely to lead to misfolding. However, the addition of a tag might still cause proteins to be mistrafficked or otherwise disrupt function of N- or C-terminal domains. Hence, I decided to generate most plasmids in an N- and C-terminally tagged version, unless a cursory literature review indicated one tag to be highly likely to disrupt function or be cleaved. This is the case, for example, for methylenetetrahydrofolate dehydrogenase 2 (Mthfd2), which has a mitochondrial translocation sequence in its N-terminus, that is cleaved upon transport into the mitochondria. Consequently, I did not generate the N-terminally tagged (ntag) version of Mthfd2. Additionally, to have the expression of GFP, we decided to include it on the expression vector, driven by a separate promoter. While the expression of the GOI is driven by a strong CMV promoter, GFP is expressed from human synapsin (hSyn) promoter. All plasmids were generated *de novo* from mouse cDNA libraries.

Finally, before starting the screen, I conducted a preliminary literature search to exclude a number of candidates. GOIs were excluded for reasons such as already being known RAGs, like Basp1, which also sits in the same pathway as Stmn2, being clearly related to growth modulating processes, for example the aforementioned Ncdn or being known modulators of the cytoskeleton, like microtubuli associated protein tau, as the cytoskeleton is

well established as a main driver of axon regeneration and we aimed to find novel growth mechanisms. This led to the generation of 56 constructs of 31 different GOIs.

Overexpression screen of genes of interest

Of the 112 tested conditions (56 constructs x 2 time points), 43 returned a significant growth effect, with 12 constructs having a consistent growth effect over both time points. Interestingly, of these 12, 7 showed a robust growth effect only in one of the tagged constructs, reaffirming the merit of this approach (Table 1). Figure 11 shows only one construct per GOI, preferentially the one with an effect, if there was a discrepancy between constructs. In total, I detected a robust growth effect for 10 different GOIs, with the largest effect from Gpc1. This not only confirmed the validity of the theoretical approach and the culture system, but also offered up Gpc1 as a fascinating candidate for more in depth mechanistic studies.

Table 1: Statistical overview of the overexpression screen results.

Indicated GOIs show a positive axon growth effect. Underlined GOIs show a robust increase in axon growth over both time points in at least one construct. Empty grey cells indicate constructs that have not been generated or the absence of a statistical comparison because one construct is missing. The first four columns are statistical comparisons to empty vector. The last column indicates a comparison in axon growth between c- and ntag constructs. n = 3, N = 90. *p<0.05, **p<0.01, ***p<0.001.

GOI	ctag		ntag		Difference
	48 h	72 h	48 h	72 h	ctag vs ntag
Brap	***	*	ns	ns	***
Copg2	ns	ns	***	***	***
Ddx18	ns	*	ns	**	ns
Dnajc6	ns	ns	*	ns	ns
Dnm1l	ns	ns	ns	ns	ns
Dync1i1	*	*	***	***	ns
Eepd1	***	*	ns	ns	*
G3bp2	**	ns	ns	ns	***
Gap43	*	ns	ns	ns	***
Gpc1	***	***	***	***	***
Hsd17b7	ns	***	***	ns	***
Kiaa45			**	ns	
Kif5a			**	***	
Map7d1			ns	ns	
Map7d2	ns	***	ns	ns	***
Mthfd2	ns	ns			
Nestin	***	***	***	ns	***
Osbpl3	ns	ns	*	ns	ns
Pcbp3	***	ns	*	ns	ns
Pgm2l1			ns	ns	
Plcb3			ns	ns	
Ppp1r2	ns	***	ns	***	ns
Pygb	ns	ns	ns	ns	ns
Rbms1	ns	ns	*	ns	ns
Rcc1	ns	*	*	***	ns
Scpep1	ns	**	ns	ns	ns
Sh3glb2	ns	ns	**	ns	**
Stmn2	***	***	ns	ns	***
Trim2	ns	ns	ns	ns	ns
Tusc5	ns	ns	ns	ns	ns
Vti1b	ns	ns	***	***	***

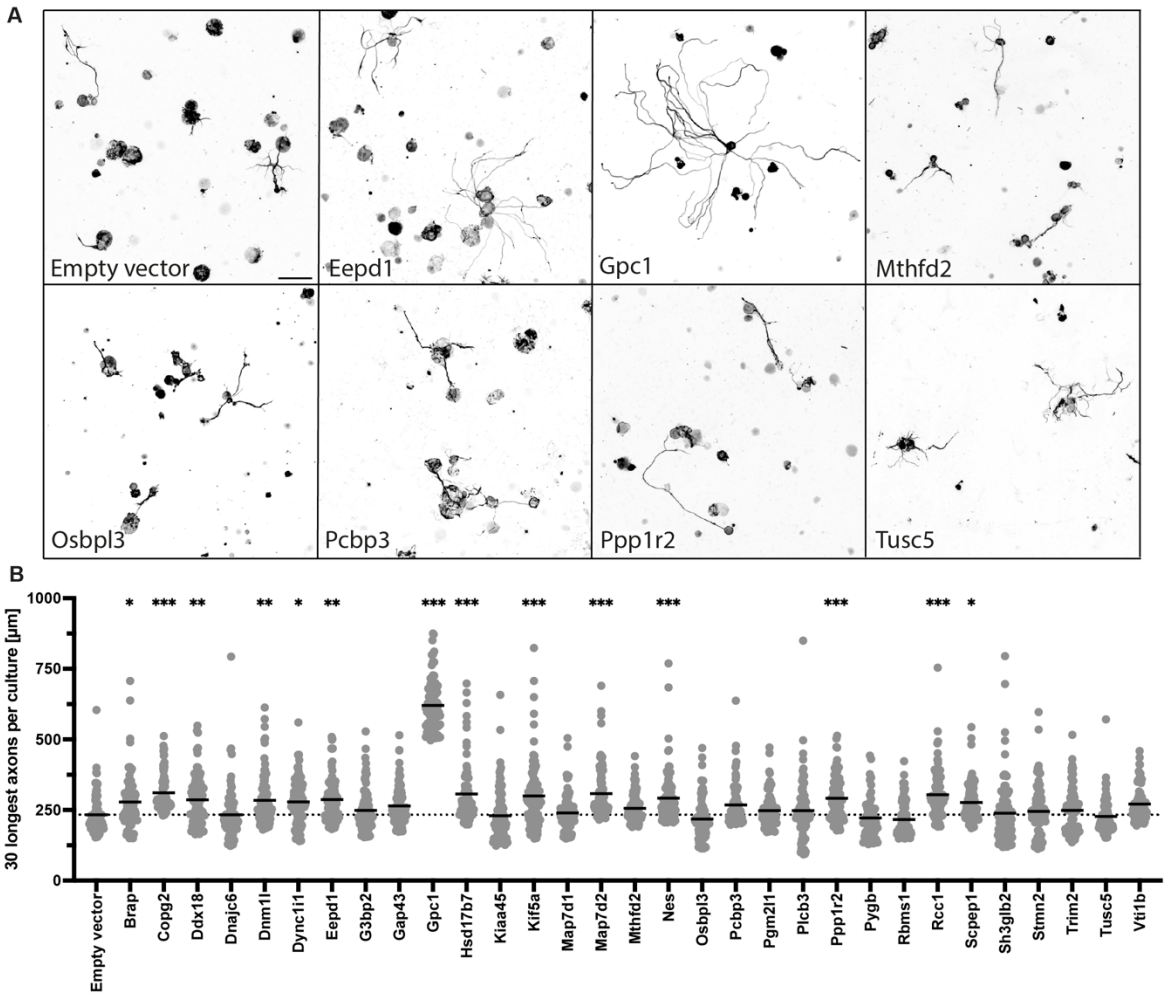

Figure 11: Multiple GOIs show a positive growth effect in the overexpression screen.

A) Representative images of DRGs from selected GOIs from the overexpression screen. ßIII-tubulin staining. Scale bar 100 µm. B) Longest axons per culture of overexpression experiments with mean indicated. Dotted line indicates the mean of the empty vector control. N = 90, n = 3. One-way ANOVA with Dunnett's multiple comparison test. All groups compared to empty vector. *p<0.05, **p<0.01, ***p<0.001.

Gpc1-overexpression overcomes the growth inhibition of chondroitin sulfate proteoglycans

As the screen was designed to have neurons grow slowly, but not actively inhibit axon growth, I tested, whether Gpc1-overexpression would overcome the growth inhibition of the CNS. Consequently, I plated DRGs on PLL and laminin plus chicken-derived CSPGs, to mirror the inhibitory environment of the spinal cord. While laminin itself is a potent activator of axon growth, it was necessary to allow the plated neurons to attach in the first place when CSPGs are present. Still, overexpression of Gpc1 overcame the inhibition conferred by the CSPGs and acted synergistically with the growth effect conferred by laminin (Fig. 12). This implies that of the many possible signalling pathways, via which Gpc1 could activate growth (as reviewed in an earlier chapter), integrin signalling, which is activated by laminin, is likely not a major factor. Furthermore, by demonstrating Gpc1 can overcome this proxy for the CNS growth inhibition, it was revealed as an interesting candidate to activate axon growth in an *in vivo* SCI model.

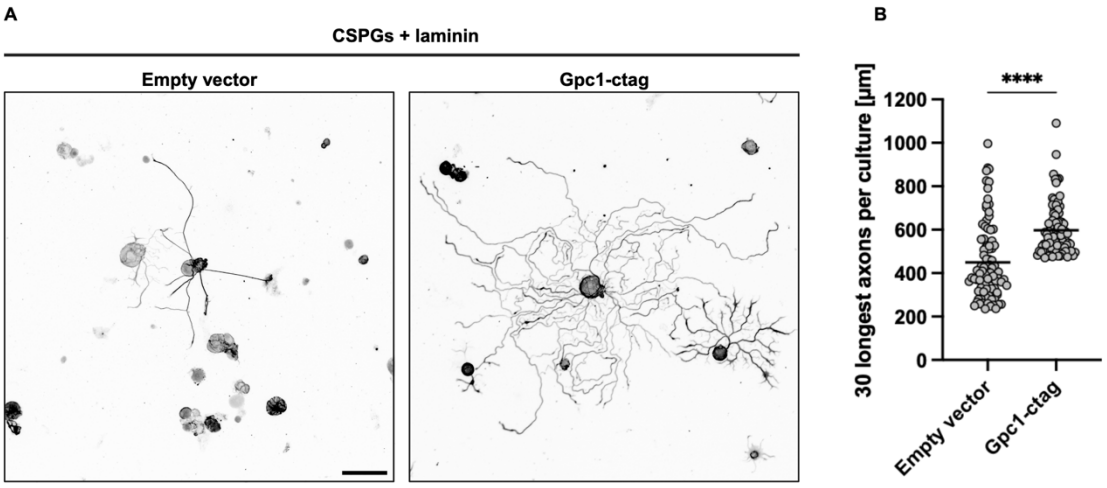

Figure 12: Gpc1-overexpression overcomes the growth inhibition of CSPGs.

(A) Representative images of DRGs expressing Gpc1-ctag or the control empty vector from cultures plated on CSPGs and laminin. ßIII-tubulin staining. Scale bar 100 µm. B) Longest axons per culture of overexpression experiments on CSPGs and laminin with mean indicated. Student's t-test. ****p<0.0001.

Identification of Gpc1 functional domains from multiple sequence alignment

Gpc1 is viewed as a modulator of extracellular signalling receptors (Pan and Ho, 2021). To this end, Gpc1 is trafficked outside of the cell via an N-terminal signalling domain. Following translocation, this signal peptide is cleaved. Via a C-terminal GPI anchor domain, Gpc1 is anchored to the outside of the PM, where it interacts with signalling receptors, such as FGFR, VEGFR and BMPR2. The anchor domain is truncated upon anchoring (Fig. 6). Gpc1's receptor interaction is facilitated by HS chains, which induce conformational changes of the receptors upon formation of a tertiary complex. Via this interaction, Gpc1 can act as a coactivator, making receptors more receptible to their respective activators, or as an inhibitor, reducing the responsiveness of receptors to their activators. The HS chains responsible for this interaction are attached to a HS binding cassette of three alternating serine and glycine residues. As studies of Gpc1 have mostly focussed on the human protein, for its relevance in cancer migration, I needed to confirm the position of these functional domains in the murine protein, in order to generate functional KOs. To this end, I used multiple sequence alignment, comparing the murine protein to all available confirmed protein sequences for Gpc1, that being, chicken, cow, human, mouse, rat, and zebra (Fig. 13). I included the other species besides mouse and human, to indicate high percent identity domains which would indicate motifs that are important for the interaction with modifying enzymes or the establishment of relevant secondary and tertiary structures. In general, mouse and human Gpc1 have a high identity of 89%. With 558 AAs, the human version is one AA longer than the murine protein. This insertion is L184 in the human protein. In the human protein, the secretory signal peptide is described to span AAs 1-24 and terminate in aspartic acid D24. The high number of identities between the murine and human protein in the first 24 AAs, as well as the presence of D24 in 5/6 species, suggests that the secretory signalling peptide also spans AAs 1-24 in the murine protein (Fig. 13A). The HS-binding serine residues of the human protein are located at S486, S488, and S490. The murine protein shows a high identity motif starting from glycine G481 to G499, with perfect alignment to the human protein and near-perfect alignment to the other species. Thus, S494, S496, and S498 are likely to be the HS-binding residues of the murine protein (Fig. 13B). Finally, in the human protein AAs 531–558 constitute the GPI anchor domain, which is initialised by S531. While the immediate upstream sequence of S531 is perfectly conserved between mouse and human, as well as highly with the other species, the downstream sequences show some variability. However, the high identity of key AAs, such as

S531, E532, E534, P546, and L552, indicate that in the murine protein, the anchor domain also begins at S531 (Fig. 13C). In conclusion, via multiple sequence alignment, I confirmed the position of the relevant domains of murine Gpc1 to generate functional KOs for further mechanistic studies.

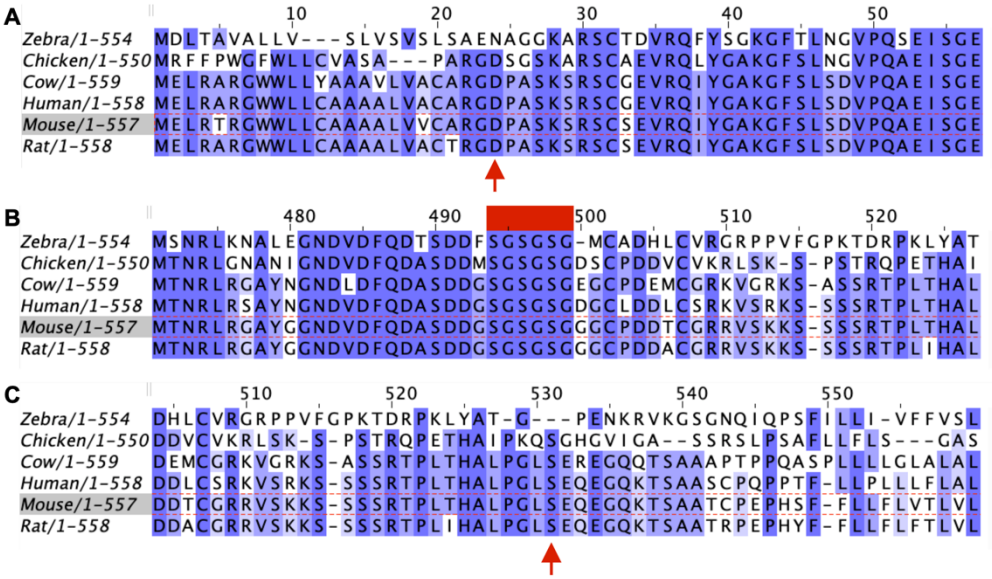

Figure 13: The multiple sequence alignment of six species of Gpc1 confirms the localization of key functional domains.

The colour code indicates percent identity, darker shades of blue indicate higher percentage. The mouse sequence is highlighted in the red dotted box. Red arrows indicate the AAs that start (A) the secretory peptide or (C) the GPI anchor domain. (B) The solid red box indicates the alternating SG residues required for HS binding.

Gpc1 needs to be secreted but not anchored to the cell membrane to induce regeneration

In the overexpression screen, the C- and N-terminally tagged (ctag and ntag, respectively) Gpc1 constructs showed significantly different growth effects, with the ctag version growing longer (Table 1 and Fig. 14B). When considering the domain structure, I wondered whether the ntag might hinder correct trafficking, thus diminishing the growth effect (Fig. 14A). This would indicate that trafficking of Gpc1 to the outside of the cell membrane is necessary to facilitate its growth effect. Based on the multiple sequence alignment, I generated functional KOs to investigate the trafficking behaviour of murine Gpc1. The noSec-Gpc1 construct was still expressed without the secretory peptide, but stained mostly in the soma with only weak signal in the axon in close proximity to the ßIII-tubulin signal. Comparatively, the ntag construct stained the axon well and spread out from the ßIII-tubulin signal, indicating localization to the outside of the PM (Fig. 11C). Thus, removal of the secretory peptide did, indeed, hinder proper localization to the PM. Further, removing the secretory peptide fully abrogated the growth effect conferred by Gpc1. Next, I wondered whether Gpc1 must be anchored to the plasma membrane in order to confer its growth effect. Interestingly, while diminishing the growth effect, removing the anchoring domain did not fully negate it (Fig. 14C). Thus, Gpc1 needs to be secreted to the plasma membrane but not anchored to it to activate axon growth.

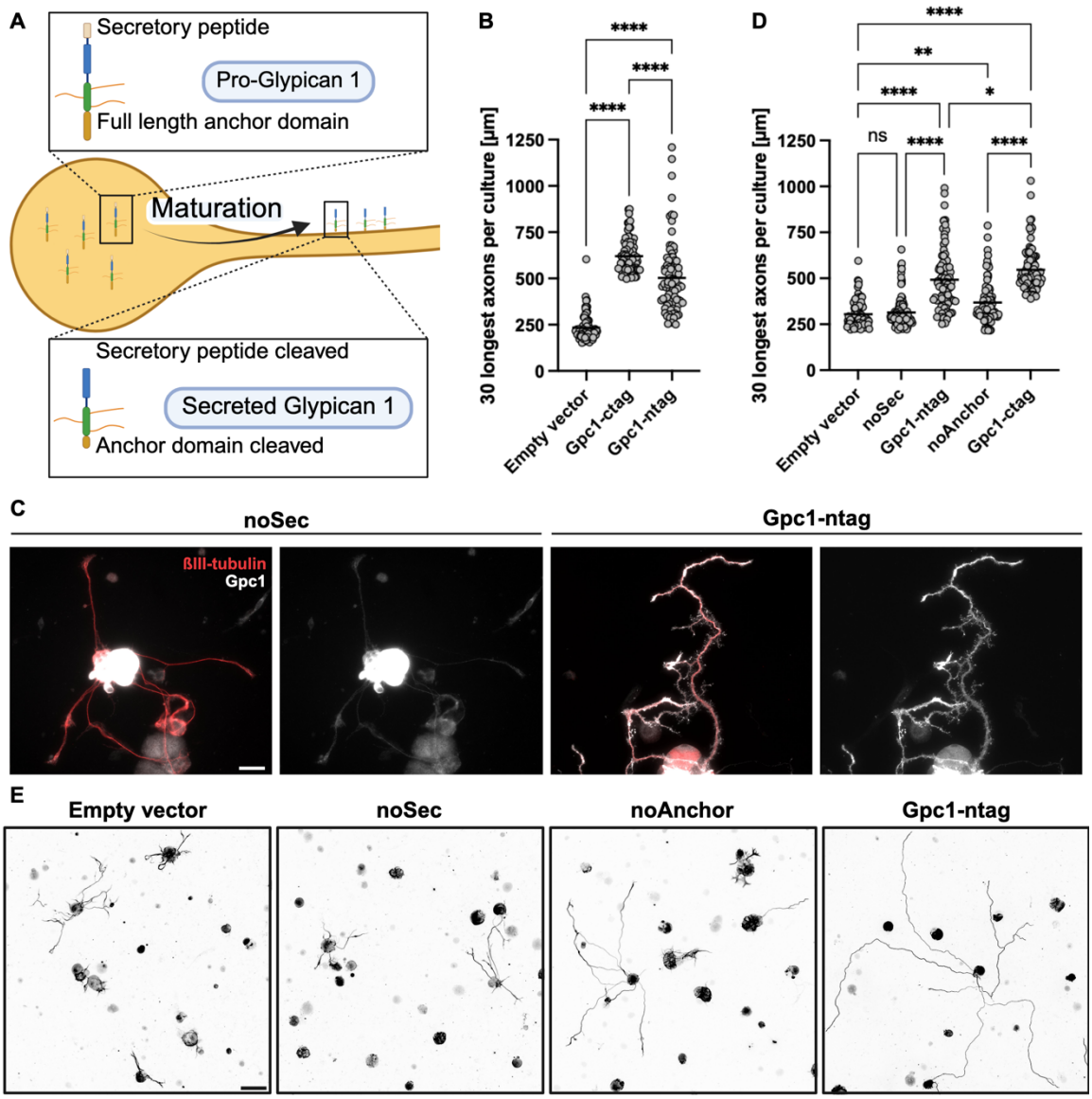

Figure 14: Gpc1 must be secreted but not anchored to the plasma membrane to elicit axon growth.

(A) Schematic of Gpc1 maturation. Pro-Glypican 1 is trafficked from the soma to the plasma membrane via a secretory peptide, which is cleaved upon translocation. Via an anchoring domain, the secreted Gpc1 is GPI-anchored to the outside of the plasma membrane. The anchor domain gets partially cleaved upon anchoring. (B) Longest axons per culture for amino- and carboxy-terminally tagged Gcp1 constructs with mean indicated. Gpc1-ctag is the same data as Fig. 11C Gpc1. (C) Representative cells stained for Gpc1 and ßIII-tubulin expressing the noSec or Gpc1-ntag construct. Scale bar 25 µm. (D) Longest axons for trafficking-related Gpc1 functional KO constructs with mean indicated. N = 90, n = 3. One-way ANOVA with Dunnett's multiple comparison test. All calculated comparisons indicated. *p<0.05, **p<0.01, ***p<0.001, ****p<0.0001. (D) Representative images of DRGs expressing the indicated constructs. ßIII-tubulin staining. Scale bar 100 µm.

Deletion of heparan sulfate binding serine residues abolishes axon growth effect conferred by Gpc1

After confirming that the canonical trafficking of Gpc1 is required to induce axon growth, I wanted to confirm, that the growth effect is conferred via extracellular signalling receptors, as is the case in the dysregulated signalling of Gpc1-positive cancers. To this end, I replaced the HS-binding serine residues, identified in the multiple sequence alignment, with glycine residues, terminating the binding of HS-chains. This confirmed, that the interaction with cell surface receptors via HS chains is necessary to induce axon growth, as the growth effect is fully depleted via this functional KO (Fig. 15).

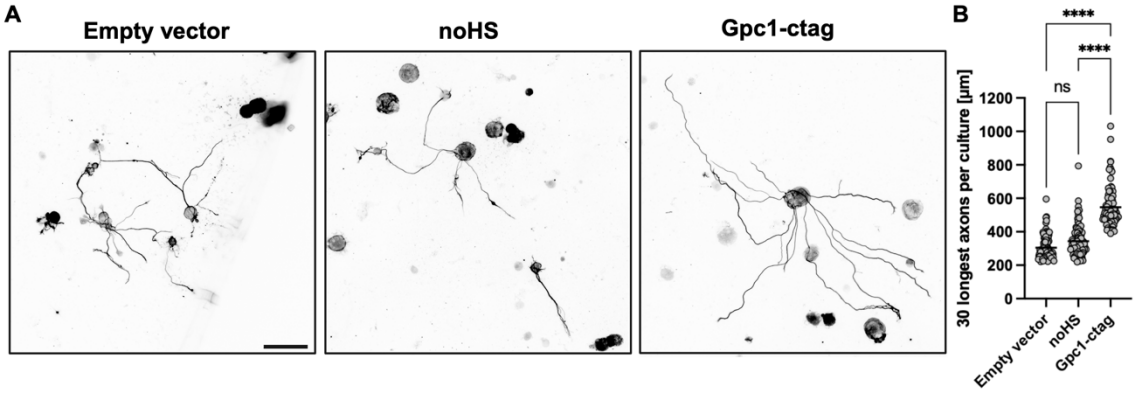

Figure 15: Removal of HS binding serine residues abolishes the growth effect of Gpc1.

(A) Representative images of DRGs expressing the indicated constructs. ßIII-tubulin staining. Scale bar 100 µm. (B) Longest axons for heparan sulfate binding functional KO constructs with mean indicated. N = 90, n = 3. One-way ANOVA with Dunnett's multiple comparison test. All calculated comparisons indicated. ****p<0.0001.

Gpc1 conditioned media induces growth in untreated DRGs

As my studies on the trafficking of Gpc1 indicated that it needs to be secreted, but not anchored, to activate growth, I wondered whether overexpressed Gpc1 was enriched in the culture media and whether conditioned media from Gpc1-overexpressing cultures could induce growth in wildtype cell cultures. Subsequently, I raised nucleofected donor cultures, expressing either Gpc1-ctag, noSec-Gpc1 or noAnchor-Gpc1, concentrated and replenished their media and transferred it to wildtype cultures (Fig. 16A). Both the noAnchor and ctag conditioned media induced growth in the receiving cultures (Fig. 16B-C), thus indicating that either Gpc1 itself or an unknown growth factor secreted by Gpc1 expression in the conditioned media can activate growth in a paracrine fashion.

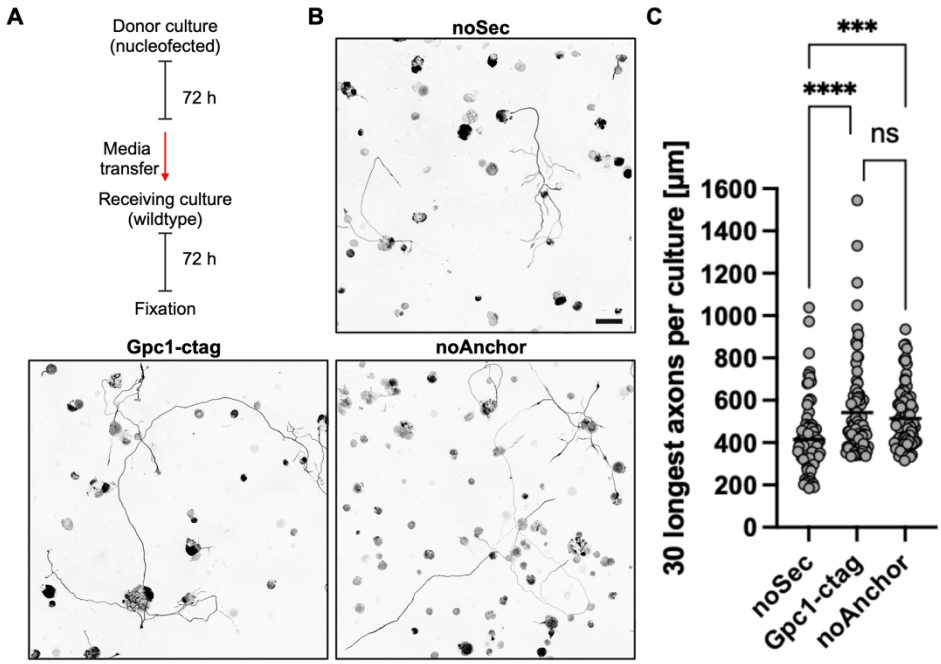

Figure 16: Gpc1-overexpressing cells condition their growth media to confer a growth effect to wildtype cultures.

(A) Schematic representation of the media transfer experiment. Donor cultures were nucleofected with Gpc1 constructs and grown for 72 h. Consequently, the media was concentrated, replenished and used to grow wildtype cultures for another 72 h. (B) Representative images of DRGs from the receiving cultures. ßIII-tubulin staining. Scale bar 100 µm. (C) Longest axon analysis for the receiving cultures with mean indicated. N = 90, n = 3. One-way ANOVA with Dunnett's multiple comparison test. All calculated comparisons indicated. ***p<0.001, ****p<0.0001.

Isolated Gpc1 protein does not induce axon growth

As conditioned media from Gpc1-overexpressing cultures activated growth in wildtype cultures, I wondered whether Gpc1 could be detected in the media of Gpc1-overexpressing cells. An enzyme-linked immunosorbent assay (ELISA) against the 3x-HA tag indicated that only the noAnchor protein was present in the media (Fig. 17A). Considering the maturation process of Gpc1, the c- and ntag are likely to be cleaved thus avoiding detection in the ELISA when using the HA-tag antibody. Consequently, I developed a Gpc1-construct with the 3xHA tag between the secretory peptide and the core protein. The "hidden" HA tag construct (hHA-Gpc1) was readily detectable in ELISA of the culture media (Fig. 17B), as well as immuno fluorescence and conserved the growth effect (Fig. 17C-D). In accordance with the literature that Gpc1 is trafficked to the outside of the PM, the staining showed PM localization.

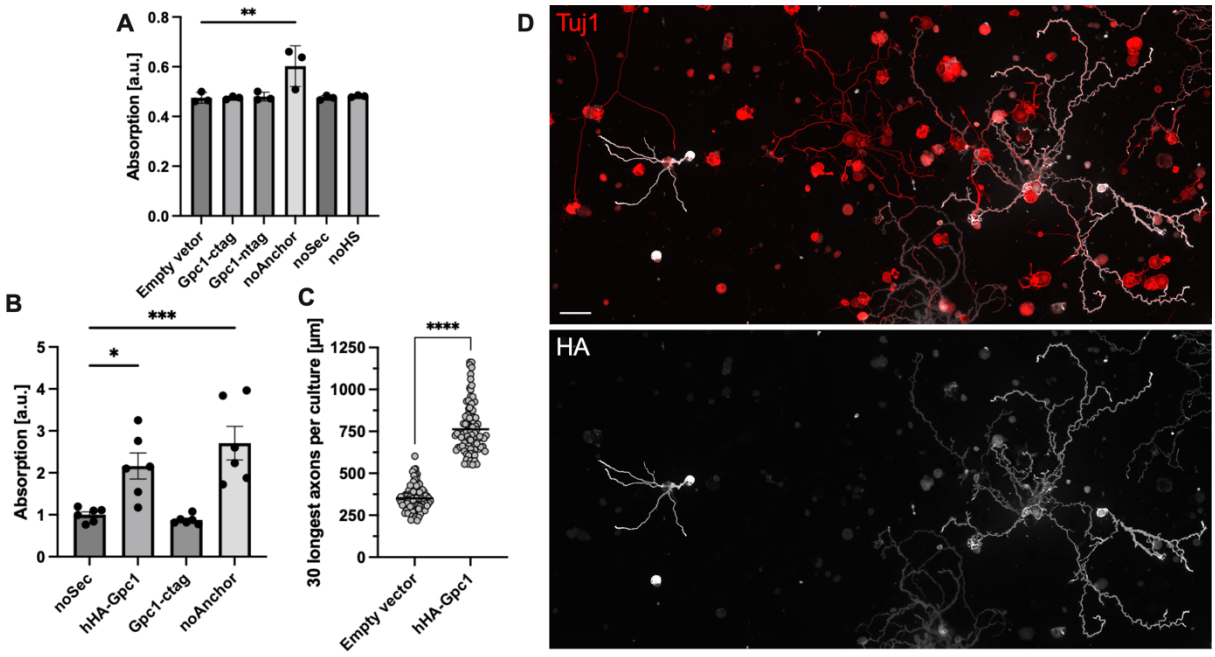

Figure 17: "hidden-HA" Gpc1 is readily detectable in ELISA and immunocytochemistry.

(A) ELISA against HA-tag of cell culture media from overexpression cultures. Mean ± SD, n = 3. One-way ANOVA with Dunnett's multiple comparison test. All groups compared to empty vector. (B) ELISA against HA-tag of cell culture media from "hidden-HA" Gpc1 (hHA-Gpc1). Mean ± SD, N = 6, n = 3. One-way ANOVA with Dunnett's multiple comparison test. All groups compared to noSec. (C) Longest axon analysis for hHA-Gpc1-overexpressing cultures with mean indicated. N = 90, n = 3. *p<0.05, **p<0.01, ***p<0.001, ****p<0.0001. (D) Representative images of DRGs overexpressing hHA-Gpc1. Scale bar 200 µm.

As I now confirmed that Gpc1 was available in the media of overexpressing cultures, I posed the question, whether the isolated protein could induce growth when added to the media of DRG cultures. We acquired the Gpc1 protein commercially, expressed from our ctag vector. To achieve higher yields, the company also generated a histidine-tagged version of Gpc1, where the histidine-tag replaced the C-terminal 3x-HA tag (Gpc1_trunc). Both protein isolates where serially diluted to achieve final concentrations ranging from 110 µg/µL to 1.1 pg/µL. Interestingly, none of the tested concentrations induced growth, while the higher concentrations even had a negative impact on the growth of the treated axons (Fig. 18A).

To verify the correct folding of the isolated protein, we employed size-exclusion chromatography (SEC) and circular dichroism (CD) spectroscopy. The SEC showed that the protein eluted at the expected rate in a sharp peak at 14-15 mL, indicating an absence of misfolded aggregates (Fig. 18B). Additionally, the CD spectrum indicated the presence of alpha helices via a positive peak at 192 nm and a negative peak at 222 nm (Fig. 18C) (Kumagai et al., 2017), consistent with the crystal structure of the Gpc1 core protein, which shows alpha helices as the main structural element of the tertiary structure (Madej et al., 2014). Thus, while the protein we used appeared correctly folded, it did not induce growth in DRG cultures. Together, I could show that there is a detectable amount of Gpc1 in the media of overexpressing cultures, but while the transfer of media from overexpressing to naïve cultures sparked growth, the isolated protein did not. This indicated that it is not the soluble Gpc1 protein, that confers the growth effect, but rather a different kind of secreted factor.

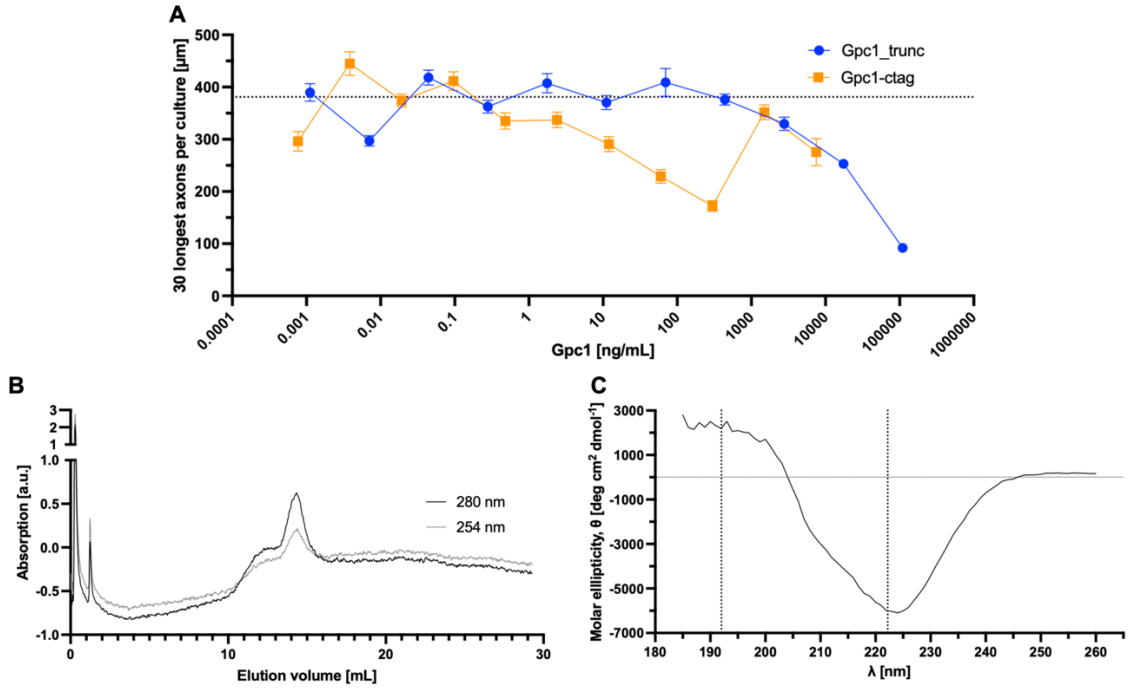

Figure 18: Isolated Gpc1 does not induce growth, even when correctly folded.

(A) Longest axon analysis for cultures treated with Gpc1-ctag or Gpc1_trunc isolated protein. The dotted line indicates the average for the non-treated control, which cannot be plotted on a logarithmic x-axis. Mean plus SEM. Gpc1-ctag n = 1, N = 30, Gpc1_trunc n = 1-3, N = 30-90. (B) Absorption of the size exclusion chromatography eluate of Gpc1_trunc at 254 and 280 nm. (C) Circular dichroism spectrum of Gpc1_trunc. The vertical dotted lines indicate the expected peaks for alpha helices at 192 and 222 nm.

Gpc1-loaded extracellular vesicles activate axon growth

Besides soluble Gpc1, another way Gpc1 could interact with other cells is via secretion in extracellular vesicles (EVs). Gpc1-positive EVs have been reported by multiple proteomic studies (Chitti et al., 2023; Garcia-Silva et al., 2021) and are investigated as a biomarker for different cancers (Adel et al., 2025; Tripathi et al., 2023). Consequently, I stained Gpc1 in hHA-Gpc1 expressing DRGs, to investigate its cellular localization. Confirming the hypothesis that Gpc1 is trafficked in EVs, I observed many intensely fluorescent puncta in the staining (Fig. 19).

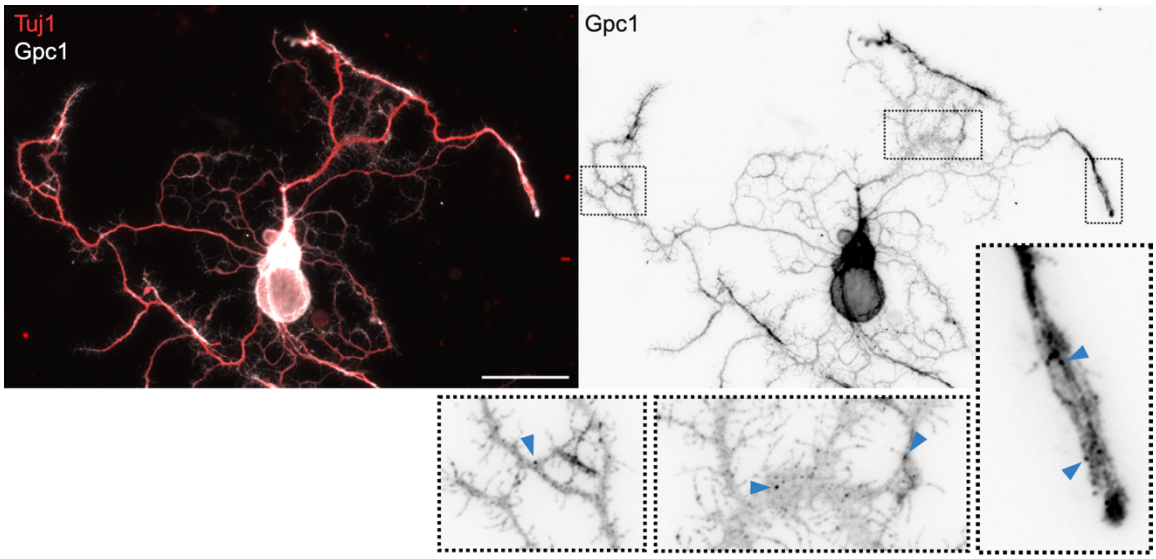

Figure 19: Gpc1 staining in overexpressing cells shows punctate Gpc1 signal.

Representative image of a DRG overexpressing hHA-Gpc1 stained for ßIII-tubulin (Tuj1) and Gpc1. Blue arrows in the zoomed in panels indicate clearly defined puncta in the Gpc1 signal. Scale bar 100 µm.

Subsequently, I isolated EVs from DRG cultures nucleofected with hHA-Gpc1 or the empty vector control. The EV-enriched fraction stained positive for Gpc1 and HA-tag, as well as CD9, a marker for EVs (Fig. 20A). Finally, treating DRG cultures with EVs from either hHA-Gpc1 or empty vector expressing cultures, elicited a growth effect in the hHA-Gpc1 EV treated neurons. Thus, extracellular vesicles from Gpc1-overexpressing cultures are positive for Gpc1 and confer a paracrine growth effect on wildtype cells (Fig. 20B-D).

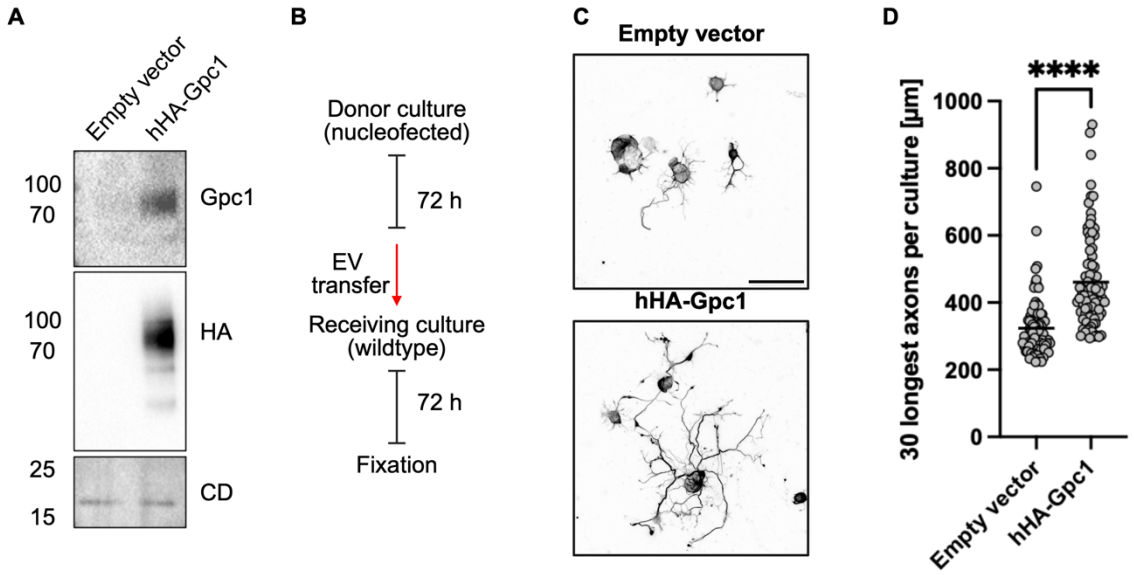

Figure 20: Gpc1-positive extracellular vesicles elicit growth in wildtype DRGs.

(A) Western blot from the EV enriched fraction following EV isolation. Molecular weight in kDa. Antibodies indicated on the right. (B) Schematic representation of the EV transfer experiment. Donor cultures were nucleofected with the indicated constructs and grown for 72 h. Consequently, the EVs were isolated and used to grow wildtype cultures for another 72 h. (C) Representative images of DRGs from the receiving cultures. ßIII-tubulin staining. Scale bar 100 µm. (D) Longest axon analysis for the receiving cultures with mean indicated. N = 90, n = 3. One-way ANOVA with Dunnett's multiple comparison test. Student's t-test. ****p<0.0001.

Gpc1-overexpression changes the phosphorylation state of the cell and regulates growth essential processes

The cell surface receptors modulated by Gpc1 largely signal inside the cell via phosphorylation cascades. Consequently, to elucidate which receptors are involved in the Gpc1 growth effect, we generated whole and phosphoproteomic data sets for DRGs overexpressing hHA-Gpc1 or empty vector controls. Interestingly, while the whole proteome analysis of empty vector and hHA-Gpc1 samples showed roughly equal numbers of proteins detected, 7632 and 7579, respectively (Fig. 21A), there was a significant reduction on detectable phosphorylated peptides in the hHA-Gpc1 samples; 12696 vs. 14180 (Fig. 21B). When analysing the GO terms of up- and downregulated proteins in the whole proteome, I detected largely terms associated to the PM, mitochondria and the ribosome. Interestingly, however, I also detected "negative regulation of smooth muscle cell migration". As discussed above, the processes of cell migration and axon growth are often similar (Fig. 21C). The responsible downregulated genes in this GO term include slit homolog 2 (drosophila) and ras homolog gene family, member a (Rhoa), which are known to be negative regulators of axon growth (Piper et al., 2006; Stern et al., 2021) and bone morphogenic protein receptor type 1a (Bmpr1a), which is negatively regulated by Gpc1 (Dwivedi et al., 2013). Thus, the GO analysis of these proteomes indicates that canonically inhibitory pathways for axon growth are downregulated upon Gpc1-overexpression.

GO term analysis of proteins which change their phosphorylation state, meaning at least one phospho peptide was significantly enriched between groups, reenforced the focus on cytoskeletal interactors. Processes such as "regulation of microtubule depolymerization" and "regulation of microtubule binding", the components "cytoskeletal part" and "microtubule" as well as the function "actin binding", "cytoskeletal protein binding", and "GTPase regulator activity" directed our attention toward Rho family GTPases, as the master regulators of the cytoskeleton. Consequently, I analysed the phosphoproteomic data with regards to Rhoa interactors. While Rhoa itself was not detected in this data set, multiple of its interactors, like rho gtpase activating protein (Arhgap)39, Arhgap21, Arhgap32, and rhogef (arhgef) and pleckstrin domain protein 1 (chondrocyte-derived) (Farp1), changed their phosphorylation state upon Gpc1-overexpression. This observation was underlined by canonical pathway analysis via the Ingenuity pathway analysis tool, for which RHO GTPase cycle was the top hit ($p = 2{,}97e\text{-}21$, overlap 49/450). Together, this indicated that overexpression of Gpc1 activates signalling cascades that lead to Rho inactivation, which enables axon growth.

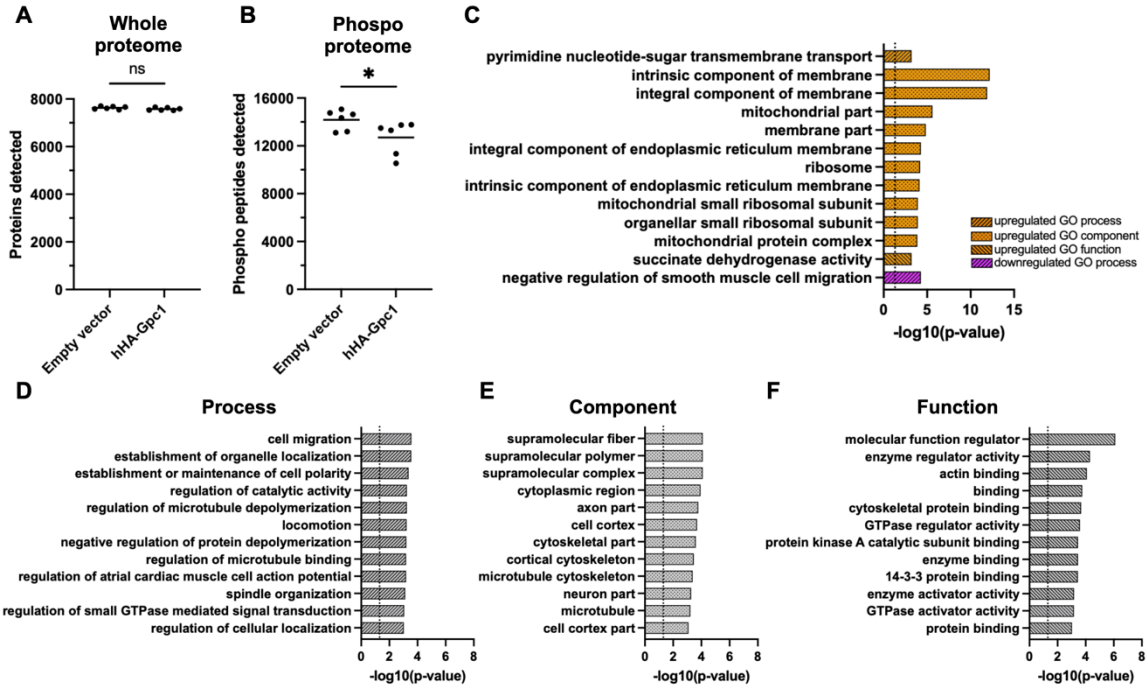

Figure 21: Gpc1-overexpression changes the phosphorylation state and proteome of DRGs.

Number of detected proteins in the whole proteomics (A) and number of detected phospho peptides (B) of hHA-Gpc1 and empty vector-overexpressing DRGs. Student's t-test. n = 6, *p<0.05. (C) enriched GO terms of up and down regulated proteins from the whole proteome of hHA-Gpc1 and empty vector-overexpressing DRGs. (D-F) Top 12 enriched GO terms of proteins which change their phosphorylation state from hHA-Gpc1 and empty vector-overexpressing DRGs. Dotted line indicates p=0.05.

Discussion

CNS axons fail to regenerate, because both intracellular and extracellular signalling mechanisms hinder them from growing. The aim of this thesis was to identify proteins which would overwrite those inhibitory signals, thus enabling axons to regenerate. Using proteomics of different growth paradigms, I established 31 GOIs. Following an overexpression screen, I observed a growth effect in 10 different proteins, chief among them, Glypican 1. I provide data indicating that correct trafficking of Gpc1 is imperative for Gpc1 to facilitate growth, which it does by interacting with extracellular cell surface receptors. I show that the activation of signalling cascades via these receptors is powerful enough to overcome the growth inhibition of the CNS as approximated by CSPGs. Consequent mechanistic analysis showed that Gpc1 is enriched in extracellular vesicles upon overexpression, and such Gpc1-positive vesicles induce growth in naïve cells.

Glypican 1 as an effector of axon growth

In this thesis, I provided data about the discovery as well as characterization of Gpc1 as an effector of axon growth. Following an unbiased screen, we detected Gpc1 as a novel candidate to induce axon regeneration, which led back to known growth mechanisms, such as growth regulation via Rho family proteins (Ahnert-Hilger et al., 2004; Arakawa et al., 2003; Da Silva et al., 2003; Stern et al., 2021). It is important to reiterate that we are not the first group to observe Gpc1 as being related to neural development or spinal cord injury. Gpc1 has been described in association to netrin-mediated axon guidance (Blanchette et al., 2015) and as a modulator of Sonic hedgehog signalling (Stoeckli, 2018). Its drosophila homologue dally-like protein is required for correct circuit assembly in the fly's visual system (Rawson et al., 2005). Furthermore, Gpc1 was shown to be regulated on the transcriptional level by neurotraumatic injury in rats (Bloechlinger et al., 2004), a result we confirm. My work, however, presents the first causal link between high levels of Gpc1 and axon regeneration. We also show Gpc1 as having both autocrine and paracrine activity.

Interestingly, we show that this growth activity is related to the regulation of cell signalling receptors, as confirmed by removal of the HS chains, which facilitate such interactions, fully abrogating the growth effect (Fig. 15). Which specific receptors are coactivated or inhibited by Gpc1 in our setting will need to be focus of further studies. Our experiment with CSPGs exclude the integrin signalling pathway. That is because, to plate DRGs on CSPG they require laminin to form their initial adhesion. Typically, as a growth activator,

laminin was excluded from our over expression culture system. The fact that Gpc1-over-expression in an environment of CSPGs and laminin still had a major growth effect implies that Gpc1 acts synergistically with laminin, thus, the original effect is likely independent of it.

One key finding of this thesis is the ability of Gpc1 to confer a growth effect via EVs. As mediators of cell-cell communication, EVs have recently been discussed as drug delivery vectors that facilitate cellular uptake of cargos and can confer tropism to specific cell populations (Elsharkasy et al., 2020; Herrmann et al., 2021). As such, our findings indicate a clinical relevance that might not be given by a protein that acts only in an autocrine manner. To pursue this avenue, further research will be needed into the mechanism of Gpc1 EV genesis and paracrine interaction. Our findings indicate that Gpc1-loaded vesicles confer a growth effect. They do not, however, conclusively show that this growth effect is due to Gpc1 directly. Possibly, Gpc1-overexpression leads to loading of other growth-affecting molecules into vesicles, a mechanism that has been described for FGF2 (Sparn et al., 2022). The presence of Gpc1 on or in these vesicles might just be a consequence of the overexpression. On the other hand, Gpc1 on the surface of EVs might confer tropism for neurons, as has been shown for other HSPGs (Christianson et al., 2013; Hagey et al., 2023). Interestingly, this would give hints to the formation of Gpc1 positive vesicles. As Gpc1 is wholly extracellular, i.e., having no intracellular domains, for it to confer tropism, Gpc1 needs to be presented on the outside of the vesicle. This would indicate such vesicles are the result of outward budding of the PM, which is then pinched from the mother cell. Such vesicles are typically referred to as micro vesicles, though the nomenclature is inconsistent (Zhang et al., 2024).

The question whether Gpc1 presents on the outside or within the lumen of EVs carries some translational implications. Were Gpc1 on the inside of vesicles, transported as a cargo, it could possibly be delivered to cells in liposomes, synthetic membrane bilayers which have been researched as drug delivery systems (Sercombe et al., 2015). The advantage of this approach is that liposomes can be generated free of cell culture systems (Lombardo and Kiselev, 2022), modified chemically to avoid clearance via immune cells (Gabizon et al., 1993) and can be loaded with the exact ratio of cargoes desired. There are also techniques of embedding GPI-anchored proteins into the outer lipid layer of liposomes (Fotoran et al., 2020), this approach, however, is less well established and would need to be developed further to facilitate Gpc1 delivery in a therapeutic context. This assumes, furthermore, that the uptake of Gpc1-loaded vesicles into host cells is only dependent on

Gpc1 and entry receptors on the PM of the host cell. However, as has been observed of viral peptides, cellular uptake and tropism can depend on multiple proteins (Bannach et al., 2020). Consequently, only loading liposomes with Gpc1 might not facilitate cellular uptake. Isolating Gpc1-loaded EVs from a donor culture seems to be the more straight forward approach. These vesicles are functional, as indicated by their ability to confer growth (Fig. 20) and thus possess all the necessary machinery for uptake or membrane integration, assuming these processes occur. However, physiologically appearing EVs face the aforementioned issues of clearance via the immune system.

Regardless of via liposomes or in EVs isolated from appropriate donor cultures, Gpc1-loaded vesicles would pose a fascinating avenue for therapy in SCI. EVs could conceivably be injected intrathecally or epidurally. The former, having the advantage of delivering Gpc1 directly into the cerebrospinal fluid surrounding the spinal cord, but being more invasive and a more complex surgical intervention. The latter, only being delivered outside of the dura, but being less invasive. Both application routes are routine methods practised in most hospitals (Kearns et al., 2024; Traynor et al., 2016). Since SCIs disrupt the blood-spinal-cord-barrier (BSCB) (Noble and Wrathall, 1988) and dorsal root ganglia locating outside of the dura, epidural injection might suffice to deliver Gpc1 to where it can have a therapeutic impact following SCI. With the afore mentioned disruption of the BSCB, systemic administration of EVs could also be possible, however, due to the effect on cancer cell migration observed in Gpc1-overexpressing tumours, that avenue appears the least advisable, while the more invasive intrathecal injections seems most favourable.

The merits of an overexpression screen

To evaluate our GOIs we choose an overexpression screen, focusing on the longest axon as an outcome measure. However, most of the GOIs we detected, were shown to be downregulated upon acquisition of growth competence (28/39) (Fig. 9). Would it then not have been more reasonable to screen the downregulation of these proteins? Partially. Overexpression is easy to achieve and easy to detect. As all constructs from the screen included an HA-tag, I could confirm their overexpression in the image acquisition process. Knock down (KD) or knock out (KO) of a protein is much harder to confirm, and requires specific probes, such as antibodies or quantitative PCR primers, which in turn have to be validated. Achieving KO of a GOI is quite difficult. Techniques such as Cre-Lox mediated KO take months to establish for individual GOIs and are consequently unfeasible for screening 31 GOIs. CRISPR-based KOs are easier to achieve, but still need thorough validation of guides. Furthermore, they require the ectopic expression of multiple vectors, which is quite hard to achieve in samples with few neurons, like our DRG culture, that are additionally hard to transfect. KD via small hairpin RNAs (shRNA) is easier to achieve, but also more prone to off-target effects (Neumeier and Meister, 2020).

Studies with shRNAs routinely use multiple constructs to target the same gene, which would multiply the work involved. Furthermore, both KO and KD follow their own kinetics, meaning it takes some time for the KO/KD to go into effect, and then the depletion of the target protein follows its own kinetic once again. As neurons are long-lived cells, much of their proteome also exhibits exceptionally long half-lives, in the range of days to weeks (Cohen and Ziv, 2019). Consequently, in DRGs, the slow removal of the knocked-down or knocked-out hypothetically growth inhibiting protein might get lost in the inherent high growth competence of cultured DRGs. Of course, it would be possible to KO/KD the GOI before culture, for example via sciatic nerve injection or dorsal root ganglion electroporation (Saijilafu et al., 2011), this however, would require a massive amount of surgeries and could be ethically questioned, with regards to the harm caused to the animals versus the knowledge gained.

An additional issue arises from the difficulty of detecting transfected cells. In our hands, DRGs do not express fluorescent proteins to sufficiently high levels for detection within the first 72 h post plating. When overexpressing a tagged protein, that is less of an issue then when co-expressing an inhibitory RNA or CRISPR components with a fluorescent protein. So, in a hypothetical KO/KD screen, the matter of detecting KO/KD cells would need to be solved.

Finally, on the matter of KO/KD screens, the question arises what value the detection of a candidate has, which decreases axon growth. If the depletion of a protein of interest can be causally linked to an increase in axon growth, that might reveal druggable targets. Indeed, our group has identified two drugs that increase axon growth in models of SCI in this manner, Pregabalin and Baclofen (Hilton et al., 2022; Tedeschi et al., 2016). Some might argue that the downregulation of a pathway is more effortlessly achieved than pathway upregulation. However, our group has also identified beneficial drugs in models of SCI, derived from axon growth activating processes, Taxol and Epothilones (Hellal et al., 2011; Ruschel et al., 2015b). Summarizing, there is no inherent benefit to studying growth inhibitors over growth activators, when the end goal is to identify translatable interventions in SCI.

Thus, the merits of an overexpression screen are easy detectability of overexpression compared to KO/KD, the technical feasibility of the generation and expression of GOI constructs for a large screen, the absence of off-target effects and the maintained possibility to reveal translationally relevant processes.

Analysis of the 30 longest axons

In my screen, I choose to forgo identification of overexpressing cells and analysed the 30 longest axons per culture instead, from images of the whole coverslip. I reasoned, that if a GOI increases growth, the 30 longest axons per culture would be positively transfected. Even if these were not transfected and the growth effect was conferred by overexpressing cells to naïve cells, if the average outcome is a growth increase, that could yield interesting candidates to follow up on. Following this logic, it is not surprising that the largest effect size is produced by a protein that has both an autocrine and paracrine effect (Fig. 11, Fig. 16, and Fig. 20). Additionally, focusing on the 30 longest axons per culture made the comparisons more robust. Firstly, when analysing cells, one always has to choose which cells to analyse. In a highly heterogeneous population of neurons, such as in a DRG culture, there is always a chance to accidentally choose only well growing cells, thus biasing the results of the analysis. By following a simple rule to choose which cells to include in the analysis, I eliminated my own bias which cells to analyse. Secondly, primary cell cultures are highly variable from batch to batch. Axon growth is an exceptional readout for the health and stress level of a cell. Just as famines decrease the growth of humans (Gorgens and Meng, 2007; Portrait et al., 2017), axon length is highly sensitive to any and all changes in their environment. Sheer uncountable factors can influence the overall "happiness" of a culture. Variations in batches of growth factors or the quality of cover slips and even the diameter of pipette tips used for dissociation can affect axons length. In most experimental timelines, these factors can often be neglected, but with hundreds of cultures produced and almost 100.000 axons quantified for one comparison (Table1 and Fig. 11), reducing the variability in the analysis was imperative to avoid false positive or false negative results. Analysing the 30 longest axons per culture empirically showed to quench such variability from the analysis.

Conversely, the question still stands, why analyse the longest axons when most of the overexpressed proteins are expected to hinder growth? The answer is again the technical variability of the primary cultures. Again, axons length is very sensitive to all manner of factors. In a DRG culture following my culture conditions, 30-50% of cells might not even form an axon, irrespective of treatment, so analysing which GOIs make growth worse can be difficult. Additionally, disruptions to cellular pathways might hinder growth, without the pathway itself being directly growth activating. For example, while cells require energy in the form of ATP to grow, supplying cells with more ATP does not on its own boost axon growth. Or, ATP is necessary for growth, but not sufficient to induce it. So, detecting

shorter axons after expression of GOIs requires another step of establishing causality, that is avoided when directly detecting axon growth. Finally, with overexpression of modified proteins, there is always a risk of a loss of function, for example via misfolding or disruption of functional domains. Consequently, there was a chance for each of our overexpression constructs to result in a dominant negative protein, which is partially supported by the 7 GOIs that showed a robust growth effect only in one of the two generated constructs.

Now, is a similar analysis possible for detecting the shortest axons? Analysing the 30 shortest axons would in all likelihood yield the exact same result in all samples. Because of the heterogeneity of DRG cultures there are always 30 neurons which just manage to produce an axon below 10 µm within 72 h. Alternatively, one might analyse the percentage of axons below a certain threshold. This threshold would have to be fine-tuned and experimentally validated, but it could give insights into GOIs that hinder growth. Considering the discussion above about growth hindering interventions, this might still yield interesting insights and should be focus of further studies.

In conclusion, this analysis method was chosen for both practical as well as scientific reasons. It proved effective in enabling me to analyse large data sets of axon growth and filter out at least one, possible multiple, interesting candidates to research axon regeneration.

Gpc1 receptors and downstream pathways

I provided data indicating that the Gpc1 growth effect relies on interactions with cell surface signalling receptors (Fig. 14 and Fig. 15), consistent with the literature on Gpc1 signalling. However, which receptors are involved in the growth effect is not clear. Gpc1 is known to interact with many receptors, including FGFR, VEGFR, TGF-ßRI+II, Frizzled and BMPRI+II (Pan and Ho, 2021). Clearly, deciphering which receptors facilitate the Gpc1 growth effect is a fascinating and impactful question for further study. Downstream of this elusive receptor or receptors, Gpc1 has a major impact on the cytoskeleton. Both, the whole- and phospho proteomics of Gpc1-overexpressing cells strongly implicated the cytoskeleton generally, and the Rho family GTPase RhoA specifically in the Gpc1 axon growth effect (Fig. 21). As the cytoskeleton is the major effector of axon growth and Rho family GTPases are the major effectors of the cytoskeleton, this finding is fully conclusive with the current literature. Interestingly, Gpc1 appears to activate pathways that are similar to physiological growth, as the GO term analysis showed that overexpression of Gpc1 also affects the cells energy metabolism ("mitochondrial part" "succinate dehydrogenase activity"), protein synthesis ("ribosome", "intrinsic component of the endoplasmic reticulum membrane"), production of membranes ("membrane part") and the transcriptome ("14-3-3 protein binding"). This indicates that Gpc1 not only bolsters one process that enables axon regeneration, like for example application of Taxol to stabilize MT (Hellal et al., 2011), but resets the cell to a more growth competent state as a whole. Furthermore, it partly aligns with the GO term analysis of the Tedeschi paradigms -which all reflect growth competent states in DRGs- where "plasma membrane" and "plasma membrane part" were consistently upregulated between growth paradigms (Fig. 8).

Outlook

The presented data positions Gpc1 as a promising candidate to enable axon regeneration through scar tissue in SCIs and as a regenerative therapeutic in other diseases, that are accompanied by the loss of axons. To ensure the efficacy and safety of such therapies, a number of key experiments need be performed on the basic biology of Gpc1 in neurons. The first major question is whether Gpc1-overexpression causes regeneration of the DRG tracts in *in vivo* models of SCI. If so, the next experiments should involve the application of EVs or liposomes in rodent models of SCI. Here, the optimal mean of delivery could be identified. As discussed above, possible application routes would be intrathecal or epidural injections or systemic administration. Gpc1-loaded cuffs or titan nano tubes could also be conceived as drug delivery approaches (Bariana et al., 2018; Elyahoodayan et al., 2020). Of course, the time line of treatment would have to be elucidated. Immediate treatment with Gpc1 following an injury might be beneficial for setting axons in a growth competent state, before the fibrotic scar poses a physical barrier. However, Gpc1 might also affect the migration of other cell types, responsible for wound healing, so later application might be more beneficial. The duration of treatment would have to be carefully determined as well. A fascinating follow up question on any *in vivo* studies would be whether Gpc1-overexpression leads to improvements in motor recovery. To this end, a more severe injury model would be required. In such experiments, Gpc1 treatment could also be combined with other promising approaches for the treatment of SCIs, such as rehabilitation, epothilones or Nogo inhibition.

The receptors which Gpc1 modulates to achieve axon growth are yet elusive. To identify which receptors are involved in the Gpc1 growth effect, western blot analysis or proteomics of Gpc1 pull-downs could be employed. However, membrane-bound proteins are notoriously hard to detect in these methods, so these experiments would have to be thoroughly optimised for their respective targets. It would also be possible to block receptors with antibodies or small molecule inhibitors, however, such approaches are prone to off-target effects and would have to be well controlled. Optimally, a combination of all of these approaches would be utilized to pinpoint which receptors are involved in the Gpc1 growth effect.

It also remains unclear whether it is the Gpc1 on the EVs or the content of the EVs which triggers the growth effect. Here, proteomics of the EVs could inform us, whether they are loaded with specific growth factors. To this end, ELISAs of Gpc1-overexpressing culture media could also be used to detect specific growth factors. This approach, however, would

introduce candidate specific bias, which is absent in the proteomic approach. Then, the question of EV uptake should be investigated. Typically, EVs are internalized via endocytosis and then release their cargo to multi vesicular bodies, which then release specific cargoes to specific subcellular locations (Joshi et al., 2020). For cancer exosomes, this process depends on EV surface HSPG (Christianson et al., 2013), consistent with our data that deletion of HS binding serines hinders the Gpc1 growth effect (Fig. 15). They can, however, also fuse directly with host cells (Papareddy et al., 2024). Deciphering the Gpc1-EV uptake mechanism could have therapeutic implication regarding target cell tropism or engineering EVs to also traffic other compounds that are beneficial to axon regeneration.

Finally, this work opens up many questions of the physiological role of Gpc1. From our data it could be speculated that Gpc1 is a main driver of the regenerative conditioning effect observed upon a PNL. To follow this speculation, KO/KD studies of Gpc1 in DRGs could be informative. If deletion of Gpc1 in DRGs hindered the conditioning effect, that could mean that the retrograde signal described by Smith and Skene (Smith and Skene, 1997) could be derived from Gpc1-positive vesicles. Interestingly, Gpc1 can itself localize to the nucleus (Bloechlinger et al., 2004), so conceivably, Gpc1 itself could be that cue. Furthermore, being a secreted growth signal, Gpc1-positive EVs could confer the regenerative effect that is observed in non-injured ganglia following PNL (Dubovy et al., 2019).

Materials and Methods

Materials

Chemicals

Name	Supplier	Product number
Ammonium chloride	Merck	168320
B-27 Supplement	Life technologies	17504-044
Borax	Sigma	71996
Boric acid	Sigma	B6768
Bovine serum albumin (BSA)	Sigma	A3294
Collagenase IV-S	Sigma Aldrich	C1889
DMEM/F12	Life technologies	11330032
Fetal Calf Serum (FCS)	Invitrogen	10270106
Fish gelatin	Sigma	G7765
Fluoromount mounting medium	Sigma	F4680-25ml
HBSS	Gibco	14025-100
HEPES Buffer solution (1 M)	Gibco	15630-056
Hydrochloric acid (≥37%)	Merck	1003141000
Hydrochloric acid (HCl, 1 N)	Fisher Scientific	124210010
L-Glutamine (200 mM; 100x)	Thermo fisher scientific	25-030-081
Laminin (500 µg/mL)	Roche	11 243 217 001
P3 Primary Cell 4D X Kit S (32 RCT)	Lonza	V4XP-3032
Paraformaldehyde	Roth	0335.3
PBS (10x) powder	AppliChem	A0965
Penicillin/Streptomycin	Life technologies	15140-122
Poly-L-lysine	Sigma	P-2636-1G
Sodium bicarbonate	Merck	1.06329.0500
Sodium chloride (NaCl)	Merck	106404
Sodium hydroxide pellets (NaOH)	Merck	1064821000
Triton X-100	Sigma	X100-100ML
Trypsin-EDTA (0.05%), phenol red	Life technologies	25300096

Drugs

Equipment

Name	Supplier	Model
Anaesthesia system	VetEquip Inc.	931401
Centrifuge	Eppendorf	5427R
Cold light source	Schott	KL 1500 LCD
Fine Scale	Kern	APJ-NM
Hot bead sterilizer	FST	18000-45
Incubator	HERAcell	240i
Magnetic stirrer	IKA	RH Basic 2
Microscope	Zeiss	PrimoVert
Nucleofector	Lonza	4D-Nucleofector Core Unit and X Unit
pH meter	METTLER Toledo	Seven Easy
Pipetting controller	Integra	Pipetboy
Scale	Scout	Scout Pro 400g
Stereomicroscope	Leica	M651
Sterile hood	Thermo Scientific	SAFE 2020
Tabletop centrifuge	Corning LSE	Mini Microcentrifuge
Temperature Controller	WPI	ATC 1000
Thermo oven	Thermo Scientifc	HERA THERM
Ultra-centrifuge	Optima	L80-XP
Vacuum pump	Vacuubrand	BVC21
Vortex	Corning LSE	VortexMixer
Waterbath	Thermo Fisher	Lab Armor

Surgery materials

Name	Supplier	Product number
Askina gauze compress 7.5x7.5 cm	B. Braun Melsungen AG	9031316
Baytril 2.5% Vet injection solution (Enrofloxacin)	Bayer	03543238

Bepanthen. Eye- and nose ointment	Bayer Vital GmbH	PZN1578675
Braunol. povidon iodine solution	B. Braun Melsungen AG	3864235
Dumont #5 forceps	Fine Science Tools	11251-30
Friedman Pearson Rongeur	Fine Science Tools	16221-14
Glucose 5% (G5) solution – 100 ml	B. Braun Melsungen AG	3154910
Metacam. (Meloxicam)	Boehringer Ingelheim	PZN 8890217
Noyes Spring Scissors	Fine Science Tools	15514-12
Scalpel blades #10	Fine Science Tools	10010-00
Scalpel handle #3 – 12 cm	Fine Science Tools	10003-12
Sofsilk 4.0 suture material	Covidien	S-1174
Sugi. – Sterile Absorption Spears	Kettenbach Medical	30601
Vannas Spring Scissors	Fine Science Tools	15000-00
Vetflurane (Isoflurane)	Virbac	24279 WDT
Wound clip applicator	Fine Science Tools	12018-12
Wound clips Reflex 7	CellPoint Scientific	203-1000

Consumables

Name	**Supplier**	**Product number**
4 well dish Nunclon Delta Surface	Thermo Scientific	176740
13 mm, #01-115 30	Marienfeld	0111530
Amicon Ultra-15, PLTK Ultracel-PL Membran, 30 kDa	Merck	UFC903024
Eppendorf tubes 1.5 mL, 2 mL	Eppendorf	VB-0306
Falcon 70 µm cell strainer	Neolab	352350
Falcon tubes 15 mL, 50 mL	Corning	CLS430053-500EA
Frosted Microscope Slides, 90°	Fisher Scientific	16245172
MaxiSorp Immuno Plates	Thermo Scientific	442404

Pipette filter tips	nerbeplus	06-602-5300, 06-662-5300, 06-695-5300
Pipette tips	nerbeplus	06-360-2018, 06-375-2018, 06-379-2018

Media, buffers, and solution

Name	**Recipe**	**Preparation and storage**
Ammonium chloride 50 mM for quenching	1.34 g ammonium chloride in 500 mL PBS	Store at RT
Blocking solution	2% fetal calf serum 2% bovine serum albumin 0.2% fish gelatin in dH2O	Aliquot and store at -20 °C
Borate buffer	1.24 g boric acid 1.9 g Borax (Sodium borate) in 400 mL H2O	Adjust to pH 8.5
CD dialysis buffer	20 mM KH2PO4 50 mM Na2SO4	Adjust pH to pH 7.4
Collagenase solution	Dissolve 50 mg in DMEM/F12 to achieve min. 1000 U/mL Collagen activity and 2 U/mL FALGPA activity	Aliquot in 20 µL and store at -20 °C
Digestion media	1.8 mL DMEM/F12 + FCS 200 µL Collagenase solution	Make fresh for DRG culture

DMEM/F12 complete	48 mL DMEM/F12 0.5 mL Pen/Strep (100x) 0.5 mL L-Glutamine (100x) 1 mL B-27 supplement	Filter sterilize with 0.22 µm filter and store at 4 °C, Use within a week
DMEM/F12+FCS	45 mL DMEM/F12, 5 mL FCS 0.5 mL Pen/Strep (100x)	Filter sterilize with 0.22 µm filter and store at 4°C, Use within a week
ELISA blocking solution	4% milk powder In PBS-T	Always use fresh
HBSS + HEPES	5 mL Hepes (1 M, pH 7.25) in 500 mL HBSS	Store at 4°C
Laminin solution	Laminin (500 µg/mL) in PBS (1:200)	Prepare fresh before coating cover slips
5x Laemmli buffer	4 ml 1.5 M Tris-Cl pH 6.8 10 ml glycerol 5 ml 2-mercaptoethanol 2 g sodium dodecyl sulfate 1 ml 1% bromophenol blue	Store aliquots at -20 °C
20 x MOPS Buffer	52.31 g MOPS 30.29 g Tris-Base 5 g SDS 10 mL 0.5 M EDTA Fill up to 250 mL with ddH_2O	Dilute to 1x before use
Paraformaldehyde/sucrose	16 g	Adjust to pH 7.4, filter

(16%) for ICC	Paraformaldehyde 16 g sucrose in 100 ml PBS	sterilize, aliquot and store at -20 °C, 4% dilutions are prepared from this stock in PBS
PBS	114.9 g Na_2HPO_4 26.41 g NaH_2PO_4 90 g NaCl Add 1000 mL with H2O	Add ingredients and preheat to 50°C until solution is clear, adjust pH to 7.4 with HCl or NaOH, store at RT
PBS-T	0.1 % Tween20 In PBS	Store at RT
Poly-L-lysine solution (PLL)	1 mg/mL poly-Lysine hydrobromide in borate buffer	Solution is sterile filtered and stored at 4°C for up to 1 week
10x TBS	48.4 g Trizma (Tris) 160 g NaCl Adjust pH to 7.6 with HCl Fill up to 2 L with ddH_2O	Dilute to 1x before use
10x Transfer Buffer	144 g Glycine 30 g Tris Fill up to 1 L with ddH_2O	Dilute to 1x before use, including 20% methanol
Triton 0.1%	5 mL Triton X-1000 45 mL PBS Dilute this 1:100 in PBS	Store at RT
Trypsin 0.05%	100 mL Trypsin/EDTA 700 µL HEPES	Aliquot and store at -20°C

Antibodies

Target	Host species	Dilution	Supplier	Product number
ßIII-Tubulin	Mouse	1:500	BioLegend	801201
ßIII-Tubulin	Rabbit	1:1000	Sigma Aldrich	T2200
CD9	Rabbit	1:1000	Cell Signaling Technology	13403
Gpc1	Rabbit	1:500	Thermo Fisher Scientific	PA5-28055
HA-tag	Mouse	1:500	Abcam	ab49969
HA-tag	Rabbit	1:500	Cell Signaling Technology	3724
Alexa Fluor. 488 Anti-Mouse	Goat	1:1000	Invitrogen	A11029
Alexa Fluor. 488 Anti-Rabbit	Goat	1:1000	Invitrogen	A11034
Alexa Fluor. 555 Anti-Mouse	Goat	1:1000	Invitrogen	A21422
Alexa Fluor® 555 Anti-Rab-bit	Donkey	1:1000	Invitrogen	A31572
Alexa Fluor® 647 Anti-mouse	Donkey	1:1000	Invitrogen	A31571
Alexa Fluor® 647 Anti-Rab-bit	Goat	1:1000	Invitrogen	A21244

Methods

Animals

All animal experiments were conducted in accordance with the Animal Welfare Act and the guidelines of the Landesamt für Natur, Umwelt und Verbraucherschutz (LANUV). Adult wildtype female mice (C57BL/6J) were purchased from Janiver Labs or Charles River or bred in house. Wildtype animals were used in experiments between 8-16 weeks of age. The wildtype mice used were predominantly female.

DRG culture

Adult mice were sacrificed with CO_2 using a Medres rodent euthanasia system. Afterwards, the spine was excised, and opened rostral-caudally. The first lumbar (L1) DRG was identified via its position below the lowest rib. The DRGs where collected in Hank's buffered salt solution + 7 mM HEPES before being washed once in DMEM for washes and digested in 500 µL collagenase solution at 37 °C for 45 min. Consequently, the ganglia were washed three times and digested in 500 µL 0.05% trypsin at 37 °C for 10 min. After two washes in 1000 µL DMEM + FCS, the ganglia were dissociated mechanically in 1000 µL DMEM + FCS via a P1000 pipette. Following filtration through a 70 µm nylon mesh, the filter was washed with 500 µL DMEM + FCS, the cell suspension was transferred into a clean tube and centrifuged for 6.5 min at 100 x*g*. For nucleofection, the cell pellet was resuspended in 20 µL P3 solution with 3 µg of DNA. After nucleofection with the program "Neuron, rat, brain Hi/Cx HE" using the Lonza P3 Primary Cell 4D-Nucleofector™ X Kit S, cells where quickly mixed with 100 µL of warm culture media and incubated at 37 °C for 10 min. After this recovery period, 140 µL of the neuron solution were recovered from the cuvette and mixed into 1900 µL culture media. Neurons were then plated on two poly-L-lysine (PLL) coated coverslips (1 mg/mL, 37 °C for 1 h) per mouse. For experiments with CSPGs, after coating with PLL, the coverslips were washed and then coated with 5 mg/mL Laminin plus 3 µg/mL in PBS. For the 6 h – 36 h cell culture time points in paradigm two, cells were plated on coverslips coated with PLL and Laminin. For the media transfer experiments, the media was collected from two overexpressing cultures and concentrated in 30 kD molecular weight cut off membrane filter tubes (Amicon Ultra-15, PLTK Ultracel-PL Membran, 30 kDa) at 4000 x*g* at 4 °C for 10 min. The concentrated media was then mixed with fresh culture media at a 1:6 ratio before using it to plate non-nucleofected cells.

Anaesthesia, analgesia and general (post) surgical care

At different time points and project-dependent, surgeries were conducted according to different protocols approved by LANUV. As such some details of surgical interventions differ between experiments. Where medications had to be replaced for animal welfare reasons, great care was taken that new medications would not interfere with the experimental purposes of the respective surgeries.

For conditioning lesions, animals were anesthetized in 5% (v/v in O_2) isoflurane, before being transferred to a respirator that supplied 2-2.5% isoflurane for the duration of the surgery. Eye ointment was applied to prevent drying of the eyes. Baytril (5 mg/kg) was administered subcutaneously as an antibiotic.

Early sciatic nerve lesions, as for the sample generation for the proteomics data, were conducted using Metacam (0.5 mg/mL, 50 µL) once a day for two days post-surgery for analgesia. Later surgeries used Tramadol (1mg/mL in drinking water) from one day before surgery until three days after surgery, plus Buprenorphine (0.1 mg/kg) 30 min before the surgery and 4-6 h after the first injection for pain management. Before being removed from the anaesthesia, all animals received 10 µL/g glucose (5%) subcutaneously to counteract fluid loss during surgery and were left to wake up on a 37 °C heat pad or under a UV heat lamp.

Conditioning lesion

After confirming complete anaesthesia by testing the interdigital- and tail-base reflex, the hindlimbs of the animal were shaved and the incision site disinfected with 70% ethanol and Braunol or just Braunol. The animal was then turned onto its side and the hip ridge was located. An incision was made into the skin via scalpel below the hip ridge at mid-thigh level. The muscle was then punctured with scissors and bluntly dissected. The sciatic nerve was localized and carefully propped up via fine tweezers. The nerve was ligated and transected distally to the ligation site. Consequently, the skin was clamped and the animals were left to recover for 7 days before dissection of the dorsal root ganglia. For experiments in cell culture, both sciatic nerves were lesioned.

Generation of expression vectors and viruses

All vectors were generated via NEB HiFi assembly. GOIs were fished from murine cDNA libraries generated via the SuperScript™ VILO™ cDNA Synthesis Kit. For GOIs from the screen, some genes were first cloned into a pJet expression vector, before generating overhang fragments for HiFi assembly. To this end, Primer-Blast (Ye et al., 2012) was used to generate a primer pair 100-300 bp upstream and downstream of the coding sequence of transcript version 1 of the respective GOI. After blunt-end ligating this product into the pJet vector using the CloneJET PCR Cloning Kit and validating the sequence, this vector was used as a specific template for adding 20 bp overhangs to the coding sequence for assembly. In the screen, a pAAV1 vector harbouring the C- or N-terminal 3xHA tag was linearized using NotI and XhoI restriction sites. Via the corresponding overhangs, the GOIs were inserted into these vectors to generate the N- and C-tagged constructs. All transfections were carried out in NEB® Stable Competent *E. coli* to preserve viral inverted terminal repeats.

To generate functional KOs of Gpc1, primers were generated to exclude the respective domains. The generated fragments were cloned into the same above vector. To introduce point mutations, assembly primers with long overhangs (25-35 bp) were generated, that included the desired point mutations in the binding region. This fragment was then assembled with another fragment covering the rest of Gpc1 into the same above vector. All sequences were confirmed via Sanger sequencing.

Immunocytochemistry

Cells were fixed with 4% PFA at RT for 20 minutes, washed 3x with PBS, quenched with 50 mM NH_4Cl at RT for 15 min, washed 3x with PBS and permeabilized with 0.1% triton in PBS at RT for 3 min. Consequently, cells were blocked in blocking solution at RT for 1 h and incubated with primary antibodies in 10% blocking solution in PBS. After washing 3x in PBS, secondary antibodies were applied in 10% blocking solution in PBS, before washing 3x in PBS and 1x in distilled water before mounting onto microscopy slides using Fluoromount. Both antibody incubations at RT for 1 h. Before microscopy, slides were allowed to dry at RT protected from light for a minimum of 16 h.

Enzyme-linked immunosorbent assay

Cell culture media were used either immediately after collecting from the cultures, or after flash freezing in liquid nitrogen and storage at -80 °C. 100 µL of media were applied to Nunc 96-Well Flat Bottom MaxiSorp Immuno Plates and incubated at 4 °C over night. Consequently, the medium was discarded and wells were blocked with 200 µL ELSIA blocking solution at 37 °C for 2 h, washed 3x with 200 µL PBS-T and 3x with 200 µL PBS, before applying 100 µL of the primary antibody in ELISA blocking solution at 4 °C over night with mild agitation. After discarding the primary antibody, the wells were washed as before, and 100 µL of the secondary antibody in ELISA blocking solution were added. Following RT incubation for 2 h with mild agitation, the secondary antibody was discarded and the wells were washed as before, while taping on tissue paper to remove excess washing buffers. Consequently, 100 µL of TMB were added to each well and incubated in the dark at RT for 30 min. The reaction was stopped with 100 µL 1 M HCl, before measuring the absorption at 450 nm.

Microscopy

Imaging of whole cover slips was conducted using a fully motorized AxioObserver.D1(Zeiss) inverted epifluorescence widefield microscope. Up to 4 microscopy slides were mounted onto the sample holder before setting up the tile scan regions for the individual cover slips in the ZenBlue software. To this aim, a 13 mm circular tile region was created and its edge was aligned with the edge of the actual cover slip. To maintain focus, a 9-point focus map was generated to capture the focus plane of the axons. After acquisition, the tile regions were stitched from a 10% overlap and the scenes were split before saving.

Mass-spectrometry of DRG growth states

For paradigm one, embryonic developmental stage, the lumbar DRGs of 4 embryos were collected in ice cold HBSS at E12.5 and E17.5. After centrifugation at 21000 x*g* at 4 °C for 5 min, the media was removed and the ganglia were flash frozen on dry ice. For paradigm two, *in vitro* time points, the cultures were prepared as above from 4 animals per sample and the cells were harvested by washing with ice cold PBS once, scraping the cells in PBS and centrifugation at 21000 x*g* at 4 °C for 5 min. Consequently, the media was removed and the cells were flash frozen on dry ice. For paradigm three, peripheral nerve

lesion, surgeries and isolation of the ganglia was performed as described above. After isolation the ganglia were centrifuged and frozen as were the embryonic ganglia.

Consequently, DRGs were prepared for MS proteome analysis by in-solution digestion. DRGs were lysed in urea buffer (6 M urea, 2 M thiourea), incubated for 15 min, and sonicated to facilitate lysis. Protein concentrations were determined using the Pierce Protein Assay (Thermo Fisher). BSA standard solutions (0.05 mg/mL to 1.0 mg/mL) were generated by diluting 2 mg/mL BSA solution (Thermo Fisher). Protein samples were diluted 1:10 in H2O and absorption was measured at 660 nm using an EnSpire® Multimode Plate Reader (Perkin Elmer). 30 µg of each sample were reduced and alkylated by applying (tris(2-carboxyethyl)phosphine) TCEP at a final concentration of 10 mM and chloroacetamide (CAA) at a final concentration of 40 mM at room temperature (RT) for 1 h. The samples were incubated with LysC at an enzyme:substrate ratio of 1:100 at RT for 2 h, diluted to a urea concentration of 2 M with 50 mM ammonium bicarbonate (ABC), and incubated with trypsin at an enzyme:substrate ratio of 1:100 at RT overnight. Digestion was stopped by acidifying the samples with formic acid (FA) to a final concentration of 1% and purified using StageTips(Rappsilber et al., 2007). In brief, StageTips (containing two layers of styrene divinylbenzene-reverse phase sulfonate (SDB-RPS) in a 200 µl pipette tip) were equilibrated by loading 20 µl methanol followed by centrifugation at 500 x*g* for 2 minutes. This step was repeated once with 20 µl of buffer B (0.1% FA, 80% ACN) and twice with 20 µl of buffer A (0.1% FA). After equilibration, the acidified samples were loaded onto the StageTips and the samples were centrifuged at 500 x*g* for 5 minutes. After loading, the StageTips were washed once with 30 µl buffer A and twice with 30 µl buffer B centrifuging at 500 x*g* for 3 minutes in between. The StageTips were finally dried using a syringe and stored until further use at 4 °C. To elute the proteins for mass spectrometry analysis, 30 µl 1% ammonia in 60% ACN were added onto the StageTips and incubated for 15 minutes. Elution into a 96-well plate was performed manually by using a syringe. The plate was then dried in a Speed Vac and 10 µl buffer R (0.1% FA, 5% ACN) were added before measurement.

Phosphoproteomics of Gpc1-overexpressing DRGs

Samples were analyzed by the CECAD Proteomics Facility on an Orbitrap Exploris 480 mass spectrometer (Thermo Scientific, granted by the Deutsche Forschungsgemeinschaft

INST 216/1163-1 FUGG) coupled to an Evosep ONE. The Evosep was run with its Whisper Zoom 20 SPD gradient using the recommended column, the mass spectrometer was operated using a WHISH-DIA approach (Petrosius et al., 2023). MS2 spectra were acquired in the range of 400 to 1000 m/z at 60k resolution in 15 m/z windows, resulting in 40 scans total. Fragments were acquired in a range of 250 to 1500 m/z with a normalized AGC target of 1000% and 30% normalized HCD collision energy. Every 10 scans, an MS1 scan was inserted, which was acquired at a resolution of 180k in the range of 390 – 1010 m/z and 300% AGC target.

Samples were analyzed in Spectronaut 19 (Biognosys) in directDIA mode using the canonical murine Uniprot reference database (UP0589, downloaded 15/01/24) and standard settings, but quantifications were performed on MS1 level. For phospho analyses, PTM localization filter was set a threshold of 0.75. Afterwards, reports were loaded into Perseus 1.6.15 (Tyanova et al., 2016), wrongly quantified signals removed and filtered for data completeness in at least one comparison group. Afterwards, FDR-controlled T-tests were performed.

Extracellular vesicle isolation and quantification

Extracellular vesicles (EV) were harvested from overexpressing cell cultures at 72 h post plating. The medium was filtered through a 0.8 µm syringe filter and then processed as per the exoEasy Maxi Kit instructions. All optional steps from the protocol were included. The EVs were eluted in 300 µL of the supplied elution buffer. For use in cell culture, the eluted fraction was diluted to a total volume of 1.5 mL with PBS. Consequently, EVs were pelleted at 100.000 x*g* at 4 °C for 1 h washed once in 1.5 mL PBS, pelleted again, and then diluted into an appropriate amount of PBS. For quantification of EVs, the Zeta View particle reader with the respective software were used. Before measurement, the device was set to a chamber temperature of 22 °C, and allowed to fully come to temperature for about 4 h. Before each measurement, the device was thoroughly rinsed with 20 mL of fresh sterile ddH_2O. Then, the device was calibrated with the particle standard at a sensitivity of 85 and a shutter speed of 120. Measurements were conducted with appropriate dilutions of the samples, ranging from 1:1000 – 1:5000, averaging 11 positions over 3 cycles.

Western blot

For western blot of EV samples, EVs were concentrated via ultracentrifugation as described above omitting the second wash. Consequently, the pellet was resuspended in a

small volume of PBS. Samples were then mixed with 6x Laemmli buffer and boiled at 95 °C for 10 minutes, before loading onto 4-12% Bis-Tris gradient gels. After running the gel to completion at 120-150 V in 1x MOPS buffer, the proteins were transferred to a PVDF membrane at 240 mA per gel in 1x transfer buffer with 20% methanol. Consequently, the membrane was washed once with TBS-T before blocking in 4% milk in TBS-T for 1 h. Antibodies diluted in 4% milk in TBS-T were added after blocking and incubated either at RT for 2 h or at 4 °C overnight, in both variants under agitation. Subsequently, the membranes were washed 3x with TBS-T for 10 min each. Secondary antibodies were applied at RT for 2 h. Following three washes as above, the blots' chemiluminescence was read a ChemiDoc imaging system, using Pierce ECL reagent pico or dura.

Size exclusion chromatography and circular dichroism measurement

For size-exclusion chromatography, 110 µg of Gpc1_trunc were diluted in 200 µL PBS and run on a Superdex™ 200 Increase 10/300 SEC column connected to an Aekta Pure FPLC System (Cytiva) against PBS, the absorbance at 254 and 280 nm was monitored. Fractions of 500 µL were collected until 29 mL were eluted. The two fractions below the peak from 14-15 mL were pooled and analysed in SDS-PAGE, showing a clear band at the molecular weight for Gpc1 (ca. 60 kDA, data not shown). For a circular dichroism measurement, the same sample was dialysed against 80 mL CD dialysis buffer at 4 °C, with slight agitation overnight. Consequently, 500 µl protein solution (c = 0.04 mg/ml) were measured in a CD spectrometer at 10 °C from 185-265 nm to detect circular dichroism.

Use of generative artificial intelligence

Generative artificial intelligence (AI), was used to aid in the generation of python scripts and ImageJ macros, for the analysis of experimental data. Furthermore, the large language models ChatGPT and Perplexity.ai were used in the discovery of relevant literature. No text or images generated by AI were copied over into this manuscript.

Analysis

Length of the longest axon and 30 longest axons per culture

Images of whole cover slips were converted into 8bit files, where necessary split into their different channels and saved as .tiff files. Whenever possible, image files were blinded before analysis. The longest axons were then annotated manually for the whole coverslip using NeuronJ (Meijering et al., 2004). Where applicable, the data was sorted via a custom python script to output the 30 longest axons per condition.

Growth state MS-based proteome analysis

Proteome samples were analyzed using a liquid chromatography tandem mass spectrometry set up in a Q-Exactive™ Plus Hybrid Quadrupole-Orbitrap™ (Thermo Fisher). Chromatographic peptide separation was achieved on PoroShell 120 packed 50 cm analytical columns coupled to an EASY-nLC 1000 HPLC system and a binary buffer system consisting of buffer A (0.1% FA) and B (0.1% FA, 80% ACN). Samples were analyzed over a 240 min gradient, raising the content of buffer B from 5 to 34% over 215 min, from 34 to 55% over 5 min, and from 55% to 90% over 5 min. This was followed by washing with 90% buffer B for 5 min, reducing buffer B to 5% over 5 min and re-equilibration with 5% buffer B over 5 min. Full MS spectra (300–1750 m/z) were recorded at a resolution (R) of 70000, maximum injection time (max. IT) of 20 ms and AGC target of 3e6. The ten most abundant ion peptides in each full MS scan were selected for HCD fragmentation at nominal collisional energy (NCE) of 28. MS2 spectra were recorded at R = 17500, maximum IT of 60 ms, and AGC target of 5e5.

Growth state MS data processing and analysis

Raw MS data were analyzed using MaxQuant analysis software and the implemented Andromeda software (1.5.3.8)(Cox and Mann, 2008; Cox et al., 2011). Peptides and proteins were identified using the mouse UniProt database with common contaminants. All MaxQuant parameters were set to default values. Trypsin was selected as the digestion enzyme; a maximum of two missed cleavages was allowed.

Methionine oxidation and N-terminal acetylation were set as variable modifications; carbamidomethylation of cysteines was chosen as a fixed modification. The label-free quantification (LFQ) algorithm was used to quantify the measured peptides and the “match between runs” option was enabled to quantify peptides with a missing MS2 spectrum.

Statistical analysis was performed using Perseus (1.5.5.3-1.6.5.0) software. Potential contaminants and reverse peptides were excluded, and values were log2 transformed. Two-sided t-tests were used to identify differentially expressed proteins between conditions. Identified peptides were annotated with the following Gene Ontology terms: Biological Process, Molecular Function, Cellular Compartment, and the Reactome database terms. Graphical visualizations were achieved using Instant Clue software (Nolte et al., 2018).
The canonical pathway analysis were generated through the use of QIAGEN IPA (QIAGEN Inc., https://digitalinsights.qiagen.com/IPA) (Kramer et al., 2014).

Gene ontology of proteomics data

Gene ontology (GO) analysis was conducted in the Gene Ontology enRIchment anaLysis and visuaLizAtion tool (GORILLA) web application (Eden et al., 2007; Eden et al., 2009). Unranked target and background lists of respective protein gene names were compared to the Mus musculus GO term database. For whole proteomics, respective gene names were separated into lists of significantly up or downregulated proteins and compared separately, to the background list of all detected proteins. For phospho proteomics, the target list included all proteins which significantly changed at least one phosphorylation site while the background list consisted of all proteins for which at least one phospho peptide was detected. Directionality of change and the effect of specific site phosphorylation were not considered.

Statistics

Analysis was performed with GraphPad Prism 10. Where only two groups are compared a Student's t-Test was performed, whereas multiple comparison were drawn via ANOVA with a post-hoc test applicable to the respective experimental design. Which comparisons were made is indicated in the respective figure legends.

References

Adel, I., Mahmoud, H.A., Khater, A.I., and Hafez, F.S. 2025. Diagnostic value of glypican-1; a new marker differentiating pulmonary squamous cell carcinoma from adenocarcinoma: immunohistochemical study on Egyptian series. *Clin Exp Med* 25:35.

Ahnert-Hilger, G., Holtje, M., Grosse, G., Pickert, G., Mucke, C., Nixdorf-Bergweiler, B., Boquet, P., Hofmann, F., and Just, I. 2004. Differential effects of Rho GTPases on axonal and dendritic development in hippocampal neurones. *J Neurochem* 90:9-18.

Alfadil, E., and Bradke, F. 2023. Moving through the crowd. Where are we at understanding physiological axon growth? *Semin Cell Dev Biol* 140:63-71.

Alizadeh, A., Dyck, S.M., and Karimi-Abdolrezaee, S. 2019. Traumatic Spinal Cord Injury: An Overview of Pathophysiology, Models and Acute Injury Mechanisms. *Front Neurol* 10:282.

Altmann, K.H., Wartmann, M., and O'Reilly, T. 2000. Epothilones and related structures--a new class of microtubule inhibitors with potent in vivo antitumor activity. *Biochim Biophys Acta* 1470:M79-91.

Alto, L.T., and Terman, J.R. 2017. Semaphorins and their Signaling Mechanisms. *Methods Mol Biol* 1493:1-25.

Arakawa, Y., Bito, H., Furuyashiki, T., Tsuji, T., Takemoto-Kimura, S., Kimura, K., Nozaki, K., Hashimoto, N., and Narumiya, S. 2003. Control of axon elongation via an SDF-1alpha/Rho/mDia pathway in cultured cerebellar granule neurons. *J Cell Biol* 161:381-391.

Bandtlow, C.E., and Zimmermann, D.R. 2000. Proteoglycans in the developing brain: new conceptual insights for old proteins. *Physiol Rev* 80:1267-1290.

Bannach, C., Brinkert, P., Kuhling, L., Greune, L., Schmidt, M.A., and Schelhaas, M. 2020. Epidermal Growth Factor Receptor and Abl2 Kinase Regulate Distinct Steps of Human Papillomavirus 16 Endocytosis. *J Virol* 94:

Bariana, M., Dwivedi, P., Ranjitkar, S., Kaidonis, J.A., Losic, D., and Anderson, P.J. 2018. Glypican-based drug releasing titania implants to regulate BMP2 bioactivity as a potential approach for craniosynostosis therapy. *Nanomedicine* 14:2365-2374.

Barnat, M., Benassy, M.N., Vincensini, L., Soares, S., Fassier, C., Propst, F., Andrieux, A., von Boxberg, Y., and Nothias, F. 2016. The GSK3-MAP1B pathway controls neurite branching and microtubule dynamics. *Mol Cell Neurosci* 72:9-21.

Bian, Y., The, M., Giansanti, P., Mergner, J., Zheng, R., Wilhelm, M., Boychenko, A., and Kuster, B. 2021. Identification of 7 000-9 000 Proteins from Cell Lines and Tissues by Single-Shot Microflow LC-MS/MS. *Anal Chem* 93:8687-8692.

Bielefeld, P., Martirosyan, A., Martin-Suarez, S., Apresyan, A., Meerhoff, G.F., Pestana, F., Poovathingal, S., Reijner, N., Koning, W., Clement, R.A., Van der Veen, I., Toledo, E.M., Polzer, O., Dura, I., Hovhannisyan, S., Nilges, B.S., Bogdoll, A., Kashikar, N.D., Lucassen, P.J., Belgard, T.G., Encinas, J.M., Holt, M.G., and Fitzsimons, C.P. 2024. Traumatic brain injury promotes neurogenesis at the cost of astrogliogenesis in the adult hippocampus of male mice. *Nat Commun* 15:5222.

Biswas, S., and Kalil, K. 2018. The Microtubule-Associated Protein Tau Mediates the Organization of Microtubules and Their Dynamic Exploration of Actin-Rich Lamellipodia and Filopodia of Cortical Growth Cones. *J Neurosci* 38:291-307.

Blanchette, C.R., Perrat, P.N., Thackeray, A., and Benard, C.Y. 2015. Glypican Is a Modulator of Netrin-Mediated Axon Guidance. *PLoS Biol* 13:e1002183.

Bloechlinger, S., Karchewski, L.A., and Woolf, C.J. 2004. Dynamic changes in glypican-1 expression in dorsal root ganglion neurons after peripheral and central axonal injury. *Eur J Neurosci* 19:1119-1132.

Bock, T., Turk, C., Aravamudhan, S., Keufgens, L., Bloch, W., Rozsivalova, D.H., Romanello, V., Nogara, L., Blaauw, B., Trifunovic, A., Braun, T., and Kruger, M. 2021. PERM1 interacts with the MICOS-MIB complex to connect the mitochondria and sarcolemma via ankyrin B. *Nat Commun* 12:4900.

Bond, A.M., Bhalala, O.G., and Kessler, J.A. 2012. The dynamic role of bone morphogenetic proteins in neural stem cell fate and maturation. *Dev Neurobiol* 72:1068-1084.

Bouquet, C., Soares, S., von Boxberg, Y., Ravaille-Veron, M., Propst, F., and Nothias, F. 2004. Microtubule-associated protein 1B controls directionality of growth cone migration and axonal branching in regeneration of adult dorsal root ganglia neurons. *J Neurosci* 24:7204-7213.

Boyer, N.P., and Gupton, S.L. 2018. Revisiting Netrin-1: One Who Guides (Axons). *Front Cell Neurosci* 12:221.

Bradbury, E.J., and Burnside, E.R. 2019. Moving beyond the glial scar for spinal cord repair. *Nat Commun* 10:3879.

Bradbury, E.J., Moon, L.D., Popat, R.J., King, V.R., Bennett, G.S., Patel, P.N., Fawcett, J.W., and McMahon, S.B. 2002. Chondroitinase ABC promotes functional recovery after spinal cord injury. *Nature* 416:636-640.

Bradke, F., and Dotti, C.G. 1999. The role of local actin instability in axon formation. *Science* 283:1931-1934.

Bradke, F., and Dotti, C.G. 2000. Establishment of neuronal polarity: lessons from cultured hippocampal neurons. *Curr Opin Neurobiol* 10:574-581.

Brunet, A., Datta, S.R., and Greenberg, M.E. 2001. Transcription-dependent and -independent control of neuronal survival by the PI3K-Akt signaling pathway. *Curr Opin Neurobiol* 11:297-305.

Burton, P.R., and Paige, J.L. 1981. Polarity of axoplasmic microtubules in the olfactory nerve of the frog. *Proc Natl Acad Sci U S A* 78:3269-3273.

Burute, M., Jansen, K.I., Mihajlovic, M., Vermonden, T., and Kapitein, L.C. 2022. Local changes in microtubule network mobility instruct neuronal polarization and axon specification. *Sci Adv* 8:eabo2343.

Campa, C.C., Ciraolo, E., Ghigo, A., Germena, G., and Hirsch, E. 2015. Crossroads of PI3K and Rac pathways. *Small GTPases* 6:71-80.

Cao, L., Li, F., Cai, S., Zhang, J., Guo, C., Ali, S., Zhou, J., Jing, X., Wang, X., Qin, Y., and Wu, F. 2024. Pan-cancer analysis and the oncogenic role of Glypican 1 in hepatocellular carcinoma. *Sci Rep* 14:15870.

Carmeliet, P., and Ruiz de Almodovar, C. 2013. VEGF ligands and receptors: implications in neurodevelopment and neurodegeneration. *Cell Mol Life Sci* 70:1763-1778.

Caroni, P., and Schwab, M.E. 1988a. Antibody against myelin-associated inhibitor of neurite growth neutralizes nonpermissive substrate properties of CNS white matter. *Neuron* 1:85-96.

Caroni, P., and Schwab, M.E. 1988b. Two membrane protein fractions from rat central myelin with inhibitory properties for neurite growth and fibroblast spreading. *J Cell Biol* 106:1281-1288.

Carulli, D., de Winter, F., and Verhaagen, J. 2021. Semaphorins in Adult Nervous System Plasticity and Disease. *Front Synaptic Neurosci* 13:672891.

Chacon, M.R., Navarro, A.I., Cuesto, G., del Pino, I., Scott, R., Morales, M., and Rico, B. 2012. Focal adhesion kinase regulates actin nucleation and neuronal filopodia formation during axonal growth. *Development* 139:3200-3210.

Chandrasekaran, A., Giniger, E., and Papoian, G.A. 2022. Nucleation causes an actin network to fragment into multiple high-density domains. *Biophys J* 121:3200-3212.

Chen, G., Wu, H., Zhang, L., and Wei, S. 2020. High glypican-1 expression is a prognostic factor for predicting a poor clinical prognosis in patients with hepatocellular carcinoma. *Oncol Lett* 20:197.

Chitti, S.V., Kang, T., Fonseka, P., Marzan, A.L., Stewart, S., Shahi, S., Bramich, K., Ang, C.S., Pathan, M., Gummadi, S., and Mathivanan, S. 2023. Proteomic analysis of the small extracellular vesicles and soluble secretory proteins from cachexia inducing and non-inducing cancer cells. *Proteomics* 23:e2100314.

Christianson, H.C., Svensson, K.J., van Kuppevelt, T.H., Li, J.P., and Belting, M. 2013. Cancer cell exosomes depend on cell-surface heparan sulfate proteoglycans for their internalization and functional activity. *Proc Natl Acad Sci U S A* 110:17380-17385.

Cohen, L.D., and Ziv, N.E. 2019. Neuronal and synaptic protein lifetimes. *Curr Opin Neurobiol* 57:9-16.

Coles, C.H., and Bradke, F. 2015. Coordinating neuronal actin-microtubule dynamics. *Curr Biol* 25:R677-691.

Cox, J., and Mann, M. 2008. MaxQuant enables high peptide identification rates, individualized p.p.b.-range mass accuracies and proteome-wide protein quantification. *Nat Biotechnol* 26:1367-1372.

Cox, J., Neuhauser, N., Michalski, A., Scheltema, R.A., Olsen, J.V., and Mann, M. 2011. Andromeda: a peptide search engine integrated into the MaxQuant environment. *J Proteome Res* 10:1794-1805.

Da Silva, J.S., Medina, M., Zuliani, C., Di Nardo, A., Witke, W., and Dotti, C.G. 2003. RhoA/ROCK regulation of neuritogenesis via profilin IIa-mediated control of actin stability. *J Cell Biol* 162:1267-1279.

Dateki, M., Horii, T., Kasuya, Y., Mochizuki, R., Nagao, Y., Ishida, J., Sugiyama, F., Tanimoto, K., Yagami, K., Imai, H., and Fukamizu, A. 2005. Neurochondrin negatively regulates CaMKII phosphorylation, and nervous system-specific gene disruption results in epileptic seizure. *J Biol Chem* 280:20503-20508.

Davy, A., Gale, N.W., Murray, E.W., Klinghoffer, R.A., Soriano, P., Feuerstein, C., and Robbins, S.M. 1999. Compartmentalized signaling by GPI-anchored ephrin-A5

requires the Fyn tyrosine kinase to regulate cellular adhesion. *Genes Dev* 13:3125-3135.

Davy, A., and Robbins, S.M. 2000. Ephrin-A5 modulates cell adhesion and morphology in an integrin-dependent manner. *EMBO J* 19:5396-5405.

Denny, S.K., Yang, D., Chuang, C.H., Brady, J.J., Lim, J.S., Gruner, B.M., Chiou, S.H., Schep, A.N., Baral, J., Hamard, C., Antoine, M., Wislez, M., Kong, C.S., Connolly, A.J., Park, K.S., Sage, J., Greenleaf, W.J., and Winslow, M.M. 2016. Nfib Promotes Metastasis through a Widespread Increase in Chromatin Accessibility. *Cell* 166:328-342.

Dent, E.W., Gupton, S.L., and Gertler, F.B. 2011. The growth cone cytoskeleton in axon outgrowth and guidance. *Cold Spring Harb Perspect Biol* 3:

Dogterom, M., and Koenderink, G.H. 2019. Actin-microtubule crosstalk in cell biology. *Nat Rev Mol Cell Biol* 20:38-54.

Dorskind, J.M., and Kolodkin, A.L. 2021. Revisiting and refining roles of neural guidance cues in circuit assembly. *Curr Opin Neurobiol* 66:10-21.

Dubey, R., van Kerkhof, P., Jordens, I., Malinauskas, T., Pusapati, G.V., McKenna, J.K., Li, D., Carette, J.E., Ho, M., Siebold, C., Maurice, M., Lebensohn, A.M., and Rohatgi, R. 2020. R-spondins engage heparan sulfate proteoglycans to potentiate WNT signaling. *Elife* 9:

Dubovy, P., Klusakova, I., Hradilova-Svizenska, I., Brazda, V., Kohoutkova, M., and Joukal, M. 2019. A Conditioning Sciatic Nerve Lesion Triggers a Pro-regenerative State in Primary Sensory Neurons Also of Dorsal Root Ganglia Non-associated With the Damaged Nerve. *Front Cell Neurosci* 13:11.

Dwivedi, P.P., Grose, R.H., Filmus, J., Hii, C.S., Xian, C.J., Anderson, P.J., and Powell, B.C. 2013. Regulation of bone morphogenetic protein signalling and cranial osteogenesis by Gpc1 and Gpc3. *Bone* 55:367-376.

Eden, E., Lipson, D., Yogev, S., and Yakhini, Z. 2007. Discovering motifs in ranked lists of DNA sequences. *PLoS Comput Biol* 3:e39.

Eden, E., Navon, R., Steinfeld, I., Lipson, D., and Yakhini, Z. 2009. GOrilla: a tool for discovery and visualization of enriched GO terms in ranked gene lists. *BMC Bioinformatics* 10:48.

Egea, J., and Klein, R. 2007. Bidirectional Eph-ephrin signaling during axon guidance. *Trends Cell Biol* 17:230-238.

Elie, A., Prezel, E., Guerin, C., Denarier, E., Ramirez-Rios, S., Serre, L., Andrieux, A., Fourest-Lieuvin, A., Blanchoin, L., and Arnal, I. 2015. Tau co-organizes dynamic microtubule and actin networks. *Sci Rep* 5:9964.

Elsharkasy, O.M., Nordin, J.Z., Hagey, D.W., de Jong, O.G., Schiffelers, R.M., Andaloussi, S.E., and Vader, P. 2020. Extracellular vesicles as drug delivery systems: Why and how? *Adv Drug Deliv Rev* 159:332-343.

Elyahoodayan, S., Larson, C., Cobo, A.M., Meng, E., and Song, D. 2020. Acute in vivo testing of a polymer cuff electrode with integrated microfluidic channels for stimulation, recording, and drug delivery on rat sciatic nerve. *J Neurosci Methods* 336:108634.

Emperador-Melero, J., Huson, V., van Weering, J., Bollmann, C., Fischer von Mollard, G., Toonen, R.F., and Verhage, M. 2018. Vti1a/b regulate synaptic vesicle and dense core vesicle secretion via protein sorting at the Golgi. *Nat Commun* 9:3421.

Enes, J., Langwieser, N., Ruschel, J., Carballosa-Gonzalez, M.M., Klug, A., Traut, M.H., Ylera, B., Tahirovic, S., Hofmann, F., Stein, V., Moosmang, S., Hentall, I.D., and Bradke, F. 2010. Electrical activity suppresses axon growth through Ca(v)1.2 channels in adult primary sensory neurons. *Curr Biol* 20:1154-1164.

Erck, C., Peris, L., Andrieux, A., Meissirel, C., Gruber, A.D., Vernet, M., Schweitzer, A., Saoudi, Y., Pointu, H., Bosc, C., Salin, P.A., Job, D., and Wehland, J. 2005. A vital role of tubulin-tyrosine-ligase for neuronal organization. *Proc Natl Acad Sci U S A* 102:7853-7858.

Ezkurdia, I., Juan, D., Rodriguez, J.M., Frankish, A., Diekhans, M., Harrow, J., Vazquez, J., Valencia, A., and Tress, M.L. 2014. Multiple evidence strands suggest that there may be as few as 19,000 human protein-coding genes. *Hum Mol Genet* 23:5866-5878.

Farmer, W.T., Altick, A.L., Nural, H.F., Dugan, J.P., Kidd, T., Charron, F., and Mastick, G.S. 2008. Pioneer longitudinal axons navigate using floor plate and Slit/Robo signals. *Development* 135:3643-3653.

Fife, C.M., McCarroll, J.A., and Kavallaris, M. 2014. Movers and shakers: cell cytoskeleton in cancer metastasis. *Br J Pharmacol* 171:5507-5523.

Flynn, K.C. 2013. The cytoskeleton and neurite initiation. *Bioarchitecture* 3:86-109.

Forscher, P., and Smith, S.J. 1988. Actions of cytochalasins on the organization of actin filaments and microtubules in a neuronal growth cone. *J Cell Biol* 107:1505-1516.

Fotoran, W.L., Kleiber, N., Muntefering, T., Liebau, E., and Wunderlich, G. 2020. Production of glycosylphosphatidylinositol-anchored proteins for vaccines and directed binding of immunoliposomes to specific cell types. *J Venom Anim Toxins Incl Trop Dis* 26:e20200032.

Freund, P., Weiskopf, N., Ashburner, J., Wolf, K., Sutter, R., Altmann, D.R., Friston, K., Thompson, A., and Curt, A. 2013. MRI investigation of the sensorimotor cortex and the corticospinal tract after acute spinal cord injury: a prospective longitudinal study. *Lancet Neurol* 12:873-881.

Gabizon, A.A., Barenholz, Y., and Bialer, M. 1993. Prolongation of the circulation time of doxorubicin encapsulated in liposomes containing a polyethylene glycol-derivatized phospholipid: pharmacokinetic studies in rodents and dogs. *Pharm Res* 10:703-708.

Gage, F.H. 2019. Adult neurogenesis in mammals. *Science* 364:827-828.

Ganguly, A., Tang, Y., Wang, L., Ladt, K., Loi, J., Dargent, B., Leterrier, C., and Roy, S. 2015. A dynamic formin-dependent deep F-actin network in axons. *J Cell Biol* 210:401-417.

Garcia-Silva, S., Benito-Martin, A., Nogues, L., Hernandez-Barranco, A., Mazariegos, M.S., Santos, V., Hergueta-Redondo, M., Ximenez-Embun, P., Kataru, R.P., Lopez, A.A., Merino, C., Sanchez-Redondo, S., Grana-Castro, O., Matei, I., Nicolas-Avila, J.A., Torres-Ruiz, R., Rodriguez-Perales, S., Martinez, L., Perez-Martinez, M., Mata, G., Szumera-Cieckiewicz, A., Kalinowska, I., Saltari, A., Martinez-Gomez, J.M., Hogan, S.A., Saragovi, H.U., Ortega, S., Garcia-Martin, C., Boskovic, J., Levesque, M.P., Rutkowski, P., Hidalgo, A., Munoz, J., Megias, D., Mehrara, B.J., Lyden, D., and Peinado, H. 2021. Melanoma-derived small extracellular vesicles induce lymphangiogenesis and metastasis through an NGFR-dependent mechanism. *Nat Cancer* 2:1387-1405.

Geary, L., and LaBonne, C. 2018. FGF mediated MAPK and PI3K/Akt Signals make distinct contributions to pluripotency and the establishment of Neural Crest. *Elife* 7:

Gengrinovitch, S., Berman, B., David, G., Witte, L., Neufeld, G., and Ron, D. 1999. Glypican-1 is a VEGF165 binding proteoglycan that acts as an extracellular chaperone for VEGF165. *J Biol Chem* 274:10816-10822.

Gerthoffer, W.T. 2008. Migration of airway smooth muscle cells. *Proc Am Thorac Soc* 5:97-105.

Ghazalpour, A., Bennett, B., Petyuk, V.A., Orozco, L., Hagopian, R., Mungrue, I.N., Farber, C.R., Sinsheimer, J., Kang, H.M., Furlotte, N., Park, C.C., Wen, P.Z., Brewer, H., Weitz, K., Camp, D.G., 2nd, Pan, C., Yordanova, R., Neuhaus, I., Tilford, C., Siemers, N., Gargalovic, P., Eskin, E., Kirchgessner, T., Smith, D.J., Smith, R.D., and Lusis, A.J. 2011. Comparative analysis of proteome and transcriptome variation in mouse. *PLoS Genet* 7:e1001393.

Girgis, J., Merrett, D., Kirkland, S., Metz, G.A., Verge, V., and Fouad, K. 2007. Reaching training in rats with spinal cord injury promotes plasticity and task specific recovery. *Brain* 130:2993-3003.

Goethals, S., and Brette, R. 2020. Theoretical relation between axon initial segment geometry and excitability. *Elife* 9:

Gorgens, T., and Meng, X. 2007. Stunting and selection effects of famine a case study of the great Chinese famine. In Discussion paper no 2543. IZA,, Bonn, Germany.

GrandPre, T., Nakamura, F., Vartanian, T., and Strittmatter, S.M. 2000. Identification of the Nogo inhibitor of axon regeneration as a Reticulon protein. *Nature* 403:439-444.

Graziano, A., Foffani, G., Knudsen, E.B., Shumsky, J., and Moxon, K.A. 2013. Passive exercise of the hind limbs after complete thoracic transection of the spinal cord promotes cortical reorganization. *PLoS One* 8:e54350.

Griffin, J.M., and Bradke, F. 2020. Therapeutic repair for spinal cord injury: combinatory approaches to address a multifaceted problem. *EMBO Mol Med* 12:e11505.

Guan, B., Anderson, D.B., Chen, L., Feng, S., and Zhou, H. 2023. Global, regional and national burden of traumatic brain injury and spinal cord injury, 1990-2019: a systematic analysis for the Global Burden of Disease Study 2019. *BMJ Open* 13:e075049.

Guillemot, F., and Zimmer, C. 2011. From Cradle to Grave: The Multiple Roles of Fibroblast Growth Factors in Neural Development. *Neuron* 71:574-588.

Hagemann, C., Moreno Gonzalez, C., Guetta, L., Tyzack, G., Chiappini, C., Legati, A., Patani, R., and Serio, A. 2022. Axonal Length Determines Distinct Homeostatic Phenotypes in Human iPSC Derived Motor Neurons on a Bioengineered Platform. *Adv Healthc Mater* 11:e2101817.

Hagey, D.W., Ojansivu, M., Bostancioglu, B.R., Saher, O., Bost, J.P., Gustafsson, M.O., Gramignoli, R., Svahn, M., Gupta, D., Stevens, M.M., Gorgens, A., and El

Andaloussi, S. 2023. The cellular response to extracellular vesicles is dependent on their cell source and dose. *Sci Adv* 9:eadh1168.

Hall, Z.W., and Sanes, J.R. 1993. Synaptic structure and development: the neuromuscular junction. *Cell* 72 Suppl:99-121.

Hansen, C.N., Faw, T.D., White, S., Buford, J.A., Grau, J.W., and Basso, D.M. 2016. Sparing of Descending Axons Rescues Interneuron Plasticity in the Lumbar Cord to Allow Adaptive Learning After Thoracic Spinal Cord Injury. *Front Neural Circuits* 10:11.

Harati, S., Phan, J.H., and Wang, M.D. 2014. Investigation of factors affecting RNA-seq gene expression calls. *Annu Int Conf IEEE Eng Med Biol Soc* 2014:5232-5235.

Harrison, R.E., and Turley, E.A. 2001. Active erk regulates microtubule stability in H-ras-transformed cells. *Neoplasia* 3:385-394.

Hausott, B., and Klimaschewski, L. 2019. Promotion of Peripheral Nerve Regeneration by Stimulation of the Extracellular Signal-Regulated Kinase (ERK) Pathway. *Anat Rec (Hoboken)* 302:1261-1267.

Heidemann, S.R., Landers, J.M., and Hamborg, M.A. 1981. Polarity orientation of axonal microtubules. *J Cell Biol* 91:661-665.

Hellal, F., Hurtado, A., Ruschel, J., Flynn, K.C., Laskowski, C.J., Umlauf, M., Kapitein, L.C., Strikis, D., Lemmon, V., Bixby, J., Hoogenraad, C.C., and Bradke, F. 2011. Microtubule stabilization reduces scarring and causes axon regeneration after spinal cord injury. *Science* 331:928-931.

Herrmann, I.K., Wood, M.J.A., and Fuhrmann, G. 2021. Extracellular vesicles as a next-generation drug delivery platform. *Nat Nanotechnol* 16:748-759.

Hilton, B.J., Blanquie, O., Tedeschi, A., and Bradke, F. 2019. High-resolution 3D imaging and analysis of axon regeneration in unsectioned spinal cord with or without tissue clearing. *Nat Protoc* 14:1235-1260.

Hilton, B.J., Husch, A., Schaffran, B., Lin, T.C., Burnside, E.R., Dupraz, S., Schelski, M., Kim, J., Muller, J.A., Schoch, S., Imig, C., Brose, N., and Bradke, F. 2022. An active vesicle priming machinery suppresses axon regeneration upon adult CNS injury. *Neuron* 110:51-69 e57.

Hobert, O. 2011. Regulation of terminal differentiation programs in the nervous system. *Annu Rev Cell Dev Biol* 27:681-696.

Hollis, E.R., 2nd, Ishiko, N., Pessian, M., Tolentino, K., Lee-Kubli, C.A., Calcutt, N.A., and Zou, Y. 2015. Remodelling of spared proprioceptive circuit involving a small number of neurons supports functional recovery. *Nat Commun* 6:6079.

Homman-Ludiye, J., Kwan, W.C., de Souza, M.J., Rodger, J., and Bourne, J.A. 2017. Ephrin-A2 regulates excitatory neuron differentiation and interneuron migration in the developing neocortex. *Sci Rep* 7:11813.

Honma, Y., Kawano, M., Kohsaka, S., and Ogawa, M. 2010. Axonal projections of mechanoreceptive dorsal root ganglion neurons depend on Ret. *Development* 137:2319-2328.

Hu, H.Z., Granger, N., Pai, S.B., Bellamkonda, R.V., and Jeffery, N.D. 2018. Therapeutic efficacy of microtube-embedded chondroitinase ABC in a canine clinical model of spinal cord injury. *Brain* 141:1017-1027.

Hubbert, C., Guardiola, A., Shao, R., Kawaguchi, Y., Ito, A., Nixon, A., Yoshida, M., Wang, X.F., and Yao, T.P. 2002. HDAC6 is a microtubule-associated deacetylase. *Nature* 417:455-458.

Huber, A.B., Kolodkin, A.L., Ginty, D.D., and Cloutier, J.F. 2003. Signaling at the growth cone: ligand-receptor complexes and the control of axon growth and guidance. *Annu Rev Neurosci* 26:509-563.

Hutson, T.H., Kathe, C., Palmisano, I., Bartholdi, K., Hervera, A., De Virgiliis, F., McLachlan, E., Zhou, L., Kong, G., Barraud, Q., Danzi, M.C., Medrano-Fernandez, A., Lopez-Atalaya, J.P., Boutillier, A.L., Sinha, S.H., Singh, A.K., Chaturbedy, P., Moon, L.D.F., Kundu, T.K., Bixby, J.L., Lemmon, V.P., Barco, A., Courtine, G., and Di Giovanni, S. 2019. Cbp-dependent histone acetylation mediates axon regeneration induced by environmental enrichment in rodent spinal cord injury models. *Sci Transl Med* 11:

Iseki, K., Hagino, S., Nikaido, T., Zhang, Y., Mori, T., Yokoya, S., Hozumi, Y., Goto, K., Wanaka, A., and Tase, C. 2012. Gliosis-specific transcription factor OASIS coincides with proteoglycan core protein genes in the glial scar and inhibits neurite outgrowth. *Biomed Res* 33:345-353.

Jen, Y.H., Musacchio, M., and Lander, A.D. 2009. Glypican-1 controls brain size through regulation of fibroblast growth factor signaling in early neurogenesis. *Neural Dev* 4:33.

Jo, H., Loison, F., and Luo, H.R. 2014. Microtubule dynamics regulates Akt signaling via dynactin p150. *Cell Signal* 26:1707-1716.

Johnson, K., and D'Mello, S.R. 2005. p21-Activated kinase-1 is necessary for depolarization-mediated neuronal survival. *J Neurosci Res* 79:809-815.

Joshi, B.S., de Beer, M.A., Giepmans, B.N.G., and Zuhorn, I.S. 2020. Endocytosis of Extracellular Vesicles and Release of Their Cargo from Endosomes. *ACS Nano* 14:4444-4455.

Jurkiewicz, M.T., Crawley, A.P., Verrier, M.C., Fehlings, M.G., and Mikulis, D.J. 2006. Somatosensory cortical atrophy after spinal cord injury: a voxel-based morphometry study. *Neurology* 66:762-764.

Jurkiewicz, M.T., Mikulis, D.J., McIlroy, W.E., Fehlings, M.G., and Verrier, M.C. 2007. Sensorimotor cortical plasticity during recovery following spinal cord injury: a longitudinal fMRI study. *Neurorehabil Neural Repair* 21:527-538.

Kaneko, S., Iwanami, A., Nakamura, M., Kishino, A., Kikuchi, K., Shibata, S., Okano, H.J., Ikegami, T., Moriya, A., Konishi, O., Nakayama, C., Kumagai, K., Kimura, T., Sato, Y., Goshima, Y., Taniguchi, M., Ito, M., He, Z., Toyama, Y., and Okano, H. 2006. A selective Sema3A inhibitor enhances regenerative responses and functional recovery of the injured spinal cord. *Nat Med* 12:1380-1389.

Kato, D., Yaguchi, T., Iwata, T., Katoh, Y., Morii, K., Tsubota, K., Takise, Y., Tamiya, M., Kamada, H., Akiba, H., Tsumoto, K., Serada, S., Naka, T., Nishimura, R., Nakagawa, T., and Kawakami, Y. 2020. GPC1 specific CAR-T cells eradicate established solid tumor without adverse effects and synergize with anti-PD-1 Ab. *Elife* 9:

Kearns, R.J., Kyzayeva, A., Halliday, L.O.E., Lawlor, D.A., Shaw, M., and Nelson, S.M. 2024. Epidural analgesia during labour and severe maternal morbidity: population based study. *BMJ* 385:e077190.

Kikuchi, K., Kishino, A., Konishi, O., Kumagai, K., Hosotani, N., Saji, I., Nakayama, C., and Kimura, T. 2003. In vitro and in vivo characterization of a novel semaphorin 3A inhibitor, SM-216289 or xanthofulvin. *J Biol Chem* 278:42985-42991.

Kim, C.H., Kim, D.E., Kim, D.H., Min, G.H., Park, J.W., Kim, Y.B., Sung, C.K., and Yim, H. 2022. Mitotic protein kinase-driven crosstalk of machineries for mitosis and metastasis. *Exp Mol Med* 54:414-425.

Kim, H.J., Saikia, J.M., Monte, K.M.A., Ha, E., Romaus-Sanjurjo, D., Sanchez, J.J., Moore, A.X., Hernaiz-Llorens, M., Chavez-Martinez, C.L., Agba, C.K., Li, H., Zhang, J., Lusk, D.T., Cervantes, K.M., and Zheng, B. 2023. Deep scRNA sequencing reveals a broadly applicable Regeneration Classifier and implicates

antioxidant response in corticospinal axon regeneration. *Neuron* 111:3953-3969 e3955.

Kim, N., Kim, S., Nahm, M., Kopke, D., Kim, J., Cho, E., Lee, M.J., Lee, M., Kim, S.H., Broadie, K., and Lee, S. 2019. BMP-dependent synaptic development requires Abi-Abl-Rac signaling of BMP receptor macropinocytosis. *Nat Commun* 10:684.

Kindberg, A.A., Srivastava, V., Muncie, J.M., Weaver, V.M., Gartner, Z.J., and Bush, J.O. 2021. EPH/EPHRIN regulates cellular organization by actomyosin contractility effects on cell contacts. *J Cell Biol* 220:

Kole, T.P., Tseng, Y., Jiang, I., Katz, J.L., and Wirtz, D. 2005. Intracellular mechanics of migrating fibroblasts. *Mol Biol Cell* 16:328-338.

Kolodkin, A.L., Matthes, D.J., and Goodman, C.S. 1993. The semaphorin genes encode a family of transmembrane and secreted growth cone guidance molecules. *Cell* 75:1389-1399.

Kramer, A., Green, J., Pollard, J., Jr., and Tugendreich, S. 2014. Causal analysis approaches in Ingenuity Pathway Analysis. *Bioinformatics* 30:523-530.

Kruger, R.P., Lee, J., Li, W., and Guan, K.L. 2004. Mapping netrin receptor binding reveals domains of Unc5 regulating its tyrosine phosphorylation. *J Neurosci* 24:10826-10834.

Kudryashov, D.S., and Reisler, E. 2013. ATP and ADP actin states. *Biopolymers* 99:245-256.

Kumagai, P.S., Araujo, A.P.U., and Lopes, J.L.S. 2017. Going deep into protein secondary structure with synchrotron radiation circular dichroism spectroscopy. *Biophys Rev* 9:517-527.

Lacroix, B., van Dijk, J., Gold, N.D., Guizetti, J., Aldrian-Herrada, G., Rogowski, K., Gerlich, D.W., and Janke, C. 2010. Tubulin polyglutamylation stimulates spastin-mediated microtubule severing. *J Cell Biol* 189:945-954.

Lassek, M., Weingarten, J., and Volknandt, W. 2015. The synaptic proteome. *Cell Tissue Res* 359:255-265.

Lebensohn, A.M., and Rohatgi, R. 2018. R-spondins can potentiate WNT signaling without LGRs. *Elife* 7:

Ledbetter, M.C., and Porter, K.R. 1964. Morphology of Microtubules of Plant Cell. *Science* 144:872-874.

Lehninger, A.L., Nelson, D.L., and Cox, M.M. 2013. Lehninger principles of biochemistry. W.H. Freeman, New York.

Ley, R., Balmanno, K., Hadfield, K., Weston, C., and Cook, S.J. 2003. Activation of the ERK1/2 signaling pathway promotes phosphorylation and proteasome-dependent degradation of the BH3-only protein, Bim. *J Biol Chem* 278:18811-18816.

Lin, C.H., Thompson, C.A., and Forscher, P. 1994. Cytoskeletal reorganization underlying growth cone motility. *Curr Opin Neurobiol* 4:640-647.

Liu, T., Cao, L., Mladenov, M., Jegou, A., Way, M., and Moores, C.A. 2024. Cortactin stabilizes actin branches by bridging activated Arp2/3 to its nucleated actin filament. *Nat Struct Mol Biol* 31:801-809.

Lombardo, D., and Kiselev, M.A. 2022. Methods of Liposomes Preparation: Formation and Control Factors of Versatile Nanocarriers for Biomedical and Nanomedicine Application. *Pharmaceutics* 14:

Lu, D., Shang, G., He, X., Bai, X.C., and Zhang, X. 2021. Architecture of the Sema3A/PlexinA4/Neuropilin tripartite complex. *Nat Commun* 12:3172.

Luo, Y., Raible, D., and Raper, J.A. 1993. Collapsin: a protein in brain that induces the collapse and paralysis of neuronal growth cones. *Cell* 75:217-227.

Madej, T., Lanczycki, C.J., Zhang, D., Thiessen, P.A., Geer, R.C., Marchler-Bauer, A., and Bryant, S.H. 2014. MMDB and VAST+: tracking structural similarities between macromolecular complexes. *Nucleic Acids Res* 42:D297-303.

Magrassi, L., Leto, K., and Rossi, F. 2013. Lifespan of neurons is uncoupled from organismal lifespan. *Proceedings of the National Academy of Sciences* 110:4374-4379.

Manini, I., Ruaro, M.E., Sgarra, R., Bartolini, A., Caponnetto, F., Ius, T., Skrap, M., Di Loreto, C., Beltrami, A.P., Manfioletti, G., and Cesselli, D. 2019. Semaphorin-7A on Exosomes: A Promigratory Signal in the Glioma Microenvironment. *Cancers (Basel)* 11:

Martin, V. 1993. Overview of paclitaxel (TAXOL). *Semin Oncol Nurs* 9:2-5.

Matson, K.J.E., Russ, D.E., Kathe, C., Hua, I., Maric, D., Ding, Y., Krynitsky, J., Pursley, R., Sathyamurthy, A., Squair, J.W., Levi, B.P., Courtine, G., and Levine, A.J. 2022. Single cell atlas of spinal cord injury in mice reveals a pro-regenerative signature in spinocerebellar neurons. *Nat Commun* 13:5628.

Matsuura, T., Narama, I., Nishikawa, T., Nishimura, M., Imagawa, T., Kitagawa, H., and Uehara, M. 1997. Morphological and morphometric features of the deformed cervical and caudal vertebrae in a new mutant knotty-tail (knt/knt) mouse. *Ann Anat* 179:277-283.

Maynard, G., Kannan, R., Liu, J., Wang, W., Lam, T.K.T., Wang, X., Adamson, C., Hackett, C., Schwab, J.M., Liu, C., Leslie, D.P., Chen, D., Marino, R., Zafonte, R., Flanders, A., Block, G., Smith, E., and Strittmatter, S.M. 2023. Soluble Nogo-Receptor-Fc decoy (AXER-204) in patients with chronic cervical spinal cord injury in the USA: a first-in-human and randomised clinical trial. *Lancet Neurol* 22:672-684.

Meijering, E., Jacob, M., Sarria, J.C., Steiner, P., Hirling, H., and Unser, M. 2004. Design and validation of a tool for neurite tracing and analysis in fluorescence microscopy images. *Cytometry A* 58:167-176.

Meng, W., Mushika, Y., Ichii, T., and Takeichi, M. 2008. Anchorage of microtubule minus ends to adherens junctions regulates epithelial cell-cell contacts. *Cell* 135:948-959.

Merriam, E.B., Millette, M., Lumbard, D.C., Saengsawang, W., Fothergill, T., Hu, X., Ferhat, L., and Dent, E.W. 2013. Synaptic regulation of microtubule dynamics in dendritic spines by calcium, F-actin, and drebrin. *J Neurosci* 33:16471-16482.

Mitchison, T., and Kirschner, M. 1988. Cytoskeletal dynamics and nerve growth. *Neuron* 1:761-772.

Mulligan, K.A., and Cheyette, B.N. 2012. Wnt signaling in vertebrate neural development and function. *J Neuroimmune Pharmacol* 7:774-787.

Mullins, R.D., Heuser, J.A., and Pollard, T.D. 1998. The interaction of Arp2/3 complex with actin: nucleation, high affinity pointed end capping, and formation of branching networks of filaments. *Proc Natl Acad Sci U S A* 95:6181-6186.

Myers, J.P., Santiago-Medina, M., and Gomez, T.M. 2011. Regulation of axonal outgrowth and pathfinding by integrin-ECM interactions. *Dev Neurobiol* 71:901-923.

Namba, T., Kibe, Y., Funahashi, Y., Nakamuta, S., Takano, T., Ueno, T., Shimada, A., Kozawa, S., Okamoto, M., Shimoda, Y., Oda, K., Wada, Y., Masuda, T., Sakakibara, A., Igarashi, M., Miyata, T., Faivre-Sarrailh, C., Takeuchi, K., and Kaibuchi, K. 2014. Pioneering axons regulate neuronal polarization in the developing cerebral cortex. *Neuron* 81:814-829.

Neumann, S., and Woolf, C.J. 1999. Regeneration of dorsal column fibers into and beyond the lesion site following adult spinal cord injury. *Neuron* 23:83-91.

Neumeier, J., and Meister, G. 2020. siRNA Specificity: RNAi Mechanisms and Strategies to Reduce Off-Target Effects. *Front Plant Sci* 11:526455.

Niu, L., Geyer, P.E., Gupta, R., Santos, A., Meier, F., Doll, S., Wewer Albrechtsen, N.J., Klein, S., Ortiz, C., Uschner, F.E., Schierwagen, R., Trebicka, J., and Mann, M.

2022. Dynamic human liver proteome atlas reveals functional insights into disease pathways. *Mol Syst Biol* 18:e10947.

Noble, L.J., and Wrathall, J.R. 1988. Blood-spinal cord barrier disruption proximal to a spinal cord transection in the rat: time course and pathways associated with protein leakage. *Exp Neurol* 99:567-578.

Nolte, H., MacVicar, T.D., Tellkamp, F., and Kruger, M. 2018. Instant Clue: A Software Suite for Interactive Data Visualization and Analysis. *Sci Rep* 8:12648.

Pan, J., and Ho, M. 2021. Role of glypican-1 in regulating multiple cellular signaling pathways. *Am J Physiol Cell Physiol* 321:C846-C858.

Papareddy, P., Tapken, I., Kroh, K., Varma Bhongir, R.K., Rahman, M., Baumgarten, M., Cim, E.I., Gyorffy, L., Smeds, E., Neumann, A., Veerla, S., Olinder, J., Thorlacus, H., Ryden, C., Bartakova, E., Holub, M., and Herwald, H. 2024. The role of extracellular vesicle fusion with target cells in triggering systemic inflammation. *Nat Commun* 15:1150.

Park, K.K., Liu, K., Hu, Y., Smith, P.D., Wang, C., Cai, B., Xu, B., Connolly, L., Kramvis, I., Sahin, M., and He, Z. 2008. Promoting axon regeneration in the adult CNS by modulation of the PTEN/mTOR pathway. *Science* 322:963-966.

Pasterkamp, R.J., Anderson, P.N., and Verhaagen, J. 2001. Peripheral nerve injury fails to induce growth of lesioned ascending dorsal column axons into spinal cord scar tissue expressing the axon repellent Semaphorin3A. *Eur J Neurosci* 13:457-471.

Perrot, G., Colin-Pierre, C., Ramont, L., Proult, I., Garbar, C., Bardey, V., Jeanmaire, C., Mine, S., Danoux, L., Berthelemy, N., Maquart, F.X., Wegrowski, Y., and Brezillon, S. 2019. Decreased expression of GPC1 in human skin keratinocytes and epidermis during ageing. *Exp Gerontol* 126:110693.

Petrie, R.J., and Yamada, K.M. 2015. Fibroblasts Lead the Way: A Unified View of 3D Cell Motility. *Trends Cell Biol* 25:666-674.

Petrosius, V., Aragon-Fernandez, P., Uresin, N., Kovacs, G., Phlairaharn, T., Furtwangler, B., Op De Beeck, J., Skovbakke, S.L., Goletz, S., Thomsen, S.F., Keller, U.A.D., Natarajan, K.N., Porse, B.T., and Schoof, E.M. 2023. Exploration of cell state heterogeneity using single-cell proteomics through sensitivity-tailored data-independent acquisition. *Nat Commun* 14:5910.

Pierret, P., Vallee, A., Mechawar, N., Dower, N.A., Stone, J.C., Richardson, P.M., and Dunn, R.J. 2001. Cellular and subcellular localization of Ras guanyl nucleotide-releasing protein in the rat hippocampus. *Neuroscience* 108:381-390.

Piper, M., Anderson, R., Dwivedy, A., Weinl, C., van Horck, F., Leung, K.M., Cogill, E., and Holt, C. 2006. Signaling mechanisms underlying Slit2-induced collapse of Xenopus retinal growth cones. *Neuron* 49:215-228.

Piperno, G., LeDizet, M., and Chang, X.J. 1987. Microtubules containing acetylated alpha-tubulin in mammalian cells in culture. *J Cell Biol* 104:289-302.

Pollard, T.D. 2007. Regulation of actin filament assembly by Arp2/3 complex and formins. *Annu Rev Biophys Biomol Struct* 36:451-477.

Poobalasingam, T., Bianco, F., Oozeer, F., and Gordon-Weeks, P.R. 2022. The drebrin/EB3 pathway regulates cytoskeletal dynamics to drive neuritogenesis in embryonic cortical neurons. *J Neurochem* 160:185-202.

Poplawski, G.H.D., Kawaguchi, R., Van Niekerk, E., Lu, P., Mehta, N., Canete, P., Lie, R., Dragatsis, I., Meves, J.M., Zheng, B., Coppola, G., and Tuszynski, M.H. 2020. Injured adult neurons regress to an embryonic transcriptional growth state. *Nature* 581:77-82.

Portrait, F.R.M., van Wingerden, T.F., and Deeg, D.J.H. 2017. Early life undernutrition and adult height: The Dutch famine of 1944-45. *Econ Hum Biol* 27:339-348.

Purves, D. 2018. Neuroscience. Oxford University Press, New York. 1 volume (various pagings) pp.

Ramon y Cajal, S. 1928. Degeneration and regeneration of the nervous system. Clarendon Press, Oxford, England.

Raper, J.A., and Kapfhammer, J.P. 1990. The enrichment of a neuronal growth cone collapsing activity from embryonic chick brain. *Neuron* 4:21-29.

Rappsilber, J., Mann, M., and Ishihama, Y. 2007. Protocol for micro-purification, enrichment, pre-fractionation and storage of peptides for proteomics using StageTips. *Nat Protoc* 2:1896-1906.

Rasool, D., and Jahani-Asl, A. 2024. Master regulators of neurogenesis: the dynamic roles of Ephrin receptors across diverse cellular niches. *Transl Psychiatry* 14:462.

Rawson, J.M., Dimitroff, B., Johnson, K.G., Rawson, J.M., Ge, X., Van Vactor, D., and Selleck, S.B. 2005. The heparan sulfate proteoglycans Dally-like and Syndecan have distinct functions in axon guidance and visual-system assembly in Drosophila. *Curr Biol* 15:833-838.

Renthal, W., Tochitsky, I., Yang, L., Cheng, Y.C., Li, E., Kawaguchi, R., Geschwind, D.H., and Woolf, C.J. 2020. Transcriptional Reprogramming of Distinct Peripheral Sensory Neuron Subtypes after Axonal Injury. *Neuron* 108:128-144 e129.

Richardson, P.M., and Issa, V.M. 1984. Peripheral injury enhances central regeneration of primary sensory neurones. *Nature* 309:791-793.

Romero, S., Le Clainche, C., Didry, D., Egile, C., Pantaloni, D., and Carlier, M.F. 2004. Formin is a processive motor that requires profilin to accelerate actin assembly and associated ATP hydrolysis. *Cell* 119:419-429.

Rouiller, I., Xu, X.P., Amann, K.J., Egile, C., Nickell, S., Nicastro, D., Li, R., Pollard, T.D., Volkmann, N., and Hanein, D. 2008. The structural basis of actin filament branching by the Arp2/3 complex. *J Cell Biol* 180:887-895.

Ruschel, J., Hellal, F., Flynn, K.C., Dupraz, S., Elliott, D.A., Tedeschi, A., Bates, M., Sliwinski, C., Brook, G., Dobrindt, K., Peitz, M., Brustle, O., Norenberg, M.D., Blesch, A., Weidner, N., Bunge, M.B., Bixby, J.L., and Bradke, F. 2015a. Axonal regeneration. Systemic administration of epothilone B promotes axon regeneration after spinal cord injury. *Science* 348:347-352.

Ruschel, J., Hellal, F., Flynn, K.C., Dupraz, S., Elliott, D.A., Tedeschi, A., Bates, M., Sliwinski, C., Brook, G., Dobrindt, K., Peitz, M., Brüstle, O., Norenberg, M.D., Blesch, A., Weidner, N., Bunge, M.B., Bixby, J.L., and Bradke, F. 2015b. Axonal regeneration. Systemic administration of epothilone B promotes axon regeneration after spinal cord injury. *Science* 348:347-352.

Sabatier, C., Plump, A.S., Le, M., Brose, K., Tamada, A., Murakami, F., Lee, E.Y., and Tessier-Lavigne, M. 2004. The divergent Robo family protein rig-1/Robo3 is a negative regulator of slit responsiveness required for midline crossing by commissural axons. *Cell* 117:157-169.

Saijilafu, Hur, E.M., and Zhou, F.Q. 2011. Genetic dissection of axon regeneration via in vivo electroporation of adult mouse sensory neurons. *Nat Commun* 2:543.

Salem, D., and Fecek, R.J. 2023. Role of microtubule actin crosslinking factor 1 (MACF1) in bipolar disorder pathophysiology and potential in lithium therapeutic mechanism. *Transl Psychiatry* 13:221.

Sanchez-Huertas, C., Bonhomme, M., Falco, A., Fagotto-Kaufmann, C., van Haren, J., Jeanneteau, F., Galjart, N., Debant, A., and Boudeau, J. 2020. The +TIP Navigator-1 is an actin-microtubule crosslinker that regulates axonal growth cone motility. *J Cell Biol* 219:

Santos, T.E., Schaffran, B., Broguiere, N., Meyn, L., Zenobi-Wong, M., and Bradke, F. 2020. Axon Growth of CNS Neurons in Three Dimensions Is Amoeboid and Independent of Adhesions. *Cell Rep* 32:107907.

Schaefer, A.W., Schoonderwoert, V.T., Ji, L., Mederios, N., Danuser, G., and Forscher, P. 2008. Coordination of actin filament and microtubule dynamics during neurite outgrowth. *Dev Cell* 15:146-162.

Schelski, M., and Bradke, F. 2017. Neuronal polarization: From spatiotemporal signaling to cytoskeletal dynamics. *Mol Cell Neurosci* 84:11-28.

Schelski, M., and Bradke, F. 2022. Microtubule retrograde flow retains neuronal polarization in a fluctuating state. *Sci Adv* 8:eabo2336.

Schiweck, J., Murk, K., Ledderose, J., Munster-Wandowski, A., Ornaghi, M., Vida, I., and Eickholt, B.J. 2021. Drebrin controls scar formation and astrocyte reactivity upon traumatic brain injury by regulating membrane trafficking. *Nat Commun* 12:1490.

Schmandke, A., Schmandke, A., and Strittmatter, S.M. 2007. ROCK and Rho: biochemistry and neuronal functions of Rho-associated protein kinases. *Neuroscientist* 13:454-469.

Sengul, G., and Watson, C. 2012. Chapter 13 - Spinal Cord. In The Mouse Nervous System. C. Watson, G. Paxinos, and L. Puelles, editors. Academic Press, San Diego. 424-458.

Serbedzija, G.N., Fraser, S.E., and Bronner-Fraser, M. 1990. Pathways of trunk neural crest cell migration in the mouse embryo as revealed by vital dye labelling. *Development* 108:605-612.

Sercombe, L., Veerati, T., Moheimani, F., Wu, S.Y., Sood, A.K., and Hua, S. 2015. Advances and Challenges of Liposome Assisted Drug Delivery. *Front Pharmacol* 6:286.

Sharma, K., Selzer, M.E., and Li, S. 2012. Scar-mediated inhibition and CSPG receptors in the CNS. *Exp Neurol* 237:370-378.

Sheng, J., Gong, J., Shi, Y., Wang, X., and Liu, D. 2022. MicroRNA-22 coordinates vascular and motor neuronal pathfinding via sema4 during zebrafish development. *Open Biol* 12:210315.

Shiau, C.E., Hu, N., and Bronner-Fraser, M. 2010. Altering Glypican-1 levels modulates canonical Wnt signaling during trigeminal placode development. *Dev Biol* 348:107-118.

Shibue, T., Brooks, M.W., Inan, M.F., Reinhardt, F., and Weinberg, R.A. 2012. The outgrowth of micrometastases is enabled by the formation of filopodium-like protrusions. *Cancer Discov* 2:706-721.

Simpson, J.H., Bland, K.S., Fetter, R.D., and Goodman, C.S. 2000. Short-range and long-range guidance by Slit and its Robo receptors: a combinatorial code of Robo receptors controls lateral position. *Cell* 103:1019-1032.

Skinnider, M.A., Gautier, M., Teo, A.Y.Y., Kathe, C., Hutson, T.H., Laskaratos, A., de Coucy, A., Regazzi, N., Aureli, V., James, N.D., Schneider, B., Sofroniew, M.V., Barraud, Q., Bloch, J., Anderson, M.A., Squair, J.W., and Courtine, G. 2024. Single-cell and spatial atlases of spinal cord injury in the Tabulae Paralytica. *Nature* 631:150-163.

Sloan, T.F., Qasaimeh, M.A., Juncker, D., Yam, P.T., and Charron, F. 2015. Integration of shallow gradients of Shh and Netrin-1 guides commissural axons. *PLoS Biol* 13:e1002119.

Smith, D.S., and Skene, J.H. 1997. A transcription-dependent switch controls competence of adult neurons for distinct modes of axon growth. *J Neurosci* 17:646-658.

Sparn, C., Dimou, E., Meyer, A., Saleppico, R., Wegehingel, S., Gerstner, M., Klaus, S., Ewers, H., and Nickel, W. 2022. Glypican-1 drives unconventional secretion of fibroblast growth factor 2. *Elife* 11:

Stankiewicz, T.R., and Linseman, D.A. 2014. Rho family GTPases: key players in neuronal development, neuronal survival, and neurodegeneration. *Front Cell Neurosci* 8:314.

Stern, S., Hilton, B.J., Burnside, E.R., Dupraz, S., Handley, E.E., Gonyer, J.M., Brakebusch, C., and Bradke, F. 2021. RhoA drives actin compaction to restrict axon regeneration and astrocyte reactivity after CNS injury. *Neuron* 109:3436-3455 e3439.

Stoeckli, E.T. 2018. Understanding axon guidance: are we nearly there yet? *Development* 145:

Stuckmann, I., Weigmann, A., Shevchenko, A., Mann, M., and Huttner, W.B. 2001. Ephrin B1 is expressed on neuroepithelial cells in correlation with neocortical neurogenesis. *J Neurosci* 21:2726-2737.

Sudo, H., and Baas, P.W. 2010. Acetylation of microtubules influences their sensitivity to severing by katanin in neurons and fibroblasts. *J Neurosci* 30:7215-7226.

Sun, T., Krishnan, R., and Swiercz, J.M. 2012. Grb2 mediates semaphorin-4D-dependent RhoA inactivation. *J Cell Sci* 125:3557-3567.

Svensson, G., Awad, W., Hakansson, M., Mani, K., and Logan, D.T. 2012. Crystal structure of N-glycosylated human glypican-1 core protein: structure of two loops evolutionarily conserved in vertebrate glypican-1. *J Biol Chem* 287:14040-14051.

Tahirovic, S., and Bradke, F. 2009. Neuronal polarity. *Cold Spring Harb Perspect Biol* 1:a001644.

Tan, C.L., Kwok, J.C., Patani, R., Ffrench-Constant, C., Chandran, S., and Fawcett, J.W. 2011. Integrin activation promotes axon growth on inhibitory chondroitin sulfate proteoglycans by enhancing integrin signaling. *J Neurosci* 31:6289-6295.

Tang, D.D., and Gerlach, B.D. 2017. The roles and regulation of the actin cytoskeleton, intermediate filaments and microtubules in smooth muscle cell migration. *Respir Res* 18:54.

Tedeschi, A., Dupraz, S., Curcio, M., Laskowski, C.J., Schaffran, B., Flynn, K.C., Santos, T.E., Stern, S., Hilton, B.J., Larson, M.J.E., Gurniak, C.B., Witke, W., and Bradke, F. 2019. ADF/Cofilin-Mediated Actin Turnover Promotes Axon Regeneration in the Adult CNS. *Neuron* 103:1073-1085 e1076.

Tedeschi, A., Dupraz, S., Laskowski, C.J., Xue, J., Ulas, T., Beyer, M., Schultze, J.L., and Bradke, F. 2016. The Calcium Channel Subunit Alpha2delta2 Suppresses Axon Regeneration in the Adult CNS. *Neuron* 92:419-434.

Teillet, M.A., Kalcheim, C., and Le Douarin, N.M. 1987. Formation of the dorsal root ganglia in the avian embryo: segmental origin and migratory behavior of neural crest progenitor cells. *Dev Biol* 120:329-347.

Teramoto, H., Crespo, P., Coso, O.A., Igishi, T., Xu, N., and Gutkind, J.S. 1996. The small GTP-binding protein rho activates c-Jun N-terminal kinases/stress-activated protein kinases in human kidney 293T cells. Evidence for a Pak-independent signaling pathway. *J Biol Chem* 271:25731-25734.

Thillai, K., Lam, H., Sarker, D., and Wells, C.M. 2017. Deciphering the link between PI3K and PAK: An opportunity to target key pathways in pancreatic cancer? *Oncotarget* 8:14173-14191.

Threadgill, R., Bobb, K., and Ghosh, A. 1997. Regulation of dendritic growth and remodeling by Rho, Rac, and Cdc42. *Neuron* 19:625-634.

Traynor, A.J., Aragon, M., Ghosh, D., Choi, R.S., Dingmann, C., Vu Tran, Z., and Bucklin, B.A. 2016. Obstetric Anesthesia Workforce Survey: A 30-Year Update. *Anesth Analg* 122:1939-1946.

Tripathi, A.D., Katiyar, S., and Mishra, A. 2023. Glypican1: A potential cancer biomarker for nanotargeted therapy. *Drug Discov Today* 28:103660.

Tropini, C., Roth, E.A., Zanic, M., Gardner, M.K., and Howard, J. 2012. Islands containing slowly hydrolyzable GTP analogs promote microtubule rescues. *PLoS One* 7:e30103.

Tse, C.M., Chisholm, A.E., Lam, T., Eng, J.J., and Team, S.R. 2018. A systematic review of the effectiveness of task-specific rehabilitation interventions for improving independent sitting and standing function in spinal cord injury. *J Spinal Cord Med* 41:254-266.

Tyanova, S., Temu, T., Sinitcyn, P., Carlson, A., Hein, M.Y., Geiger, T., Mann, M., and Cox, J. 2016. The Perseus computational platform for comprehensive analysis of (prote)omics data. *Nat Methods* 13:731-740.

van Beuningen, S.F.B., Will, L., Harterink, M., Chazeau, A., van Battum, E.Y., Frias, C.P., Franker, M.A.M., Katrukha, E.A., Stucchi, R., Vocking, K., Antunes, A.T., Slenders, L., Doulkeridou, S., Sillevis Smitt, P., Altelaar, A.F.M., Post, J.A., Akhmanova, A., Pasterkamp, R.J., Kapitein, L.C., de Graaff, E., and Hoogenraad, C.C. 2015. TRIM46 Controls Neuronal Polarity and Axon Specification by Driving the Formation of Parallel Microtubule Arrays. *Neuron* 88:1208-1226.

van de Bospoort, R., Farina, M., Schmitz, S.K., de Jong, A., de Wit, H., Verhage, M., and Toonen, R.F. 2012. Munc13 controls the location and efficiency of dense-core vesicle release in neurons. *J Cell Biol* 199:883-891.

Vandermoere, F., El Yazidi-Belkoura, I., Demont, Y., Slomianny, C., Antol, J., Lemoine, J., and Hondermarck, H. 2007. Proteomics exploration reveals that actin is a signaling target of the kinase Akt. *Mol Cell Proteomics* 6:114-124.

Vaughn, J.E., Henrikson, C.K., Chernow, C.R., Grieshaber, J.A., and Wimer, C.C. 1975. Genetically-associated variations in the development of reflex movements and synaptic junctions within an early reflex pathway of mouse spinal cord. *J Comp Neurol* 161:541-553.

Vinopal, S., Dupraz, S., Alfadil, E., Pietralla, T., Bendre, S., Stiess, M., Falk, S., Camargo Ortega, G., Maghelli, N., Tolic, I.M., Smejkal, J., Gotz, M., and Bradke, F. 2023. Centrosomal microtubule nucleation regulates radial migration of projection neurons independently of polarization in the developing brain. *Neuron* 111:1241-1263 e1216.

Voets, T., Moser, T., Lund, P.E., Chow, R.H., Geppert, M., Sudhof, T.C., and Neher, E. 2001. Intracellular calcium dependence of large dense-core vesicle exocytosis in the absence of synaptotagmin I. *Proc Natl Acad Sci U S A* 98:11680-11685.

Wang, X., Chun, S.J., Treloar, H., Vartanian, T., Greer, C.A., and Strittmatter, S.M. 2002. Localization of Nogo-A and Nogo-66 receptor proteins at sites of axon-myelin and synaptic contact. *J Neurosci* 22:5505-5515.

Webster, D.R., Gundersen, G.G., Bulinski, J.C., and Borisy, G.G. 1987. Differential turnover of tyrosinated and detyrosinated microtubules. *Proc Natl Acad Sci U S A* 84:9040-9044.

Weidner, N., Abel, R., Maier, D., Rohl, K., Rohrich, F., Baumberger, M., Hund-Georgiadis, M., Saur, M., Benito, J., Rehahn, K., Aach, M., Badke, A., Kriz, J., Barkovits, K., Killeen, T., Farner, L., Seif, M., Hubli, M., Marcus, K., Maurer, M.A., Robert, B., Rupp, R., Scheuren, P.S., Schubert, M., Schuld, C., Sina, C., Steiner, B., Weis, T., Hug, A., Bolliger, M., Weiskopf, N., Freund, P., Hothorn, T., Schwab, M.E., Curt, A., and Nogo Inhibition in Spinal Cord Injury Study, G. 2025. Safety and efficacy of intrathecal antibodies to Nogo-A in patients with acute cervical spinal cord injury: a randomised, double-blind, multicentre, placebo-controlled, phase 2b trial. *Lancet Neurol* 24:42-53.

Witte, H., Neukirchen, D., and Bradke, F. 2008. Microtubule stabilization specifies initial neuronal polarization. *J Cell Biol* 180:619-632.

Wu, N., Jia, D., Ibrahim, A.H., Bachurski, C.J., Gronostajski, R.M., and MacPherson, D. 2016. NFIB overexpression cooperates with Rb/p53 deletion to promote small cell lung cancer. *Oncotarget* 7:57514-57524.

Yang, D., Qu, F., Cai, H., Chuang, C.H., Lim, J.S., Jahchan, N., Gruner, B.M., C, S.K., Kong, C., Oudin, M.J., Winslow, M.M., and Sage, J. 2019. Axon-like protrusions promote small cell lung cancer migration and metastasis. *Elife* 8:

Ye, J., Coulouris, G., Zaretskaya, I., Cutcutache, I., Rozen, S., and Madden, T.L. 2012. Primer-BLAST: a tool to design target-specific primers for polymerase chain reaction. *BMC Bioinformatics* 13:134.

Ylera, B., Erturk, A., Hellal, F., Nadrigny, F., Hurtado, A., Tahirovic, S., Oudega, M., Kirchhoff, F., and Bradke, F. 2009. Chronically CNS-injured adult sensory neurons gain regenerative competence upon a lesion of their peripheral axon. *Curr Biol* 19:930-936.

Zhang, S., Han, J., Sells, M.A., Chernoff, J., Knaus, U.G., Ulevitch, R.J., and Bokoch, G.M. 1995. Rho family GTPases regulate p38 mitogen-activated protein kinase through the downstream mediator Pak1. *J Biol Chem* 270:23934-23936.

Zhang, Y., Lan, M., and Chen, Y. 2024. Minimal Information for Studies of Extracellular Vesicles (MISEV): Ten-Year Evolution (2014-2023). *Pharmaceutics* 16:

Zhang, Z., Coomans, C., and David, G. 2001. Membrane heparan sulfate proteoglycan-supported FGF2-FGFR1 signaling: evidence in support of the "cooperative end structures" model. *J Biol Chem* 276:41921-41929.

Zhao, R.R., Andrews, M.R., Wang, D., Warren, P., Gullo, M., Schnell, L., Schwab, M.E., and Fawcett, J.W. 2013. Combination treatment with anti-Nogo-A and chondroitinase ABC is more effective than single treatments at enhancing functional recovery after spinal cord injury. *Eur J Neurosci* 38:2946-2961.

Zhou, G.L., Zhang, H., Wu, H., Ghai, P., and Field, J. 2014. Phosphorylation of the cytoskeletal protein CAP1 controls its association with cofilin and actin. *J Cell Sci* 127:5052-5065.

Ziak, J., Dorskind, J.M., Trigg, B., Sudarsanam, S., Jin, X.O., Hand, R.A., and Kolodkin, A.L. 2024. Microtubule-binding protein MAP1B regulates interstitial axon branching of cortical neurons via the tubulin tyrosination cycle. *EMBO J* 43:1214-1243.

Acknowledgements

After eleven and a half years of study, I finally get to type these words, which conclude my doctoral thesis. Five of which – on the day I write this almost exactly – I spent with Frank, who is the first person I need to express my gratitude to. It sounds cliché, but I am truly grateful to you for providing me this opportunity and giving me the freedom to explore science in my own way. Certainly, this would not have been possible with another PI. Next, I am so thankful for those who keep the lab running. Jessy wo taught me so much and then worked hand in hand with me once I had learned the ropes. Blanca, without whom the lab wouldn't run nearly as smoothly. Sina who made all the animal work possible while keeping all of us on the right side of the law, and Andreas the good heart of the group, who welcomed me to the lab. Special thanks go out to green bay. Eissa and Juli, my favourite conference buddies and Emily H. and Shweta who always had good banter and amazing feedback. Also, big shoutout to honorary green bay member Emily B., who would always help with all things mouse or spinal cord. Thorben and Seba, who always gave support and wisdom on matters of the cytoskeleton and were always good for a laugh or a rant. Further, I would not have made it here without the great assistants, who made all the paperwork bearable and the travel almost seamless, Nasti, Nancy and Debbie, thank you so much! I also want to voice my appreciation for my favourite students, Sarah and Judith, who were not only great help, but also taught me just as much as I taught them. Finally, a big thank you to everyone else from the group, Cedric, Annika, Tien-Chen, Max, Valentina, Anh-Tuan, Barbara, Jarred and Brett, my friends and colleagues from the DZNE and my collaborators, all of you helped along the way and shaped this journey in one way or another.

Mama und Papa, ich bin unendlich dankbar, dass ihr das alles ermöglicht habt. Ohne jemals eingreifen oder vorschreiben zu wollen habt ihr darauf vertraut, dass ich meinen Weg finden werde. Das scheint funktioniert zu haben. Christian und Susanne, auch eure Unterstützung seit Beginn des Studiums war unverzichtbar. Ihr habt einen steinigen Weg etwas geebnet. Miriam und ihre Familie, meine Omas, Tanten und Cousinen, alle waren die ganze Zeit an meiner Seite, haben sich immer interessiert, für was das soll was ich da treibe und nie daran gezweifelt, dass das schon alles Sinn macht. Und zu guter Letzt Svenja, du warst so ziemlich von Anfang an dabei, hast alles Krisen mit mir durchgestanden, Hoffnungen und Enttäuschungen mitgefiebert und mir immer den Rücken gehalten. Ich kann nur hoffen, dass du auch in allen kommenden Lebensphasen an meiner Seite bist.

Natürlich wäre das alles nicht möglich gewesen, ohne Freunde die einen bei Laune halten. Die Schergen, mit denen ich teilweise gefühlt genau so viel Zeit verbracht habe wie im Labor. Pia, Anja und die restlichen Dorfkinder, die immer ein Stück Heimat sein werden. Die Burschen, bei denen ich jedes Mal wieder 18 bin, wenn man sich trifft. Die T. Gehlings und die anderen BC-Freunde, die seit den ersten Wochen des Bachelors nicht wegzudenken sind. Anika und alle anderen, die da waren, wenn ich Ablenkung brauchte, oder jemand der meine Erfolge mit mir feiert. Danke, dass ihr das mit mir durchgezogen habt.

Publications

Ricke, K. M., Paß, T., Kimoloi, S., **Fährmann, K.**, Jüngst, C., Schauss, A., Baris, O. R., Aradjanski, M., Trifunovic, A., Eriksson Faelker, T. M., Bergami, M., & Wiesner, R. J. (2020). *Mitochondrial Dysfunction Combined with High Calcium Load Leads to Impaired Antioxidant Defense Underlying the Selective Loss of Nigral Dopaminergic Neurons*. The Journal of neuroscience: the official journal of the Society for Neuroscience, 40(9), 1975–1986. https://doi.org/10.1523/JNEUROSCI.1345-19.2019